Arterial spin labeling perfusion MRI in cerebral ischemia

Reinoud P.H. Bokkers

Arterial spin labeling perfusion MRI in cerebral ischemia
PhD thesis, Utrecht University, The Netherlands

ISBN : 978-90-393-5588-6.

Cover : Bart Massee
Lay-out : Karin van Rijnbach
Printed by : PrintSupport4U

Arterial spin labeling perfusion MRI in cerebral ischemia

Arteriële spin labeling perfusie MRI in cerebrale ischemie
(met een samenvatting in het Nederlands)

Proefschrift

ter verkrijging van de graad van doctor aan de Universiteit Utrecht
op gezag van de rector magnificus, prof. dr. G.J. van der Zwaan,
ingevolge het besluit van het college voor promoties
in het openbaar te verdedigen
op vrijdag 8 juli 2011 des middags te 2.30 uur

door

Reinoud Pieter Harmen Bokkers
geboren op 28 december 1980 te Blackburn, Verenigd Koninkrijk

Promotor: Prof. dr. W.P.Th.M. Mali

Co-promotor: Dr. J. Hendrikse

The publication of this PhD thesis was financially supported by Philips, ev3, Bayer Healthcare en Covidien.

Financial support by the Dutch Heart Foundation and Röntgen Stichting Utrecht for the publication of this thesis is gratefully acknowledged.

for the patients and volunteers that
made this research possible

Contents

CHAPTER 1

GENERAL INTRODUCTION

General introduction

Cerebral perfusion is the basis for the delivery of oxygen and nutrients to the brain. A human brain is supplied on average with 750 milliliters of freshly oxygenated blood per minute. Although the human brain constitutes only 2% of the total weight of a body, it receives roughly 15% of the cardiac output.[1] Basic physiological functions such as synaptic transmission, the membrane ion pump and energy metabolism are disrupted when there is a disturbance in the supply of blood. Within minutes decreased perfusion can lead to irreversible neuronal damage.

The amount of blood that is supplied to the brain is expressed as cerebral blood flow (CBF). This is the amount of blood in milliliters flowing through 100 grams of brain tissue per minute. The two main factors that determine CBF are the cerebral perfusion pressure (CPP) and vascular resistance within the brain.[2] CPP is the main pressure gradient causing blood to flow from the supplying vasculature to the brain. The vascular resistance is the accumulative effect of the resistance with the cerebrovasculature, from the large cervical arteries up to the smallest cerebral arterioles.

Fluctuations in perfusion pressure are negligible within normal physiological conditions. Adequate oxygen and nutrient delivery is, however, at risk when there is a severe reduction in cardiac output or a restriction of blood flow through the supplying arteries. To maintain the amount of perfusion to the brain within narrow limits there are two main compensatory responses: autoregulation, and increasing the extraction of oxygen out of blood.[3] Autoregulation is the hemodynamic reflex that varies the vascular resistance within the brain.[2,4] This is possible within seconds through transitory dilatation and constriction of the small artery and arterioles walls by varying the tone of the smooth muscles.[5,6] The second compensatory response is the increase in oxygen extraction fraction. When both mechanisms are exhausted and there is a further perfusion pressure drop, adequate cell metabolism cannot be maintained and permanent cell tissue damage occurs.

Ischemic stroke

Stroke is the rapid development of brain function loss due to a disturbance in the blood supply to the brain. Previously known as cerebrovascular accident, stroke is the second cause of long-term disability and death in high-income countries.[7] The symptoms may be transient, lasting seconds to minutes, or persist for a longer period of time. Stroke can be hemorrhagic or ischemic due to hypoperfusion or a blockage in one of the brain feeding arteries.[8] Approximately 20% of strokes are hemorrhagic, and 80% ischemic caused by a lack of blood supply.

Classification of the underlying pathophysiology of a stroke is critical as the short and long-term treatments are different. Hemorrhagic stroke treatment is based on identifying the underlying cause of hemorrhage and, if required, reducing

the extent of brain damage through timely intra-cranial pressure relief. Ischemic stroke treatment is aimed at removing the blockage. This can be done either pharmaceutically with thrombolytic agents or directly by removing the occluding thrombus mechanically. Neurological symptoms and signs can help determine the location of the process in the brain. They do not however accurately reflect the stroke subtype. Non-contrast computer tomography (CT) or magnetic resonance imaging (MRI) is therefore used in clinical practice to differentiate between hemorrhagic and ischemic stroke. Imaging of the brain perfusion can help depict brain tissue with reduced cerebral blood flow and identify tissue that has not yet been permanently damaged.[9] In patients that are seen after 3 hours of stroke onset this is of particular interest, as this combination of anatomical and perfusion imaging can be used to select patients with salvageable brain tissue that may still benefit from reperfusion therapy.[10,11]

A major risk factor for ischemic stroke is a stenosis, or narrowing, in one of the brain feeding arteries.[12,13] In approximately 25% of the patients presenting with stroke, a stenosis is found in one of the internal carotid arteries (ICA).[14,15] Although the pathophysiology of cerebral ischemia occurrence is not completely understood, there are two major processes that underlie the occurrence of stroke. First, the formation of thrombus at the atherosclerotic plaque resulting in thrombo-emboli; and second, hypoperfusion of the brain tissue due to lumen reduction and decreased perfusion in the more distal circulation.[16] As the risk for future ischemic stroke is high, treatment is important.[17,18] This consists of risk factor management, antiplatelet drug therapy and medical revascularization therapy. Revascularization is done by means of either surgical carotid endarterectomy treatment or carotid artery angioplasty with stent placement. The risk of developing fatal or nonfatal stroke when treated with only antiplatelet drug therapy is 26%.[19] From the results of three high-quality prospective randomized trials it has become apparent that a stenosis larger than 60% to 70% leads to a significant incidence of stroke.[19-21] This risk is lowered to 9% when combined with a surgical carotid endarterectomy. The effectiveness for patients who have a stenosis ≤ 60% is unclear and surgical treatment is therefore not recommended. Observational studies suggest strongly however that the risk of ischemic stroke is higher in patients with impaired cerebral perfusion in the hemisphere ipsilateral to a symptomatic or asymptomatic carotid stenosis than in those with normal perfusion.[12,13] Cerebral perfusion imaging has therefore been proposed as a method to select those patients at high risk for future stroke that may benefit from revascularization.[22]

Patients with a complete occlusion of one of the ICAs are at even greater risk for future stroke. The annual risk of stroke is approximately 5 - 6% and in those with compromised cerebral perfusion and poor collateral blood flow raised to 9 - 18% per year.[23-26] Surgical treatment has been largely abandoned in clinical practice as a large, international randomized trial showed in 1985 that extracranial to intracranial

(EC/IC) bypass surgery does not prevent stroke in patients with symptomatic ICA occlusion.[27] Studies suggest however that EC/IC bypass surgery may be effective in a subgroup of patients with severely impaired cerebral perfusion.[28,29]

Imaging of cerebral perfusion

From the first method of measuring global brain perfusion in 1948 with nitrous oxide, to the development of the first cross-sectional imaging method in the 1980s with positron emission tomography (PET) in the human brain, there have been vast improvements in imaging brain perfusion.[30,31] In current clinical practice the most commonly used techniques are bolus passage computed tomography (CT) and gadolinium based dynamic susceptibility contrast (DSC) magnetic resonance imaging (MRI).[32] Both modalities use a contrast agent as a tracer to image the blood flow through the brain. There are however concerns regarding detrimental effects of ionizing radiation leading to cancer and the use of contrast agents in patients with poor renal function. The iodine based contrast agents used in CT perfusion imaging can lead to nephropathy and gadolinium based contrast agents used in DSC MR perfusion imaging have been reported to induce nephrogenic systemic fibrosis.[33,34]

Arterial spin labeling (ASL) is an alternative non-invasive MR technique that was first introduced in 1992 by Williams and Detre for visualizing brain perfusion and quantifying cerebral blood flow.[35,36] ASL-MRI uses arterial blood as endogenous contrast agent by magnetically labeling the inflowing blood with radiofrequency pulses. It therefore does not require injection of contrast agents. After the initial radiofrequency labeling there is delay to allow the labeled arterial water protons to flow through the arterial vascular tree and into the brain parenchyma. The experiment is then repeated without labeling the arterial blood to acquire a control image. Perfusion contrast is given by the difference in magnetization between the labeled and unlabeled control image induced by the exchange of magnetization at brain tissue level.

There are several different ASL-MRI approaches that vary mainly based on the labeling technique. Two main labeling strategies can be distinguished. Pulsed ASL-MRI, where the blood with the labeling volume is instantly inverted.[37-39] And continuous ASL, where blood flowing through a specific plain is inverted continuously.[35,40] In clinical studies ASL has been used to assess perfusion in neurodegenerative diseases, epilepsy, central nervous system neoplasm's and vascular malformations.[41] A difficulty with ASL-MRI however is that in patients with cerebrovascular disease the quantification of cerebral blood flow is hampered by the recruitment of additional blood flow through collateral pathways.[42] These alternative pathways of blood flow lead to a delayed arrival of the labeled blood bolus to the brain tissue.[43-45] Because most ASL-MRI techniques acquire the perfusion weighted images at a fixed time point after the initial labeling of arterial blood, it is possible that the magnetic label may not have reached the imaging plane, leading to an underestimation of CBF. By

acquiring a series of perfusion weighted images at increasing delay times after the initial labeling, it is possible to compensate for such blood transit delays without prior knowledge of the transit times.

Cerebral autoregulation

Cerebral autoregulation is the compensatory ability of the brain to sustain blood flow when there are fluctuations in the cerebral perfusion pressure. Decreased cerebral autoregulatory capacity is an early predictor of hemodynamic impairment and is associated with increased risk for developing ischemic stroke.[12,46-49] Measurements can be used to predict the risk of brain tissue ischemia and stratify patients for treatment. This is comparable to the cardiac stress test which is widely used to assess heart disease, such as the clinical significance of a coronary artery stenosis.

The brain's autoregulatory capacity can be assessed indirectly by measuring the dilatory response to a vascular challenge that dilates the cerebral vessels. It can be measured either at brain tissue level with techniques such as $H_2{}^{15}O$ PET and single photon emission tomography, or by measuring the increase in flow-velocity in the middle cerebral artery with transcranial Doppler (TCD).[24,25,50] Both approaches have limitations. Measurements of flow-velocity are rough estimates and are insensitive to recruitment through collateral pathways (such as leptomeningeal collaterals at the brain surface) and shifts in the perfusion-territories of the brain feeding arteries.[42,51] And imaging of cerebral hemodynamic status with $H_2{}^{15}O$ PET requires a cyclotron in the near vicinity and is therefore only available to a few institutions. As clinical MRI scanners are widely available, combining ASL perfusion imaging with a vasodilatory challenge may potentially be a rapid and assessable way to evaluate the cerebral autoregulatory capacity without ionizing radiation and without repeated administration of contrast agents.

Outline of this Thesis

The overall aim of this thesis was to explore imaging of cerebral blood flow and cerebral autoregulatory status of the brain in patients with acute and chronic cerebrovascular disease by means of arterial spin labeling perfusion MRI.

This thesis consists of three parts:
The first part focuses on the application of ASL techniques to assess brain perfusion and detect areas with reduced blood flow in patients with acute stroke and symptomatic large-vessel disease. In *chapter 2,* ASL perfusion imaging in patients with acute stroke is compared to gadolinium based DSC perfusion imaging. In *chapter 3*, an ASL technique that acquires a series of perfusion weighted images at increasing delay times after the initial labeling is compared with dynamic $H_2{}^{15}O$ PET. *Chapter 4* focuses on applying this same ASL technique with acquisitions at a series of delay times for the assessment of the effect of a symptomatic ICA stenosis on ASL timing parameters, and evaluating the effect of collateral flow through the circle of Willis. And in *chapter 5*, ASL at multiple delay times is utilized to assess the effect of an ICA occlusion and collateral blood flow on regional timing parameters.

The second part focuses on assessing the cerebral autoregulatory status by combining ASL perfusion imaging with a vascular challenge. In *chapter 6,* the cerebral autoregulatory status of the brain tissue supplied by the individual brain feeding arteries in patients with ICA stenosis is investigated with quantitative and selective ASL perfusion imaging. *Chapter 7* investigates the effect of a symptomatic ICA occlusion upon the cerebral autoregulatory status and whether the cerebrovascular reactivity varies within the perfusion-territories of the brain feeding arteries. And finally, in *chapter 8* the effect of steno-occlusive large vessel disease and small vessel white matter damage upon CBF and the autoregulatory status of the white matter are investigated.

A general discussion and summary of this thesis is presented in part three, *chapter 9 and 10.*

References

1. Brust JC. Cerebral circulatino: Stroke. In: Kandel ER, Schwartz JH, Jessell TM. Principles of neural science 1991:1041-1049.
2. Lassen NA. Cerebral blood flow and oxygen consumption in man. Physiol Rev 1959;39:183-238.
3. Derdeyn CP, Videen TO, Yundt KD, et al. Variability of cerebral blood volume and oxygen extraction: stages of cerebral haemodynamic impairment revisited. Brain 2002;125:595-607.
4. Aaslid R, Lindegaard KF, Sorteberg W, et al. Cerebral autoregulation dynamics in humans. Stroke 1989;20:45-52.
5. Rapela CE, Green HA. Autoregulation of canine cerebral blood flow. Circ Res 1964;15:205-211.
6. MacKenzie ET, Farrar JK, Fitch W, et al. Effects of hemorrhagic hypotension on the cerebral circulation. I. Cerebral blood flow and pial arteriolar caliber. Stroke 1979;10:711-718.
7. Roger VL, Go AS, Lloyd-Jones DM, et al. Heart disease and stroke statistics--2011 update: a report from the American Heart Association. Circulation 2011;123:e18-e209.
8. Caplan LR, Hennerici M. Impaired clearance of emboli (washout) is an important link between hypoperfusion, embolism, and ischemic stroke. Arch Neurol 1999;55:1475-1482.
9. Latchaw RE, Alberts MJ, Lev MH, et al. Recommendations for imaging of acute ischemic stroke: a scientific statement from the American Heart Association. Stroke 2009;40:3646-3678.
10. Kidwell CS, Alger JR, Saver JL. Evolving paradigms in neuroimaging of the ischemic penumbra. Stroke 2004;35:2662-2665.
11. Heiss WD, Thiel A, Grond M, et al. Which targets are relevant for therapy of acute ischemic stroke? Stroke 1999;30:1486-1489.
12. Markus H, Cullinane M. Severely impaired cerebrovascular reactivity predicts stroke and TIA risk in patients with carotid artery stenosis and occlusion. Brain 2001;124:457-467.
13. Blaser T, Hofmann K, Buerger T, et al. Risk of stroke, transient ischemic attack, and vessel occlusion before endarterectomy in patients with symptomatic severe carotid stenosis. Stroke 2002;33:1057-1062.
14. Bogousslavsky J, Hachinski VC, Boughner DR, et al. Cardiac and arterial lesions in carotid transient ischemic attacks. Arch Neurol 1986;43:223-228.
15. Markus HS, MacKinnon A. Asymptomatic embolization detected by Doppler ultrasound predicts stroke risk in symptomatic carotid artery stenosis. Stroke 2005;36:971-975.
16. Fox AJ, Eliasziw M, Rothwell PM, et al. Identification, prognosis, and management of patients with carotid artery near occlusion. AJNR Am J Neuroradiol 2005;26:2086-2094.
17. The European Carotid Surgery Trialists Collaborative Group. Randomised trial of endarterectomy for recently symptomatic carotid stenosis: final results of the MRC European Carotid Surgery Trial (ECST). Lancet 1998;351:1379-1387.
18. Barnett HJ, Taylor DW, Eliasziw M, et al. Benefit of carotid endarterectomy in patients with symptomatic moderate or severe stenosis. North American Symptomatic Carotid Endarterectomy Trial Collaborators. N Engl J Med 1998;339:1415-1425.
19. North American Symptomatic Carotid Endarterectomy Trial Collaborators. Beneficial effect of carotid endarterectomy in symptomatic patients with high-grade carotid stenosis. N Engl J Med 1991;325:445-453.
20. Mayberg MR, Wilson SE, Yatsu F, et al. Carotid endarterectomy and prevention of cerebral ischemia in symptomatic carotid stenosis. JAMA 1991;266:3289-3294.
21. European Carotid Surgery Trialists' Collaborative Group. MRC European Carotid Surgery Trial: interim results for symptomatic patients with severe (70-99%) or with mild (0-29%) carotid stenosis. Lancet 1991;337:1235-1243.
22. Barnett HJ, Meldrum HE. Endarterectomy for carotid stenosis: new approaches in patient selection. Cerebrovasc Dis 2001;11:105-111.

23. Klijn CJ, Kappelle LJ, Algra A, et al. Outcome in patients with symptomatic occlusion of the internal carotid artery or intracranial arterial lesions: a meta-analysis of the role of baseline characteristics and type of antithrombotic treatment. Cerebrovasc Dis 2001;12:228-234.
24. Vernieri F, Pasqualetti P, Passarelli F, et al. Outcome of carotid artery occlusion is predicted by cerebrovascular reactivity. Stroke 1999;30:593-598.
25. Grubb RL, Jr., Derdeyn CP, Fritsch SM, et al. Importance of hemodynamic factors in the prognosis of symptomatic carotid occlusion. JAMA 1998;280:1055-1060.
26. Klijn CJ, Kappelle LJ, van Huffelen AC, et al. Recurrent ischemia in symptomatic carotid occlusion: prognostic value of hemodynamic factors. Neurology 2000;55:1806-1812.
27. The EC/IC bypass study group. Failure of extracranial-intracranial arterial bypass to reduce the risk of ischemic stroke. Results of an international randomized trial. N Engl J Med 1985;313:1191-1200.
28. Adams HP, Jr. Occlusion of the internal carotid artery: reopening a closed door? JAMA 1998;280:1093-1094.
29. Derdeyn CP, Grubb RL, Powers WJ. Cerebral hemodynamic impairment: methods of measurement and association with stroke risk. Neurology 1999;53:251-259.
30. Kety SS, Schmidt CF. The nitrous oxide method for the quantitative determination of cerebral blood flow in man; theory, procedure and normal values. J Clin Invest 1948;27:476-483.
31. Phelps ME, Hoffman EJ, Mullani NA, et al. Application of annihilation coincidence detection to transaxial reconstruction tomography. J Nucl Med 1975;16:210-224.
32. Wintermark M, Sesay M, Barbier E, et al. Comparative overview of brain perfusion imaging techniques. Stroke 2005;36:e83-e99.
33. Penfield JG, Reilly RF, Jr. What nephrologists need to know about gadolinium. Nat Clin Pract Nephrol 2007;3:654-668.
34. Sadowski EA, Bennett LK, Chan MR, et al. Nephrogenic systemic fibrosis: risk factors and incidence estimation. Radiology 2007;243:148-157.
35. Williams DS, Detre JA, Leigh JS, et al. Magnetic resonance imaging of perfusion using spin inversion of arterial water [published erratum appears in Proc Natl Acad Sci U S A 1992;89:4220]. Proc Natl Acad Sci U S A 1992;89:212-216.
36. Detre JA, Leigh JS, Williams DS, et al. Perfusion imaging. Magn Reson Med 1992;23:37-45.
37. Edelman RR, Siewert B, Darby DG, et al. Qualitative mapping of cerebral blood flow and functional localization with echo-planar MR imaging and signal targeting with alternating radio frequency. Radiology 1994;192:513-520.
38. Kim SG. Quantification of relative cerebral blood flow change by flow- sensitive alternating inversion recovery (FAIR) technique: application to functional mapping. Magn Reson Med 1995;34:293-301.
39. Wong EC, Buxton RB, Frank LR. Quantitative imaging of perfusion using a single subtraction (QUIPSS and QUIPSS II). Magn Reson Med 1998;39:702-708.
40. Sardashti M, Schwartzberg DG, Stomp GP, et al. Spin-labeling angiography of the carotids by presaturation and simplified adiabatic inversion. Magn Reson Med 1990;15:192-200.
41. Wolf RL, Detre JA. Clinical neuroimaging using arterial spin-labeled perfusion magnetic resonance imaging. Neurotherapeutics 2007;4:346-359.
42. Liebeskind DS. Collateral Circulation. Stroke 2003;34:2279-2284.
43. Calamante F, Williams SR, van Bruggen N, et al. A model for quantification of perfusion in pulsed labelling techniques. NMR Biomed 1996;9:79-83.
44. Alsop DC, Detre JA. Reduced transit-time sensitivity in noninvasive magnetic resonance imaging of human cerebral blood flow. J Cereb Blood Flow Metab 1996;16:1236-1249.
45. Gibbs JM, Wise RJ, Leenders KL, et al. Evaluation of cerebral perfusion reserve in patients with carotid-artery occlusion. Lancet 1984;1:310-314.

46. Silvestrini M, Vernieri F, Pasqualetti P, et al. Impaired cerebral vasoreactivity and risk of stroke in patients with asymptomatic carotid artery stenosis. JAMA 2000;283:2122-2127.
47. Powers WJ. Cerebral hemodynamics in ischemic cerebrovascular disease. Ann Neurol 1991;29:231-240.
48. Yonas H, Smith HA, Durham SR, et al. Increased stroke risk predicted by compromised cerebral blood flow reactivity. J Neurosurg 1993;79:483-489.
49. Gur AY, Bova I, Bornstein NM. Is impaired cerebral vasoreactivity a predictive factor of stroke in asymptomatic patients. Stroke 1996;27:2188-2190.
50. Hirano T, Minematsu K, Hasegawa Y, et al. Acetazolamide reactivity on 123I-IMP single photon emission computed tomography in patients with major cerebral artery occlusive disease: correlation with positron emission tomography parameters. J Cereb Blood Flow Metab 1994;14:763-770.
51. van Laar PJ, Hendrikse J, Klijn CJ, et al. Symptomatic carotid artery occlusion: flow territories of major brain-feeding arteries. Radiology 2007;242:526-534.

PART 1
Arterial spin labeling perfusion imaging

CHAPTER 2

Reinoud P.H. Bokkers
Daymara A. Hernandez
José G. Merino
Raymond V. Mirasol
Matthias J.P. van Osch
Jeroen Hendrikse
Steven Warach
Lawrence L. Latour

ARTERIAL SPIN LABELING PERFUSION IMAGING IN PATIENTS WITH ACUTE STROKE

Background and purpose: Perfusion MRI can be used to identify patients with acute ischemic stroke that may benefit from reperfusion therapies. The risk of nephrogenic systemic fibrosis, however, limits the use of contrast agents. Our objective was to evaluate the ability of arterial spin labeling (ASL), an alternative non-invasive perfusion technique, to detect perfusion deficits compared with dynamic susceptibility contrast (DSC) perfusion imaging.

Methods: Consecutive patients referred for emergency assessment of suspected acute stroke within a seven-month period were imaged with both ASL and DSC perfusion MRI. Images were interpreted in a random order by two experts blinded to clinical information for image quality, presence of perfusion deficits and diffusion-perfusion mismatches.

Results: 156 patients were scanned with a median time of 5.6 (3.0–17.7) hours from last seen normal. Stroke diagnosis was clinically confirmed in 78 patients. ASL and DSC imaging were available in 64 of these patients. A perfusion deficit was detected with DSC in 39 of these patients; ASL detected 32 of these index perfusion deficits, missing 7 lesions. The median volume of the perfusion deficits as determined with DSC was smaller in patients which were evaluated as normal with ASL than in those with a deficit (median, interquartile range; 56 (10–116) vs. 114 (41–225) ml, p=0.01).

Conclusion: ASL can depict large perfusion deficits and perfusion-diffusion mismatches in correspondence with DSC. Our findings show that a fast 2½ minute ASL perfusion scan may be adequate for screening acute stroke patients with contraindications to gadolinium-based contrast agents.

Introduction

Magnetic resonance imaging (MRI) can be used to identify ischemic brain tissue and evaluate the amount of tissue at risk for infarction in patients presenting with stroke-like symptoms.[1] Perfusion imaging identifies brain tissue that has reduced blood flow, the potential target for reperfusion therapies. In patients who present to the emergency room beyond the standard time window for intravenous tissue plasminogen activator (IV-tPA) MRI has been postulated as a tool to identify individuals with salvageable brain tissue by detecting whether or not hypoperfused tissue has developed irreversible ischemic injury.[2-4]

Perfusion is assessed in routine clinical practice with dynamic susceptibility contrast (DSC) imaging. In DSC-MRI a gadolinium contrast agent is injected and a time series of fast T_2^* weighted images is acquired. The use of gadolinium-based contrast agents is however limited because of the risk of inducing nephrogenic systemic fibrosis (NSF) in patients with poor renal function. Gadolinium is therefore contraindicated in patients with an estimated glomerular filtration rate (GFR) < 30 mL/min and in those on hemodialysis.[5-7] Arterial spin labeling (ASL) is an alternative non-invasive MR technique for visualizing perfusion and quantifying cerebral blood flow. It uses blood as an endogenous contrast agent by magnetically labeling it with radiofrequency pulses and does not require gadolinium-based contrast agents. The perfusion contrast is given by the difference in magnetization induced by the exchange of these labeled spins at brain tissue level and a non-labeled control image.[8-10]

Previous studies have shown that ASL can detect perfusion deficits in patients with acute and subacute stroke.[11-13] The aims of our study were to test the feasibility of using ASL in the clinical setting for evaluating hyperacute stroke patients and to evaluate the ability of ASL to detect perfusion deficits and perfusion-diffusion mismatch of varying volumes compared with DSC perfusion imaging.

Methods

This prospective study was conducted in compliance with human subjects protection requirements.

Subjects

All patients who had an acute MRI for the assessment of suspected ischemic stroke at the Washington Hospital Center in Washington D.C. over a seven-month period were considered. At this hospital MRI is the initial imaging modality for the evaluation of acute stroke. Patients with a suspected stroke who were 18 years of age or older were included and patients who had a contraindication to MRI or were pregnant were excluded. A vascular neurologist or stroke fellow evaluated all

patients and scored the National Institutes of Health Stroke Scale (NIHSS). Patients who met standard eligibility criteria and were within 4.5 hours of symptom onset were treated with IV-tPA.[14]

MR imaging

Imaging was performed on a clinical 3 Tesla MRI scanner (Achieva, Philips Medical Systems, Best, The Netherlands) equipped with an eight-channel coil and locally developed software to enable ASL perfusion imaging. The imaging protocol was the standard imaging protocol used to screen all stroke patients was part of a quality improvement study. It included diffusion-weighted imaging (DWI), T_2weighted fluid attenuation inversion recovery (FLAIR) imaging, DSC and ASL perfusion-weighted imaging. DSC images were not acquired in patients with a GFR less than 30 mL/min in accordance with published guidelines due to the increased risk of developing nephrogenic systemic fibrosis.[15]

The DSC perfusion-weighted images were acquired with the vendor's standard commercially available gradient echo sequence. A single dose of 0.1 mmol/kg of gadolinium (gadolinium-DTPA, Magnevist, Bayer Schering Pharma, Germany) was administered at 5 ml/sec. The scan parameters were: repetition time (TR), 1000 ms; echo time (TE), 25 ms; field-of-view (FOV), 256 x 256 mm; 20 slices of 7 mm; scan time 1.43 minutes. ASL perfusion-weighted images were acquired using a pseudo-continuous labeling technique according to a previously published protocol.[16] In short, arterial spin labeling was performed by employing a train of 18 degrees, 0.5 ms, Hanning shaped RF pulses at an interval of 1 ms, for a duration of 1650 ms, with a balanced gradient scheme.[17,18] The control images were acquired by adding 180º to the phase of all even RF pulses. After a 1525 ms delay, twenty slices were acquired in ascending fashion with an in-plane resolution of 3 x 3 mm^2 with single shot echo planar imaging in combination with background suppression and parallel imaging (SENSE factor 2.5). Background suppression consisting of a saturation pulse immediately before labeling and inversion pulses at 1680 and 2830 ms after the saturation pulse.[19] The other ASL MRI parameters were: TR, 4000 ms; TE, 14 ms; pairs of control / label, 12; 20 slices with a 3 x 3 x 7 mm resolution; scan time, 2.5 minutes.

FLAIR and DWI images were acquired with the vendor's standard commercially available sequences. The FLAIR images were balanced (roughly) across field strength for conspicuity of chronic ischemic parenchyma, with the following parameters: TR/TE = 9000/120 m ; TI, 2600 ms; 40 slices with 1 x 1 x 4 mm resolution (SENSE factor, 1.75); scan time, 2.27 minutes. For DWI the parameters were: TR/TE = 4500/62.1 ms; 40 slices with 1 x 1 x 3.5 mm resolution (SENSE factor, 1.75); scan time 3.5 minutes.

Perfusion-weighted image analyses

DSC perfusion-weighted images were calculated from the acquired from series

of T_2^* weighted images with the vendor's standard available perfusion software (Advanced Brain Perfusion, Philips Healthcare, Cleveland, OH) on the MRI console. The time-to-peak (TTP) images were used for perfusion deficit analyses. ASL perfusion-weighted images were generated according to a previously published model that corrects for T_1 decay, T_2^* weighted and the different delay times of the imaging slices.[20] In patients with motion artefacts, in-plane motion was first corrected for by coregistering all dynamic pairs with SPM5 (Wellcome Trust Centre for Neuroimaging, Oxford, United Kingdom) using the normalized mutual information and a rigid body transformation.

Quantitative perfusion deficit and mismatch

The acute perfusion and diffusion ischemic volumes were measured from DWI and the DSC TTP series using a semi-automated quantitative method in Cheshire™ (Perceptive Informatics, Waltham, Massachusetts) by a core lab rater who has extensive experience and established rater reliability statistics.[21] Lesion areas were segmented on a slice-by-slice basis with user selected seed points followed by user-driven editing. DWI lesions were identified on affected hyperintense areas visible from the b = 1000 mm/s^2 trace or isotropic images. The rater was careful not to include bilateral artefacts, chronic lesions and if necessary reviewed apparent diffusion coefficient maps to isolate acute lesions. PWI lesions on the TTP maps were identified as hyperintense areas, excluding susceptibility artefacts adjacent to the paranasal sinuses. The volumes were automatically calculated by multiplying the total lesion area by the slice thickness.

Qualitative image evaluation

Unaware of the patient's identity, clinical information and diagnosis, two experienced readers (SW, JGM) reviewed the DSC and ASL perfusion-weighted images. The images were viewed independently in a random order. The readers also had access to the DWI and FLAIR images. They rated image quality, presence / absence of perfusion deficits, DWI lesions, perfusion-diffusion mismatch and significance of the mismatch. Image quality was scored as excellent, good, fair, poor and uninterpretable. When there was a discrepancy in the evaluation of a perfusion deficit between both readers, they looked at the images together and reached a consensus. The readers used commercially available software to view the images (MIPAV, NIH, Bethesda, Maryland, version 4.4.1) and were able to adjust for contrast, color scheme and size of the images.

Statistical analysis

To compare acute DWI ischemic lesion volume, acute perfusion lesion volume on TTP and diffusion-perfusion mismatch, logarithmic transformation was applied to correct for normality and comparison was performed with an independent t-test.

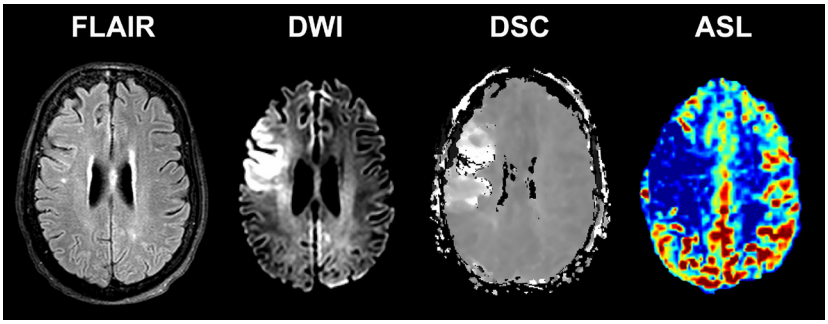

Figure 1. Transverse perfusion, diffusion and FLAIR images of a 66-year old woman presenting within 1 hour after symptom onset. Restricted diffusion and increased time-to-peak times can be appreciated in the flow territory of the right middle cerebral artery on the DWI and DSC images. The corresponding ASL image shows a corresponding decrease in perfusion. *For color figure see page 154.*

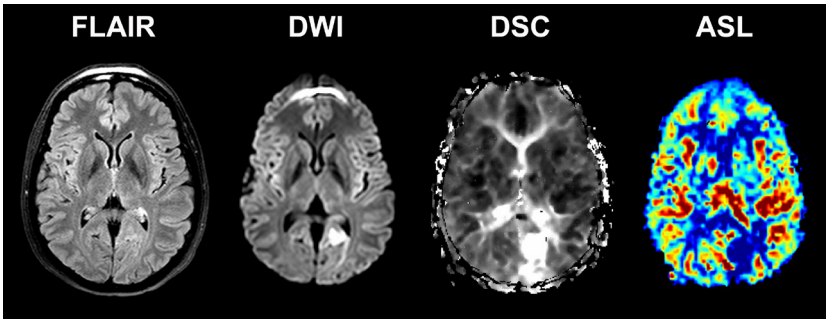

Figure 2. Transverse perfusion, diffusion and FLAIR images of a 48-year old woman presenting within 6 hours after symptom onset. Restricted diffusion and increased time-to-peak times can be appreciated in the flow territory of left posterior circulation on the DWI and DSC images. The corresponding ASL image shows a corresponding decrease in perfusion. *For color figure see page 154.*

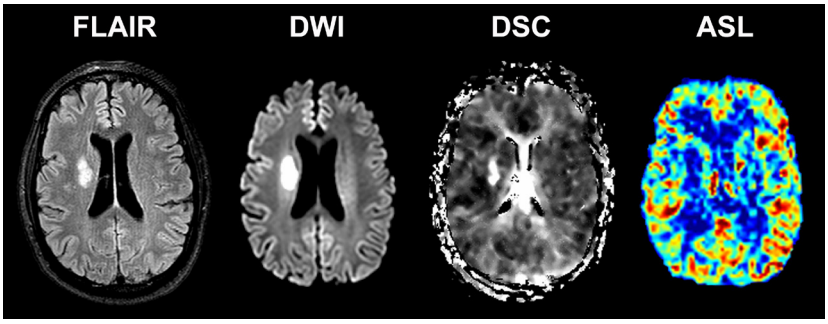

Figure 3. Transverse perfusion, diffusion and FLAIR images of a 53-year old male presenting within 10 hours after symptom onset. Restricted diffusion and increased time-to-peak times can be appreciated in the right basal ganglia on the DWI and DSC images. The perfusion deficit was however not depicted with ASL. *For color figure see page 154.*

Table 1. Agreement between the perfusion deficits depicted with ASL and DSC perfusion imaging.

	DSC *(n = 64)*	
ASL	***Yes***	***No***
Yes	32	4
No	7	21

Values are expressed as mean ± standard deviation (SD) or median (1st interquartile – 3rd interquartile) unless otherwise specified. A p-value < 0.05 was considered statistically significant. Inter-rater reliability analyses was performed using the Kappa statistic to determine consistency among raters.[22] Statistical analysis was performed using SPSS (SPSS Inc., Chicago, Illinois, USA, version 15.0.1) for Windows.

Results

One hundred fifty-six consecutive patients (83 women and 73 men, 62 ± 17 years) had an MRI as part of the initial evaluation of stroke at Washington Hospital Center between June 2009 and January 2010. The median time from symptom onset to imaging was 5.6 (3.0 – 17.7) hours. Of the 156 patients, 30 patients were excluded because they could not receive contrast due GFR less than 30 mL/min and 21 patients were excluded because of incomplete imaging data. A total of 105 patients underwent both ASL and DSC perfusion imaging. Of the 31 patients in whom DSC was contraindicated, 14 had a stroke.

The quality of the DSC and ASL images was variable. 95% of all DSC images were interpretable (100 of 105 patients): in 75 patients the DSC images were judged as good to excellent (71%), in 15 they were fair (14%), in 10 they were poor (10%), and in 5 they were uninterpretable (5%). 95% of all ASL images were interpretable (100 of 105 patients): in 76 patients the ASL images were judged as good to excellent (76%), in 17 they were fair (16%), in 9 they were poor (9%), and in 3 they were uninterpretable (3%).

Of the 105 patients with both ASL and DSC perfusion imaging, 64 (61%) had a clinically confirmed stroke. The median baseline NIHSS score was 6 (range, 0 - 33). The median time between symptom onset and imaging was 6.5 (3.0 – 23.2). Twenty-nine (45%) of the 64 patients with confirmed stroke received IV-tPA. In these patients the median time to imaging was 3.0 (1.7 – 4.0) hours.

Figure 1 and 2 illustrates two examples of ASL and DSC perfusion imaging in patients with acute stroke. A perfusion deficit was detected with DSC in 39 (61%) of the 64 patients with confirmed stroke (Table 1). ASL identified a perfusion deficit in 32 (82%) of the 39 patients with a deficit on DSC. In the seven stroke

Table 2. Agreement between the significant perfusion-diffusion mismatch depicted with ASL and DSC perfusion imaging.

	DSC *(n = 64)*	
ASL	***Yes***	***No***
Yes	18	6
No	2	38

patients with a deficit depicted on DSC but not on ASL; five of these patients had a cortical gray matter deficit and two a deficit in the basal ganglia (Figure 3). The ASL image quality was scored as poor to uninterpretable in four of the seven patients. Four of the 25 stroke patients who were classified as having normal perfusion by DSC were classified as having a perfusion deficit with ASL. The quality of the DSC images in 3 of these 4 patients was poor. A perfusion deficit was depicted in one of these four patients in the basal ganglia with ASL but not with DSC. The inter-rater agreement for detecting perfusion deficits with DSC and ASL perfusion imaging was, respectively, 0.64 and 0.6.

Table 2 lists how many patients were identified as having a significant perfusion-diffusion mismatch on ASL and DSC perfusion imaging. Twenty (31%) out of the 64 patients with a confirmed stroke had a significant mismatch on DSC, and out of these 18 (90%) were also determined to have a mismatch on ASL. The two patients that had a mismatch on DSC but not on ASL had cortical lesions; one had an uninterpretable ASL. In six (33%) out of the 18 patients the mismatch was categorized as significant with ASL, but not with DSC. The inter-rater agreement for detecting perfusion-diffusion mismatch with DSC and ASL perfusion imaging was 0.71 and 0.51, respectively.

It was not possible to measure the perfusion deficit volume in 7 (11%) of 64 patients with clinically confirmed stroke because the DSC images were too poor of quality. The median volume of the perfusion deficit on DSC for all stroke patients was 110 (35 – 215) ml. The median volume of the perfusion deficit (on DSC) in patients that did not have a defect present on ASL was 56 (10 – 116) ml. This was significantly smaller than the median volume of 114 (41 – 225) ml in patients that did have a defect on ASL, $p = 0.01$ t-test performed on log-transformation of volumes.

Discussion

This study demonstrates that fast evaluation of hyperacute stroke patients in a clinical setting is feasible with ASL perfusion imaging. Detection of large perfusion deficits and the presence of a perfusion-diffusion mismatch with ASL is comparable to that of DSC perfusion imaging. In the patients in whom a perfusion deficit was

detected with DSC but evaluated as normal with ASL, the perfusion deficit volume was smaller.

Our findings that perfusion deficits are detectable with ASL correspond with previous studies in small groups of pediatric and adult patients with both acute and subacute stroke.[23-25] Using a prototype single slice pulsed ASL sequence, Siewert et al showed that ASL could detect perfusion abnormalities in a group of 18 subacute stroke patients in comparison to gadolinium-enhanced DSC imaging.[26] With a more recent pulsed ASL scan that uses a FAIR alternating labeling scheme combined with a QUIPS2 bolus cut-off, Viallon et al showed similar results in a group of 41 acute stroke patients within two weeks of symptom onset.[27] Their results showed that ASL can identify territorial hypoperfusion in correspondence with DSC, however for lacunar infarctions, the spatial resolution of ASL was not sufficient to predict local perfusion deficits. This is in line with our findings that in those patients where ASL did not detect a perfusion deficit, the lesion volume was smaller.

There are important differences between both perfusion imaging techniques used in this study. The ASL perfusion-weighted images are based on cerebral blood flow and ischemic tissue is reflected by loss of signal. This is substantially different to DSC, where the measured mean transit times are predominantly used for lesion detection in stroke. This hemodynamic parameter reflects the transit time of the administered contrast bolus through the brain parenchyma. Ischemia will lead to increased transit times and a lesion is reflected by increased signal or hypointensity. When comparing both techniques this is an important difference, as the contrast-to-noise of the ASL perfusion-weighted maps is lower and ischemic lesions are less clearly delineated. Although our study shows correspondence, the ischemic lesions that were not detected with ASL were of smaller volume. By using an ASL technique with image acquisition at multiple delay times after the initial labeling, it is also possible to measure the arterial arrival times with ASL.[28] In a recent study of 15 patients with acute minor stroke and TIA, MacIntosh et al demonstrated that a whole-brain 3D-GRASE PASL sequence with prolonged arrival times values can be measured within the affected hemisphere.[29] With further research, this potentially may be a valuable additive to the currently acquired perfusion-weighted images, as small inconspicuous lesions, for instance in the basal ganglia, may be easier to detect.

Recent acute ischemic stroke imaging guidelines recommend MR imaging for detection of ischemic changes and to exclude potential intracerebral hemorrhage.[30] Currently, there is increasing evidence supporting that perfusion imaging may play an important role on the selection of patients beyond the strict three hour window that could benefit from thrombolysis treatment. In our study however, DSC imaging was not performed in 20% of the patients presenting with stroke-like symptoms due to increased risk of developing NSF. This significant amount of patients illustrates the importance of having an alternative non-invasive method for perfusion imaging. Since ASL uses radiofrequency pulses and does not require injection of gadolinium-

based contrast agents, it may potentially be a viable alternative for those patients with a poor GFR or on hemodialysis.

A potential limitation of our study may be that an ASL perfusion sequence was used that acquires the images after a fixed time point following the labeling. In patient with delayed inflow, for instance caused by collateralization, this may lead to an underestimation of cerebral perfusion. However, with the sequence the effective delay time from begin of labeling to the readout is 3 seconds and should allow appropriate inflow time. Also, further delay would have been an additional parameter of hemodynamic compromise.

Conclusion

ASL can depict large perfusion deficits and perfusion-diffusion mismatches in correspondence with DSC. Our findings show that a fast 2½ minute ASL perfusion scan may be adequate for screening patients with contraindications to gadolinium-based contrast agents.

References

1. Latchaw RE, Alberts MJ, Lev MH, et al. Recommendations for imaging of acute ischemic stroke: a scientific statement from the American Heart Association. Stroke 2009;40:3646-3678.
2. Warach S, Dashe JF, Edelman RR. Clinical outcome in ischemic stroke predicted by early diffusion-weighted and perfusion magnetic resonance imaging: a preliminary analysis. J Cereb Blood Flow Metab 1996;16 2005:37:53-59.
3. Heiss WD, Thiel A, Grond M, et al. Which targets are relevant for therapy of acute ischemic stroke? Stroke 1999;30:1486-1489.
4. Kidwell CS, Alger JR, Saver JL. Evolving paradigms in neuroimaging of the ischemic penumbra. Stroke 2004;35:2662-2665.
5. Penfield JG, Reilly RF, Jr. What nephrologists need to know about gadolinium. Nat Clin Pract Nephrol 2007;3:654-668.
6. Kuo PH, Kanal E, bu-Alfa AK, et al. Gadolinium-based MR contrast agents and nephrogenic systemic fibrosis. Radiology 2007;242:647-649.
7. Kanal E, Barkovich AJ, Bell C, et al. ACR guidance document for safe MR practices: 2007. AJR Am J Roentgenol 2007;188:1447-1474.
8. Williams DS, Detre JA, Leigh JS, et al. Magnetic resonance imaging of perfusion using spin inversion of arterial water [published erratum appears in Proc Natl Acad Sci U S A 1992 May 1;89 2005:37. (9):4220]. Proc Natl Acad Sci U S A 1992;89:212-216.
9. Detre JA, Leigh JS, Williams DS, et al. Perfusion imaging. Magn Reson Med 1992;23:37-45.
10. Edelman RR, Siewert B, Darby DG, et al. Qualitative mapping of cerebral blood flow and functional localization with echo-planar MR imaging and signal targeting with alternating radio frequency. Radiology 1994;192:513-520.
11. Chalela JA, Alsop DC, Gonzalez-Atavales JB, et al. Magnetic resonance perfusion imaging in acute ischemic stroke using continuous arterial spin labeling. Stroke 2000;31:680-687.
12. Chen J, Licht DJ, Smith SE, et al. Arterial spin labeling perfusion MRI in pediatric arterial ischemic stroke: initial experiences. J Magn Reson Imaging 2009;29:282-290.
13. MacIntosh BJ, Lindsay AC, Kylintireas I, et al. Multiple inflow pulsed arterial spin-labeling reveals delays in the arterial arrival time in minor stroke and transient ischemic attack. AJNR Am J Neuroradiol 2010;31:1892-1894.
14. Sacco RL, Adams R, Albers G, et al. Guidelines for prevention of stroke in patients with ischemic stroke or transient ischemic attack: a statement for healthcare professionals from the American Heart Association/American Stroke Association Council on Stroke: co-sponsored by the Council on Cardiovascular Radiology and Intervention: the American Academy of Neurology affirms the value of this guideline. Stroke 2006;37:577-617.
15. Perazella MA, Rodby RA. Gadolinium-induced nephrogenic systemic fibrosis in patients with kidney disease. Am J Med 2007;120:561-562.
16. Bokkers RP, van Osch MJ, van der Worp HB, et al. Symptomatic carotid artery stenosis: impairment of cerebral autoregulation measured at the brain tissue level with arterial spin-labeling MR imaging. Radiology 2010;256:201-208.
17. Garcia DM, de Bazelaire C, Alsop DC. Pseudo-continuous Flow Driven Adiabatic Inversion for Arterial Spin Labeling. Proceedings 13th Scientific Meeting, ISMRM; 2005:37.
18. Wu WC, Fernandez-Seara M, Detre JA, et al. A theoretical and experimental investigation of the tagging efficiency of pseudocontinuous arterial spin labeling. Magn Reson Med 2007;58:1020-1027.
19. Ye FQ, Frank JA, Weinberger DR, et al. Noise reduction in 3D perfusion imaging by attenuating the static signal in arterial spin tagging (ASSIST). Magn Reson Med 2000;44:92-100.

20. Alsop DC, Detre JA. Reduced transit-time sensitivity in noninvasive magnetic resonance imaging of human cerebral blood flow. J Cereb Blood Flow Metab 1996;16:1236-1249.
21. Luby M, Bykowski JL, Schellinger PD, et al. Intra- and interrater reliability of ischemic lesion volume measurements on diffusion-weighted, mean transit time and fluid-attenuated inversion recovery MRI. Stroke 2006;37:2951-2956.
22. Landis JR, Koch GG. The measurement of observer agreement for categorical data. Biometrics 1977;33:159-174.
23. Chalela JA, Alsop DC, Gonzalez-Atavales JB, et al. Magnetic resonance perfusion imaging in acute ischemic stroke using continuous arterial spin labeling. Stroke 2000;31:680-687.
24. Chen J, Licht DJ, Smith SE, et al. Arterial spin labeling perfusion MRI in pediatric arterial ischemic stroke: initial experiences. J Magn Reson Imaging 2009;29:282-290.
25. Siewert B, Schlaug G, Edelman RR, et al. Comparison of EPISTAR and T2*-weighted gadolinium-enhanced perfusion imaging in patients with acute cerebral ischemia. Neurology 1997;48:673-679.
26. Viallon M, Altrichter S, Pereira VM, et al. Combined use of pulsed arterial spin-labeling and susceptibility-weighted imaging in stroke at 3T. Eur Neurol 2010;64:286-296.
27. Golay X, Hendrikse J, Lim TC. Perfusion imaging using arterial spin labeling. Top Magn Reson Imaging 2004;15:10-27.
28. MacIntosh BJ, Lindsay AC, Kylintireas I, et al. Multiple inflow pulsed arterial spin-labeling reveals delays in the arterial arrival time in minor stroke and transient ischemic attack. AJNR Am J Neuroradiol 2010;31:1892-1894.
29. Latchaw RE, Alberts MJ, Lev MH, et al. Recommendations for imaging of acute ischemic stroke: a scientific statement from the American Heart Association. Stroke 2009;40:3646-3678.

CHAPTER 3

Reinoud P.H. Bokkers
Jochem P. Bremmer
Bart N.M. van Berckel
Adriaan A. Lammertsma
Jeroen Hendrikse
Josien P.W. Pluim
L. Jaap Kappelle
Ronald Boellaard
Catharina J.M. Klijn

ARTERIAL SPIN LABELING PERFUSION IMAGING AT MULTIPLE DELAY TIMES COMPARED WITH POSITRON EMISSION TOMOGRAPHY IN PATIENTS WITH A CAROTID ARTERY OCCLUSION

Background and purpose: Arterial spin labeling (ASL) perfusion MRI with image acquisition at multiple inversion times is a non-invasive ASL technique able to compensate for spatial heterogeneities in transit times caused by collateral blood flow in patients with severe stenosis of the cerebropetal blood vessels. Our aim was to compare ASL-MRI and $H_2{}^{15}O$ PET, the gold standard for cerebral blood flow (CBF) assessment, in patients with a symptomatic internal carotid artery (ICA) occlusion.

Methods: Fourteen patients (9 men and 5 women; mean age, 63±14 years) with a symptomatic ICA occlusion underwent both ASL-MRI and $H_2{}^{15}O$ PET. ASL-MRI was performed using a pulsed STAR labeling technique at multiple inversion times within 7 days of the PET. CBF was measured in the gray-matter of the anterior, middle and posterior cerebral artery, and white-matter.

Results: Both PET and ASL-MRI showed a significantly decreased CBF in the gray-matter of the middle cerebral artery in the hemisphere ipsilateral to the ICA occlusion. The average gray-matter CBF measured with ASL-MRI (71.8±4.3 mL/min/100g) was higher ($p<0.01$) than measured with $H_2{}^{15}O$ PET (43.1±1.0 mL/min/100g).

Conclusion: ASL-MRI at multiple inversion times is capable of depicting the presence and extent of regions with hypoperfusion in patients with an occlusion of the ICA, although a systematic overestimation of CBF relative to $H_2{}^{15}O$ PET was noted.

J Cereb Blood Flow Metab. 2010;30(1):222-229

Introduction

Patients with ischemic stroke or transient ischemic attacks (TIAs) and an occlusion of the internal carotid artery (ICA) have a 5 to 6% risk of developing stroke per year.[1] In those with compromised cerebral blood flow (CBF) this risk is even higher, approximately 9 – 18% per year.[2-4] For therapeutic decisions it is therefore important to be able to identify patients with hemodynamic compromise who are at high risk of recurrent ischemic stroke. Numerous techniques have been developed that are capable of assessing CBF *in-vivo*, such as positron emission tomography (PET), computed tomography (CT) perfusion, dynamic susceptibility contrast magnetic resonance imaging (MRI) and single photon emission tomography (SPECT). In clinical practice, bolus passage CT perfusion and gadolinium based MR perfusion imaging are the most widely used,[5] since PET facilities are limited. Because of the current concerns regarding the use of ionizing radiation and morbidity after contrast enhanced studies in patients with renal insufficiency,[6,7] a non-invasive alternative for *in-vivo* assessment of CBF would be of great benefit.

Arterial spin labeling (ASL) is a MRI technique that can non-invasively assess CBF by magnetically labeling the arterial water spins with a radiofrequency pulse.[8-11] In clinical studies it has been used to assess perfusion in neurodegenerative diseases, epilepsy, central nervous system neoplasms and vascular malformations.[12] However, a disadvantage of ASL-MRI is that in patients with cerebrovascular disease the quantification of cerebral blood flow is hampered by the recruitment of additional blood flow through collateral pathways.[13] These alternative pathways of blood flow lead to a delayed arrival of the labeled blood bolus to the brain.[14-16] Because most ASL-MRI techniques acquire the labeled images at a fixed time after the initial labeling of arterial blood, it is possible that the magnetic label may not have reached the imaging plane, leading to underestimation of CBF. Recently, ASL-MRI with acquisition of a series of images at increasing delay times after the initial labeling has been introduced as a method to compensate for such blood transit delays. Although researchers have previously compared the results of ASL-MRI to established perfusion imaging techniques,[17-19] no such verification has been done with ASL-MRI at multiple delay times.

The purpose of this study was to evaluate the accuracy of CBF measurements with ASL-MRI at multiple delay times in patients with a symptomatic carotid occlusion by comparing these to CBF measurements acquired with dynamic $H_2{}^{15}O$ PET measurements. We compared quantitative values of CBF in mL/min/100g tissue and qualitative CBF estimates, expressed as an ipsilateral to contralateral ratio, for different brain regions.

Methods

The institutional ethical standards committee approved the study protocol and written informed consent was obtained from all participants.

Study population

Fourteen patients (9 men and 5 women; mean ± standard deviation (SD) age, 63 ± 14 years) with a symptomatic ICA occlusion were examined with both ASL-MRI and $H_2{}^{15}O$ PET within a timeframe of seven days. All patients had transient or minor-disabling neurological deficits (modified Rankin score of 0, 1 or 2) in the supply territory of the occluded ICA within three months prior to inclusion.[20] Of the fourteen patients, one patient had symptoms within the last two weeks prior to inclusion, four patients within one month, seven within two months and two patients within three months. Occlusion of the ICA was confirmed with intra-arterial digital subtraction angiography and the stenosis grade of the contralateral asymptomatic ICA was assessed in accordance to the North American Symptomatic Carotid Endarterectomy Trial criteria.[21]

PET imaging

PET investigations were performed on an ECAT EXACT HR+ scanner (CTI/Siemens, Knoxville, Tennessee). The characteristics of this scanner have been previously described elsewhere.[22] All subjects were scanned under standard conditions: dimmed lights and music off. All scans were corrected for photon attenuation and scatter using a 10 minute transmission scan. Each study consisted of a $H_2{}^{15}O$ PET scan. To measure CBF a bolus of 1100 MBq $H_2{}^{15}O$ (bolus injection of ~5 s) was administered intravenously, while simultaneously starting a 3D emission scan (25 frames over a period of 600s). All scans were reconstructed using FORE+2D FBP reconstruction with a Hanning filter at Nyquist frequency. A matrix size of 256 x 256 and a zoom of 2.1 was applied resulting in voxel sizes of 1.2 x 1.2 x 2.4 mm^3 and the final image resolution equalled about 7 mm FWHM. For all scans the arterial input function was measured using an online continuous blood sampling device.[23] Three manual arterial blood samples, at 5.5, 8 and 10 minutes were taken for calibration purposes. Parametric CBF images were generated using a basis function implementation of the cerebral blood flow model including corrections for dispersion, delay and arterial blood volume, as described previously.[24]

MR imaging

ASL-MRI scans were performed on a clinical 3 Tesla MRI scanner (Achieva, Philips Medical Systems, Best, the Netherlands) within seven days of the PET examination. A quadrature head coil was used for radiofrequency transmission and signal reception. Anatomical MR images were acquired using a 3D T_1 weighted fast-field-

echo and a T_2weighted fluid-attenuated inversion-recovery (FLAIR) sequence with the following parameters: repetition time (TR), 18 (T_1) and 11000 (FLAIR) ms; echo time (TE), 2.1 (T_1) and 125 (FLAIR) ms; inversion time FLAIR, 2800 ms; matrix size, 240 x 240 with 64 (T_1) and 24 (FLAIR) slices; slice thickness, 2 mm; field-of-view (FOV), 240 x 240 mm.

A pulsed STAR labeling technique with a Look-Locker-like readout strategy at multiple delay times was used for ASL-MR perfusion imaging.[25,26] For image acquisition a series of thirteen 35° excitation pulses were applied, with increasing delay times from 200 to 2600 ms with a constant interval of 200 ms, followed by single shot gradient echo-planar-imaging readout. The perfusion imaging slice was planned just above the ventricles through the semioval centre and aligned parallel to the orbitomeatal angle. A 140 mm thick labeling slab was set eight millimeters below the imaging slice. Perfusion images were obtained by subtracting the control images from the labeled images. Other parameters for MR perfusion imaging were: TR/TE, 4000/23 ms; 62% partial Fourier acquisition; SENSE factor, 2.5; averages, 50; matrix, 64 x 64; FOV, 240 × 240 mm; slice-thickness, 7 mm; scan time, 5 min.

Analysis of the acquired images was performed with custom software written in IDL, version 6.0 (Research Systems Inc., Boulder, CO, USA). CBF was quantified using the perfusion model of Buxton et al,[27] with the adaptations as proposed by Gunther et al.[28] The equilibrium magnetization $M_{0,a}$ of the arterial blood was estimated by fitting the unlabeled signal in the brain tissue to a saturation-recovery curve. The CBF was calculated by a fit of the signal difference (ΔM) to the perfusion model with the following values for the physical constants: R_1 (longitudinal relaxation rate of tissue), 1.2 ms; R_{1a} (longitudinal relaxation rate of blood), 1.65 s; λ (brain/blood partition coefficient of water), 0.9 mL/g.[29,30]

Registration and CBF analysis

The anatomical MR images were coregistered with the echo-planar ASL-MR and summed PET images. Coregistration consisted of finding a rigid transformation (three rotations, three translations) based on the maximal mutual information of the images.[31] The slice corresponding to the imaging slice of the ASL-MRI examination was determined for the T_1 weighted MR images. In this slice the region of interest (ROI) selection was performed for the gray-matter in the flow territory of the anterior (ACA), middle (MCA) and posterior cerebral artery (PCA), and white-matter (Figure 1). Selection of the ROIs was performed for all subjects on the basis of established flow territory templates.[32] Areas of hyperintensities on the FLAIR MR images, depicting areas of infarction, were manually excluded from the ROIs. The obtained ROIs were subsequently transformed to the coregistered parametric PET and ASL-MR images for analysis. In this manner, the ROIs could be defined on high-resolution anatomical images, whereas the analysis was performed on PET and ASL data in the original orientation and resolution.

Figure 1. Transverse anatomical image depicting the regions of interest used for quantification of the hemodynamic parameters. In each hemisphere a ROI was drawn in the flow territory of the anterior (ACA), middle (MCA) and posterior cerebral artery (PCA) of the gray-matter, and in the white-matter.

Statistical analysis

SPSS, version 16.0.1 (SPSS Inc., Chicago, Illinois, U.S.A.), was used for statistical analysis. The obtained CBF values, and ratios between the ipsi and contralateral hemisphere, from PET and ASL were compared with a paired *t* test. A student's *t* test was used to compare the CBF in the ipsilateral and contralateral hemisphere. The linear correlation coefficient (Pearson's r) was calculated to estimate the correlation between ASL-MRI and PET CBF measurements. A p value of less than 0.05 was considered to indicate statistical significance. All data are presented as mean ± standard error of the mean (SEM), unless otherwise specified.

Results

The clinical characteristics of the study population are summarized in Table 1. Figure 2 shows the CBF maps of a 65-year-old female patient with a unilateral left-sided ICA occlusion obtained with ASL-MRI and $H_2{}^{15}O$ PET. Figure 3 shows CBF images of a 33-year-old male patient with a unilateral right-sided ICA occlusion.

Both $H_2{}^{15}O$ PET and ASL-MRI measured a significantly decreased CBF in the gray-matter of the MCA in the symptomatic hemisphere when compared to the contralateral hemisphere. The average CBF values for the hemisphere ipsilateral and contralateral to the ICA occlusion are summarized in Table 2. For $H_2{}^{15}O$ PET perfusion imaging the ratio between the contra and ipsilateral hemisphere was 1.2 ± 0.1 for the ACA, 1.3 ± 0.1 for the MCA and 1.1 ± 0.1 for the PCA region. The ratios for ASL-MRI were 1.2 ± 0.2, 1.7 ± 0.2 and 0.9 ± 0.1, respectively. The ratios for the middle ($p = 0.02$) and posterior regions ($p < 0.01$) were significantly different (paired *t* test) between $H_2{}^{15}O$ PET and ASL-MRI.

The average gray-matter CBF (ACA, MCA and PCA regions) measured with ASL-MRI (71.8 ± 4.3 mL/min/100g) was 28.7 ± 3.3 mL/min/100g (paired *t*-test, $p < 0.01$) higher than the CBF measured with $H_2{}^{15}O$ PET (43.1 ± 1.0 mL/min/100g). The

Table 1. Patient characteristics.

	Patients (n = 14)
Age, mean years ± SD	63 ± 14
Male sex, n	9 (64%)
Presenting events, n	
Transient ischemic attack	11 (79%)
Ischemic stroke	3 (21%)
Rankin score at time of interview	
0	11 (79%)
1	0
2	3 (21%)
Degree of contralateral ICA stenosis	
0 – 49%	12
50 – 69%	2
70 – 100 %	0
Vascular risk factors	
Diabetes Mellitus	9 (64%)
Hypertension	8 (57%)
Hyperlipidemia	7 (50%)
Angina pectoris	2 (14%)
Myocardial infarction	0 (0%)
Current smoker	7 (50%)
Past smoker	5 (36%)

Data are numbers (percentage) unless otherwise specified

Table 2. Cerebral blood flow values (mL/min/100g) in patients with a symptomatic ICA occlusion measured with PET and ASL-MRI.

	Gray-matter			**White-matter**
	Anterior	*Middle*	*Posterior*	
PET				
Ipsilateral	36.7 ± 2.4	39.0 ± 1.7 *	46.3 ±2.6 †	21.5 ± 1.9
Contralateral	40.1 ± 2.0	48.0 ± 2.2 †	48.7 ± 2.5 †	20.7 ± 1.8
ASL				
Ipsilateral	49.0 ± 8.7	48.9 ± 5.3 *	109.5 ± 7.5	24.7 ± 4.1
Contralateral	50.4 ± 7.2	77.2 ± 10.0	95.6 ± 11.0	24.8 ± 4.1

* Significant difference in CBF between the ipsi and contralateral hemisphere (*t* test).
† Significant difference in CBF between the ASL and PET measurements (paired *t* test).

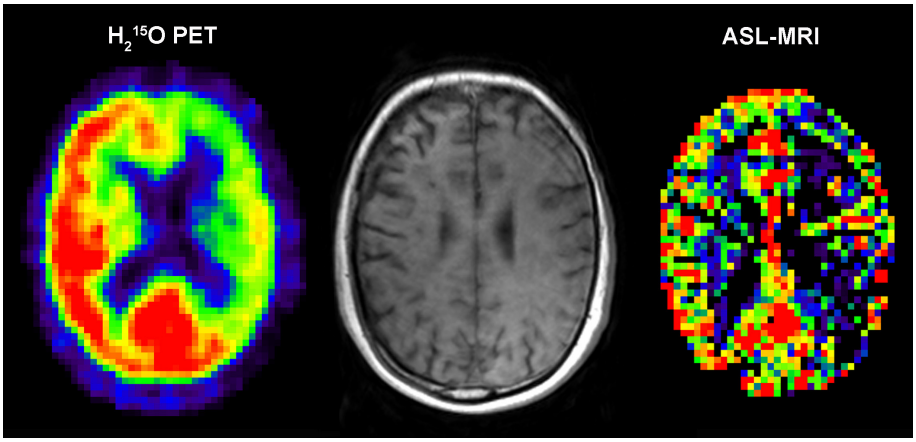

Figure 2. Transverse perfusion images in ml/min/100 g obtained with $H_2{}^{15}O$ PET (left) and ASL-MRI (right) of a 65-year-old female patient with a unilateral left-sided ICA occlusion. *For color figure see page 155.*

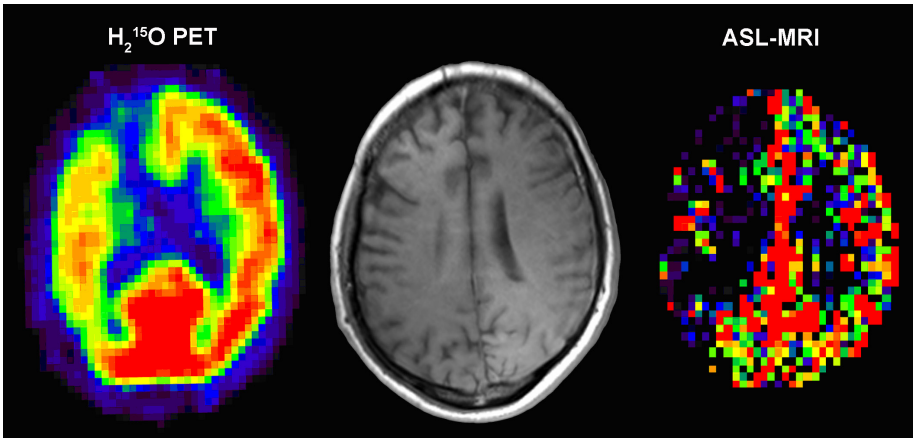

Figure 3. Transverse perfusion images in ml/min/100 g obtained with $H_2{}^{15}O$ PET (left) and ASL-MRI (right) of a 33-year-old male patient with a unilateral right-sided ICA occlusion. *For color figure see page 155.*

white-matter CBF measured with ASL-MRI (24.8 ± 2.8 mL/min/100g) was 3.7 ± 1.5 mL/min/100g ($p < 0.01$) higher than the white-matter CBF measured with $H_2{}^{15}O$ PET (21.1 ± 1.3 mL/min/100g) The Pearson's correlation coefficient for the ASL-MRI and PET CBF measurements was 0.58 ($p < 0.01$) for the combined gray matter regions and 0.37 ($p = 0.03$) for the white-matter region. The Pearson's correlation coefficients for the individual ACA gray-matter region was 0.52 ($p = 0.02$), for the MCA region 0.63 ($p < 0.01$) and for the PCA region 0.32 ($p = 0.05$) (Figure 4).

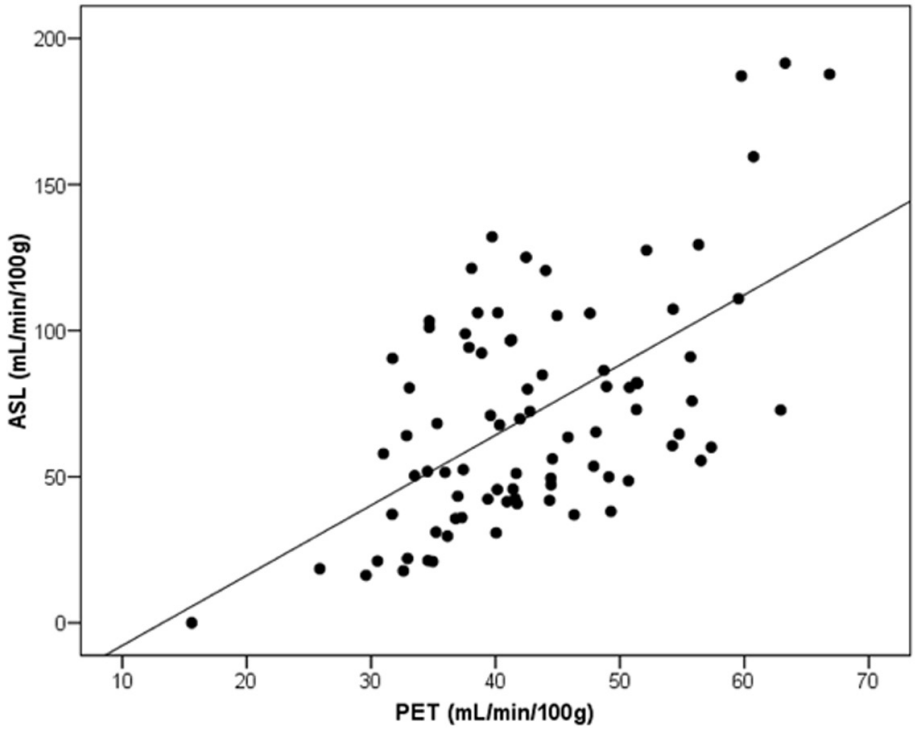

Figure 4. ROI based comparison between $H_2{}^{15}O$ PET and ASL-MRI CBF measurements over all ROI regions in the gray matter of all subjects.

Discussion

The present study demonstrates that CBF measurements obtained with ASL-MRI with acquisition of images at multiple delay times are correlated with quantitative CBF values derived with $H_2{}^{15}O$ PET in patients with a symptomatic occlusion of the ICA. The observed correlations differed between brain regions and were the best in the flow territory of the MCA. Furthermore, ASL-MRI was capable of depicting decreased CBF in the gray-matter of the MCA in patients with a symptomatic occlusion of the carotid artery similar to $H_2{}^{15}O$ PET, although an overall systematic overestimation of CBF relative to $H_2{}^{15}O$ PET was noted.

In an increasing number of institutions, ASL-MR perfusion imaging techniques are being added to the clinical MR protocols for routine assessment of CBF.[33,34] Previous studies have validated the various ASL techniques in both healthy volunteers and patients, and have applied the technique to assess cerebral perfusion in a wide range of neurological diseases.[19,35,36] Using a steady-state ASL strategy, one study found comparable CBF measurements in twelve healthy subjects when compared

to $H_2{}^{15}O$ PET.[19] In a study of eleven patients with an ICA occlusion, others found a significant correlation (r = 0.71) between CBF measurements obtained with a continuous ASL-MRI technique and steady-state O^{15}-labeled CO_2 PET.[37] In the latter study a possible underestimation of CBF in the affected hemisphere in five of the eleven patients was reported, due to longer transit times of the blood flow arriving through collateral blood flow pathways.

By performing multiple ASL experiments at increasing delay times between labeling and image acquisition, the accuracy of perfusion quantification in tissue with spatially variable tissue times can be enhanced.[26,28] Using pulsed ASL with multiple small flip angle gradient echo readouts, in a similar manner as in the Look-Locker technique used for fast T_1 mapping,[25] it is possible to measure the kinetics of the labeled blood and calculate CBF in a single scan. Previously, in a study of ten subjects, it was shown that an arterial spin labeling strategy at multiple TI with and without vascular crushers (QUASAR) provided data that correlated well with DSC-MRI results.[38] Other techniques have also been introduced to circumvent these problems associated with variable transit times for both continuous and pulsed arterial spin labeling. For pulsed ASL, in which perfusion is assessed at a single inversion time point, sequences such as QUIPSS and QUIPSS II with thin-slice TI1 periodic saturation have been introduced.[39,40] In order to minimize effects of varying arrival times, these incorporate saturation pulses into the sequence to obtain sharply defined bolus profiles. A disadvantage is that with a fixed delay between tagging and imaging, flow may possibly be underestimated when the transit times are too long. For continuous ASL, in which labeling is performed during a few seconds at one plane, insensitivity to transit delays can be increased by using a pre-delay between the continuous labeling and the readout.[41]

Although we found a significant correlation between ASL-MRI and $H_2{}^{15}O$ PET CBF measurements, higher absolute CBF values were found with ASL-MRI. This overestimation by ASL-MRI is consistent with previous studies comparing ASL-MRI with image acquisition at a single inversion time to PET,[19,37] which in those studies was attributed mainly to intravascular signal. Although water is a highly diffusible tracer, it has been shown that with ASL-MRI, even when longer post-labeling delay times are used, label may still be present in the (small) feeding arteries, leading to an overestimation of CBF.[42] Another possible explanation could be related to the CBF measurements derived with PET in this study. The $H_2{}^{15}O$ PET method used in this study was based on the assumption that delay and dispersion of the arterial blood time-activity curve between brain and radial artery was the same throughout the brain. In patients with an obstruction in the arteries feeding the brain, as seen in our patient population, and subsequent collateral blood flow through primary and secondary collateral vessels, this may not hold true, leading to a potential underestimation of CBF in comparison to the contralateral hemisphere.

In the present study we found that the relation between the ASL-MRI and PET CBF measurements varied over the different flow territories of the cerebral arteries.

The absolute differences in CBF were the largest in the flow territory of the posterior circulation. This may be caused by the course of the posterior cerebral arteries. The P2 segment distally from the posterior communicating artery runs almost parallel to the axial ASL-MR imaging slices. As a result, the diffusion of labeled blood into the brain may not yet be complete with label still being present in the vasculature. The perfusion model, however, assumes that labeled magnetization of inflowing blood has fully diffused into the tissue. This may lead to relatively higher CBF values in the posterior circulation when compared to brain tissue supplied by the ICA, which runs perpendicular to the ASL-MR imaging slice.

Our study showed a relatively low CBF in the MCA territory of the hemisphere ipsilateral to the ICA occlusion when assessed with ASL-MRI using interhemispheric comparisons of CBF. In a healthy brain, it can be assumed that the perfusion like contribution coming from remaining intravascular spins may be equal for both hemispheres, as the vasculature is roughly identical on both sides. However, our study indicates that when a ratio between hemispheres is used in patients with a carotid artery occlusion to estimate hypoperfusion, ASL-MRI may overestimate the difference between the symptomatic and contralateral hemisphere in the gray-matter of the MCA. The difference in CBF ratios between ASL-MRI and PET was less in the flow territory of the ACA and PCA. We hypothesize that when using interhemispheric ratios brain tissue with higher amounts of intravascular label, such as the gray-matter of the MCA territory, is more prone to error.

A potential limitation of our study is that we used a Look-Locker-like small flip angle gradient echo sampling strategy to acquire the series of images at increasing delay times after labeling. Although this significantly decreases scan time, making it more practical for clinical use in patients, the train of RF pulses during the readout decreases the perfusion signal. Because of this signal loss, and the natural T_1 decay of the magnetized blood, we refrained from the use of crusher gradients. Crusher gradients can be utilized to dephase the moving spins in order to eliminate the signal from the large arteries. However, despite the possible overestimation of CBF due to not using crushers, there was a significant correlation between the ASL-MRI CBF measurements and the $H_2{}^{15}O$ PET CBF measurements. An additional limitation of the study may be the seven days between the ASL-MRI and $H_2{}^{15}O$ PET examination and that both scans were performed under different environmental conditions (i.e. silence versus loudness MRI, possibly leading to a higher CBF in the auditory cortex). To control for the difference in time from symptoms to investigation, the order of both investigations were randomized.

Conclusion

CBF values obtained with ASL-MRI at multiple delay times correlated significantly with $H_2{}^{15}O$ PET, although there was a systematic overestimation of CBF by ASL-MRI.

This overestimation shows that for quantitative use ASL perfusion images should be interpreted with caution, especially when literature cut-off values for hemodynamic impairment are used which are based on other methods, such as $H_2{}^{15}O$ PET CBF. Still, the relative values of the ipsilateral to contralateral hemisphere in our patients with ICA occlusion are comparable to these values obtained with $H_2{}^{15}O$ PET. Therefore we conclude that the non-invasive ASL-MRI measurements of perfusion are useful to depict the presence and extent of areas with hypoperfusion in the vascular territory of the middle cerebral artery in patients with symptomatic ICA occlusion.

References

1. Klijn CJ, Kappelle LJ, Algra A, et al. Outcome in patients with symptomatic occlusion of the internal carotid artery or intracranial arterial lesions: a meta-analysis of the role of baseline characteristics and type of antithrombotic treatment. Cerebrovasc Dis 2001;12:228-234.
2. Vernieri F, Pasqualetti P, Passarelli F, et al. Outcome of carotid artery occlusion is predicted by cerebrovascular reactivity. Stroke 1999;30:593-598.
3. Klijn CJ, Kappelle LJ, van Huffelen AC, et al. Recurrent ischemia in symptomatic carotid occlusion: prognostic value of hemodynamic factors. Neurology 2000;55:1806-1812.
4. Grubb RL, Jr., Derdeyn CP, Fritsch SM, et al. Importance of hemodynamic factors in the prognosis of symptomatic carotid occlusion. JAMA 1998;280:1055-1060.
5. Wintermark M, Sesay M, Barbier E, et al. Comparative overview of brain perfusion imaging techniques. Stroke 2005;36:e83-e99.
6. Penfield JG, Reilly RF, Jr. What nephrologists need to know about gadolinium. Nat Clin Pract Nephrol 2007;3:654-668.
7. Sadowski EA, Bennett LK, Chan MR, et al. Nephrogenic systemic fibrosis: risk factors and incidence estimation. Radiology 2007;243:148-157.
8. Golay X, Hendrikse J, Lim TC. Perfusion imaging using arterial spin labeling. Top Magn Reson Imaging 2004;15:10-27.
9. Williams DS, Detre JA, Leigh JS, et al. Magnetic resonance imaging of perfusion using spin inversion of arterial water [published erratum appears in Proc Natl Acad Sci U S A 1992;89:4220]. Proc Natl Acad Sci U S A 1992;89:212-216.
10. Detre JA, Leigh JS, Williams DS, et al. Perfusion imaging. Magn Reson Med 1992;23:37-45.
11. Edelman RR, Siewert B, Darby DG, et al. Qualitative mapping of cerebral blood flow and functional localization with echo-planar MR imaging and signal targeting with alternating radio frequency. Radiology 1994;192:513-520.
12. Wolf RL, Detre JA. Clinical neuroimaging using arterial spin-labeled perfusion magnetic resonance imaging. Neurotherapeutics 2007;4:346-359.
13. Liebeskind DS. Collateral Circulation. Stroke 2003;34:2279-2284.
14. Calamante F, Williams SR, van Bruggen N, et al. A model for quantification of perfusion in pulsed labelling techniques. NMR Biomed 1996;9:79-83.
15. Alsop DC, Detre JA. Reduced transit-time sensitivity in noninvasive magnetic resonance imaging of human cerebral blood flow. J Cereb Blood Flow Metab 1996;16:1236-1249.
16. Gibbs JM, Wise RJ, Leenders KL, et al. Evaluation of cerebral perfusion reserve in patients with carotid-artery occlusion. Lancet 1984;1:310-314.
17. Floyd TF, Ratcliffe SJ, Wang J, et al. Precision of the CASL-perfusion MRI technique for the measurement of cerebral blood flow in whole brain and vascular territories. J Magn Reson Imaging 2003;18:649-655.
18. Pell GS, King MD, Proctor E, et al. Comparative study of the FAIR technique of perfusion quantification with the hydrogen clearance method. J Cereb Blood Flow Metab 2003;23:689-699.
19. Ye FQ, Berman KF, Ellmore T, et al. H(2)(15)O PET validation of steady-state arterial spin tagging cerebral blood flow measurements in humans. Magn Reson Med 2000;44:450-456.
20. Bamford JM, Sandercock PAG, Warlow CP, et al. Interobserver agreement for the assessment of handicap in stroke patients. Stroke 1989;20:828.
21. Fox AJ. How to measure carotid stenosis. Radiology 1993;186:316-318.
22. Brix G, Zaers J, Adam LE, et al. Performance evaluation of a whole-body PET scanner using the NEMA protocol. National Electrical Manufacturers Association. J Nucl Med 1997;38:1614-1623.
23. Boellaard R, van Lingen A, van Balen SC, et al. Characteristics of a new fully programmable blood sampling device for monitoring blood radioactivity during PET. Eur J Nucl Med 2001;28:81-89.

24. Boellaard R, Knaapen P, Rijbroek A, et al. Evaluation of basis function and linear least squares methods for generating parametric blood flow images using 15O-water and Positron Emission Tomography. Mol Imaging Biol 2005;7:273-285.
25. Look DC, Locker DR. Time saving measurement of NMR and EPR relaxation times. Rev Sci Instum 1970;41:250-251.
26. Petersen ET, Lim T, Golay X. Model-free arterial spin labeling quantification approach for perfusion MRI. Magn Reson Med 2006;55:219-232.
27. Buxton RB, Frank LR, Wong EC, et al. A general kinetic model for quantitative perfusion imaging with arterial spin labeling. Magn Reson Med 1998;40:383-396.
28. Gunther M, Bock M, Schad LR. Arterial spin labeling in combination with a look-locker sampling strategy: inflow turbo-sampling EPI-FAIR (ITS-FAIR). Magn Reson Med 2001;46:974-984.
29. Herscovitch P, Raichle ME. What is the correct value for the brain--blood partition coefficient for water? J Cereb Blood Flow Metab 1985;5:65-69.
30. Barth M, Moser E. Proton NMR relaxation times of human blood samples at 1.5 T and implications for functional MRI. Cell Mol Biol (Noisy -le-grand) 1997;43:783-791.
31. Maes F, Collignon A, van der Meulen D, et al. Multimodality image registration by maximization of mutual information. IEEE Trans Med Imaging 1997;16:187-198.
32. Tatu L, Moulin T, Bogousslavsky J, et al. Arterial territories of the human brain: cerebral hemispheres. Neurology 1998;50:1699-1708.
33. Deibler AR, Pollock JM, Kraft RA, et al. Arterial Spin-Labeling in Routine Clinical Practice, Part 2: Hypoperfusion Patterns. AJNR Am J Neuroradiol 2008;29:1235-1241.
34. Deibler AR, Pollock JM, Kraft RA, et al. Arterial Spin-Labeling in Routine Clinical Practice, Part 3: Hyperperfusion Patterns. AJNR Am J Neuroradiol 2008;29:1428-1235.
35. Donahue MJ, Lu H, Jones CK, et al. An account of the discrepancy between MRI and PET cerebral blood flow measures. A high-field MRI investigation. NMR Biomed 2006;19:1043-1054.
36. Koziak AM, Winter J, Lee TY, et al. Validation study of a pulsed arterial spin labeling technique by comparison to perfusion computed tomography. Magn Reson Imaging 2008;26:543-553.
37. Kimura H, Kado H, Koshimoto Y, et al. Multislice continuous arterial spin-labeled perfusion MRI in patients with chronic occlusive cerebrovascular disease: a correlative study with CO2 PET validation. J Magn Reson Imaging 2005;22:189-198.
38. Knutsson L, van Westen D, Petersen ET, Markenroth Block K, Holtas S, Wirestam R, Stahlberg F. Absolute quantification of cerebral blood flow using dynamic susceptibility contrast MRI: A comparison with model-free arterial spin labeling. Magn Reson Imaging 2010;28:1-7.
39. Wong EC, Buxton RB, Frank LR. Quantitative imaging of perfusion using a single subtraction (QUIPSS and QUIPSS II). Magn Reson Med 1998;39:702-708.
40. Luh WM, Wong EC, Bandettini PA, et al. QUIPSS II with thin-slice TI1 periodic saturation: a method for improving accuracy of quantitative perfusion imaging using pulsed arterial spin labeling. Magn Reson Med 1999;41:1246-1254.
41. Detre JA, Alsop DC, Vives LR, et al. Noninvasive MRI evaluation of cerebral blood flow in cerebrovascular disease. Neurology 1998;50:633-641.
42. Ye FQ, Mattay VS, Jezzard P, et al. Correction for vascular artifacts in cerebral blood flow values measured by using arterial spin tagging techniques. Magn Reson Med 1997;37:226-235.

CHAPTER 4

Reinoud P.H. Bokkers
Bart H. van der Worp
Willem P.Th.M. Mali
Jeroen Hendrikse

PERFUSION IMAGING OF ARTERIAL SPIN LABELING TIMING PARAMETERS IN PATIENTS WITH A CAROTID ARTERY STENOSIS

Background and purpose: Arterial spin labeling (ASL) perfusion MRI with image acquisition at multiple delay times can be used to measure delays in the arrival of arterial blood to the brain. We assessed the effect of a symptomatic internal carotid artery (ICA) stenosis on ASL timing parameters, and evaluated the effect of collateral flow through the circle of Willis.

Methods: Forty-four functionally independent patients (30 men and 14 women; mean age, 69±9 years) with a recently symptomatic ICA stenosis ≥50% and 34 sex- and age-matched healthy volunteers were investigated. MR angiography and 2D phase-contrast imaging were used to assess collateral flow in the circle of Willis.

Results: In the hemisphere ipsilateral to the ICA stenosis, CBF was lower ($P<0.01$) in the anterior frontal, posterior frontal, parieto-occipital, and occipital regions than in control subjects. The transit times were prolonged ($p<0.01$) in the ipsilateral anterior frontal, posterior frontal and fronto-parietal regions when compared with the control subjects. The trailing edge time was prolonged ($p<0.01$) in the ipsilateral fronto-parietal region when compared to the control subjects. In the 27 patients without a contralateral stenosis, the trailing edge was longer ($p<0.01$) in the ipsilateral posterior frontal, fronto-parietal and parieto-occipital regions than in the contralateral regions. Collateral flow via the circle of Willis did not affect CBF and transit or trailing edge times.

Conclusion: ASL MRI is a non-invasive tool for imaging CBF and delays in the arrival of arterial blood to the brain, and can potentially provide valuable information on the quality of perfusion to the brain in patients with cerebrovascular disease.

Neurology 2009;73(11):869-875

Introduction

Patients with a symptomatic stenosis of the internal carotid artery (ICA) are at high risk of future ischemic stroke.[1,2] A stenosis in the ICA leads to a reduction in the perfusion pressure of the brain and subsequent recruitment of additional blood flow through collateral pathways in order to sustain perfusion.[3] The risk of ischemic stroke is higher in patients with impaired perfusion in the hemisphere ipsilateral to the stenosis than those with normal perfusion.[4,5] At the level of the brain tissue, the presence of such impaired perfusion and collateral blood flow recruitment may be detected by a delayed arrival of blood from the arteries in the neck towards the brain.[6] Both studies using time-to-arrival and time-to-peak measurements with perfusion computed tomography (CT) and perfusion-weighted dynamic susceptibility (DSC) magnetic resonance (MR) imaging have demonstrated the occurrence of such delayed arrival in patients with an ICA stenosis.[7-9]

Arterial spin-labeling (ASL) is an MR imaging technique capable of non-invasively assessing the cerebral perfusion by labeling arterial blood with radiofrequency pulses.[10-13] In addition to measuring cerebral blood flow (CBF), ASL can also be utilized to quantify the dynamics of arterial blood inflow.[14] By acquiring a series of images at increasing delay times after the initial labeling it is possible to measure the arrival time and the duration needed for the end of the labeled bolus to reach the brain tissue: the transit and trailing edge times, respectively.[15]

The purpose of our study was to investigate the transit and trailing edge times measured with ASL at multiple delay times in patients with a symptomatic ICA stenosis, and to evaluate the effect of collateral flow via the circle of Willis on regional hemodynamics.

Methods

The institutional ethical standards committee approved the study protocol and written informed consent was obtained from all participants.

Patients and control subjects

Forty-four functionally independent patients (30 men and 14 women; mean ± standard deviation (SD) age, 69 ± 9 years) with a recently symptomatic ICA stenosis ≥ 50% were included in this study. Twenty patients had had an ischemic stroke, eighteen patients a transient ischemic attack, and fourteen patients ipsilateral retinal ischemia. Several patients had more than one presenting event. Grading of the ICA stenosis was performed with duplex ultrasonography. Forty patients had an ICA stenosis of 70 - 99% and four patients a stenosis of 50 - 69%. Six patients had a contralateral ICA stenosis of 50 – 69%, nine a stenosis of 70 – 99% and two had an occlusion of the contralateral ICA. All patients were participants of the International

Carotid Stenting Study (ICSS), a multicenter, randomized, prospective clinical trial comparing primary stenting of symptomatic carotid artery stenosis with carotid endarterectomy.[16]

The control group consisted of 34 volunteers (23 men and 11 women; mean age ± SD, 68 ± 6 years) without a history of neurological disease, vascular pathology on MRI or MR angiography of the brain, or an ICA stenosis ≥ 30%. All controls were randomly recruited from a hospital-based vascular screening study involving subjects with symptomatic atherosclerosis or risk factors for atherosclerosis.[17]

MR imaging

Imaging was performed on a clinical 1.5 Tesla MRI scanner (Gyroscan ACS-NT, Philips Medical Systems, Best, The Netherlands) using a quadrature head coil for radiofrequency transmission and signal reception. MR perfusion imaging was performed with a pulsed ASL transfer insensitive labeling technique (TURBO-TILT).[18] A single perfusion imaging slice was aligned parallel to the orbito-meatal angle and planed just above the ventricles through the centrum semiovale. The labeling slab was 140 mm thick, set 10 mm proximal to the imaging slice. Labeling was achieved by applying two consecutive slice-selective 90° radiofrequency pulses. For image acquisition, a series of thirteen 35° excitation pulses were applied with increasing delay times from 200 to 2600 ms with a constant interval of 200 ms, followed by single shot gradient echo-planar-imaging readout. The ASL signal was corrected for imperfections in slice profiles.[19]

Perfusion weighted images were obtained by subtracting the labeled images from the unlabeled control images. In addition to quantifying CBF, the perfusion signal at multiple delay times can be used to measure the transit and trailing edge times. The transit time is the duration between labeling and the first arrival of the magnetized blood into the imaging voxel. The trailing edge time is the duration needed for the end of the labeled bolus to reach the imaging voxel.[15] To quantify CBF, and the transit and trailing edge times, the perfusion signal at varying delay times was fitted to a kinetic perfusion model for signal dynamics during multiple readouts:[20]

$$\Delta M(t) = 0 \qquad 0 < t < \tau_a \qquad [1]$$

$$\Delta M(t) = \frac{-2 \cdot M_{a,0} \cdot f}{\delta R} e^{-R_{1a} \cdot t} (1 - e^{\delta R \cdot (t - \tau_a)}) \qquad \tau_a \le t \le \tau_d \qquad [2]$$

$$\Delta M(t) = \frac{-2 \cdot M_{a,0} \cdot f}{\delta R} e^{-R_{1a} \cdot t_d} (1 - e^{\delta R \cdot (t - \tau_d)}) \cdot e^{-R_{1app,eff} \cdot (t - \tau_d)} \qquad t \ge \tau_d \qquad [3]$$

where f is the perfusion value CBF in ml/min/100gr, τ_a is the transit time, τ_d is

the trailing edge time, $\delta R = R_{1a} - R_{1app,eff}$ and $R_{1app,eff} = R_1 + f/\lambda - \ln(\cos\alpha/\Delta TI)$, λ is the brain/blood partition coefficient, α is the flip angle, ΔTI is the time between consecutive readouts, R_{1a} is the longitudinal relaxation rate of arterial blood, R_1 is the longitudinal relaxation rate of tissue and $M_{a,0}$ is the equilibrium magnetization in a blood filled voxel, estimated by fitting the unlabeled signal in the sagittal sinus to a saturation-recovery curve. The following physical constants, used in equation 1 – 3, were obtained from the literature: R_1 = 1000 ms, R_{1a} = 1400 ms, λ = 0.9 mL/g.[21,22] Other MRI parameters were: repetition time (TR) 3000 ms; echo time (TE), 5.6 ms; 62% partial Fourier acquisition; averages, 50; field of view (FOV), 240 × 240 mm; 64 x 64 matrix; scan time, five minutes.

The presence of collateral flow routes in the circle of Willis was assessed with a three-dimensional time-of-flight MR angiography sequence with subsequent maximal intensity projection reconstruction (TR/TE, 30/6.9 ms; flip angle 20°; two averages; FOV, 100 x 100 mm; matrix, 256 x 256; 50 slices; slice thickness, 1.2 mm with 0.6 mm overlap; scan time, three minutes). The direction of blood flow in these collaterals was determined according to a previously published imaging protocol with two consecutive two-dimensional phase-contrast MR imaging measurements, of which one was phase-encoded in the left-right direction and one in the antero-posterior direction (TR/TE, 16/9.1 ms; flip angle, 7.5°; FOV, 250 x 188 mm; matrix, 256 x 256; eight averages; slice thickness, 13 mm; velocity sensitivity, 40 cm/s, scan time, 20 sec).[23] Anterior collateral flow was defined as flow across the anterior communicating artery with retrograde flow in the precommunicating part of the anterior cerebral artery (A1 segment). Posterior-to-anterior flow in the posterior communicating artery was considered to represent posterior collateral flow.

Data analysis

Data were analyzed with mathematic software (MATLAB, The Mathworks, Natick, Mass). Based on the ASL control images, five regions of interests (ROIs) were drawn according to a standardized template symmetrically in each hemisphere, in distinct areas of gray matter.[24] Two regions of interest were drawn in the frontal lobe, and one in the fronto-parietal, parieto-occipital, and occipital region.

Statistical analysis

SPSS (SPSS Inc., Chicago, Illinois, U.S.A.) for Windows, version 15.0.1, was used for statistical analysis. Descriptive statistical analyses were preformed to summarize patient characteristics. Mean CBF and transit and trailing edge times were calculated for all ROIs in the hemisphere ipsilateral to the symptomatic stenosis and in the contralateral hemisphere. Because no differences were found in CBF and in the transit and trailing edge times between the left and right hemispheres of the control subjects, the values of the regions in both hemispheres were averaged for analysis. A one-way ANOVA with Bonferroni correction for multiple comparisons was used

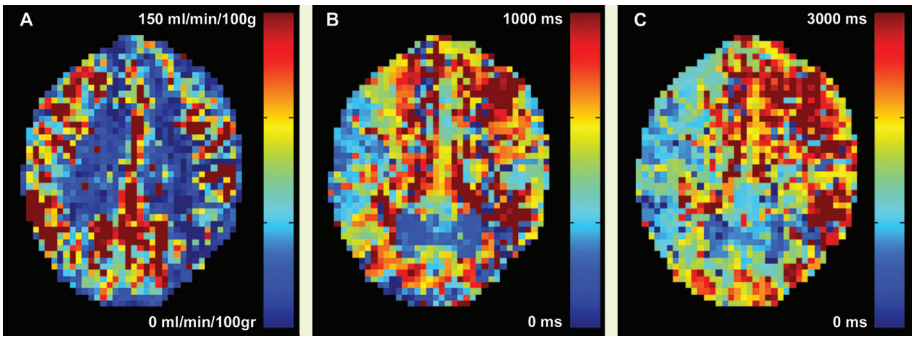

Figure 1. Transverse ASL perfusion MR images of a patient with a unilateral left-sided ICA stenosis of 90%. The images show the absolute CBF in ml/min/100gr (A), transit time in ms (B), and trailing edge time in ms (C). Decreased CBF and increasing ASL timing parameters are observed in the hemisphere ipsilateral to the internal carotid artery stenosis. *For color figure see page 156.*

to evaluate differences between CBF and transit and trailing edge times in ROIs of controls and those of hemispheres ipsi- and contralateral to the ICA stenosis in patients. The influence of collateral flow patterns on CBF and transit and trailing edge times in the hemisphere ipsilateral to the symptomatic ICA stenosis was evaluated using Student's *t*-test. A p value ≤ 0.05 was considered to indicate a significant difference. Values are expressed as mean ± standard error of the mean (SEM) unless otherwise specified.

Results

An example of an ASL MR imaging investigation of a patient with a unilateral symptomatic ICA stenosis is shown in Figure 1. Decreased CBF and increased ASL timing parameters are found in the hemisphere ipsilateral to the ICA stenosis.

Figure 2 shows the CBF values of all regions of the hemispheres ipsi- and contralateral to the symptomatic ICA stenosis, and in the control subjects. In the hemisphere ipsilateral to the symptomatic ICA stenosis, the CBF was lower than in the control subjects in the anterior frontal (31 ± 2 vs. 44 ± 3 ml/min/100gr, $p < 0.01$), posterior frontal (38 ± 3 vs. 57 ± 2 ml/min/100gr, $p < 0.01$), parieto-occipital (35 ± 3 vs. 47 ± 3 ml/min/100gr, $p = 0.03$), and occipital (38 ± 3 vs 57 ± 3 ml/min/100gr, $p < 0.01$) regions. In the hemisphere contralateral to the symptomatic ICA stenosis, the CBF was lower than in the control subjects in the anterior frontal (29 ± 2 vs. 44 ± 3 ml/min/100gr, $p < 0.01$), posterior frontal (40 ± 3 vs. 57 ± 2 ml/min/100gr, $p < 0.01$), and occipital (35 ± 3 vs 56 ± 3 ml/min/100gr, $p < 0.01$) regions.

Figure 3 shows the transit times of all regions in the hemispheres ipsi- and contralateral to the symptomatic ICA stenosis, and in the control subjects. In the

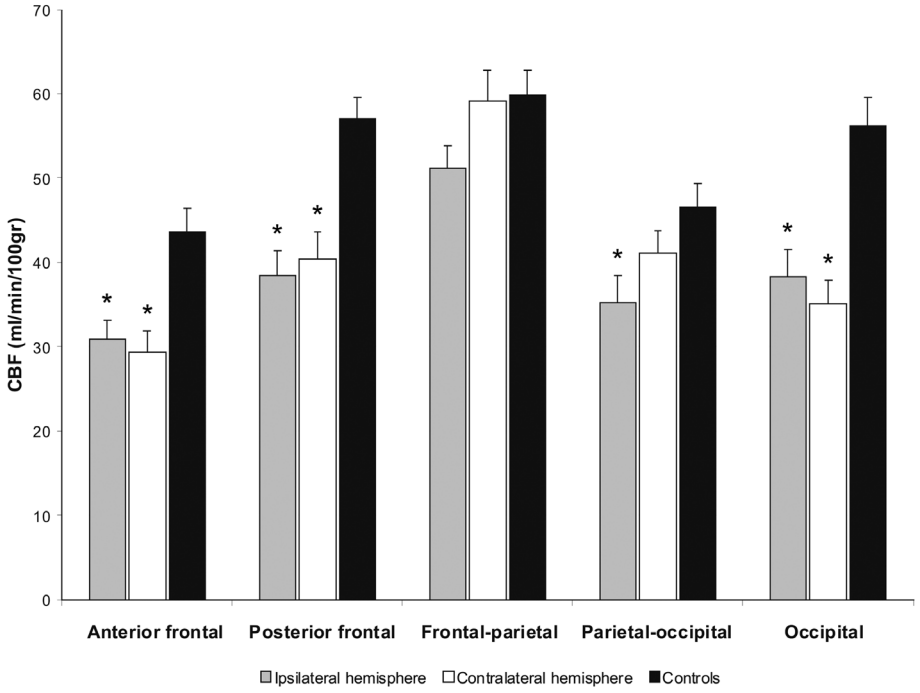

Figure 2. CBF (mean ± SEM) in the regions of the hemispheres ipsi- and contralateral to the symptomatic ICA stenosis and in those of the control group.

* significant difference between the indicated hemisphere and the control subjects.

hemisphere ipsilateral to the ICA stenosis, the transit times were longer than in the control subjects in the anterior frontal (697 ± 50 vs. 37 ± 10 ms, $p < 0.01$), posterior frontal (703 ± 50 vs. 47 ± 11, $p < 0.01$) and fronto-parietal (322 ± 32 vs. 3 ± 2 ms, $p < 0.01$) regions. In the hemisphere contralateral to the ICA stenosis, the transit times were longer than in the control subjects in the anterior frontal (592 ± 45 vs 37 ± 10 ms, $p < 0.01$), posterior frontal (614 ± 50 vs. 47 ± 11 ms, $p < 0.01$), and fronto-parietal (259 ± 27 vs. 3 ± 2 ms, $p < 0.01$) regions. Figure 4 shows the trailing edge times of all regions in the hemispheres ipsi- and contralateral to the symptomatic ICA stenosis and in the control subjects. In the hemisphere ipsilateral to the ICA stenosis, the trailing edge time was longer than in the control subjects in the fronto-parietal region (1768 ± 78 vs. 1562 ± 48 ms, $p < 0.01$ms).

In the 17 patients with an asymptomatic contralateral stenosis ≥ 50%, there were no differences between the hemodynamic parameters of the hemispheres ipsi- and contralateral to the symptomatic stenosis. In the 27 patients without a contralateral stenosis, the trailing edge was longer ($p < 0.01$) in the hemisphere ipsilateral to the ICA stenosis than in the contralateral hemisphere in the posterior

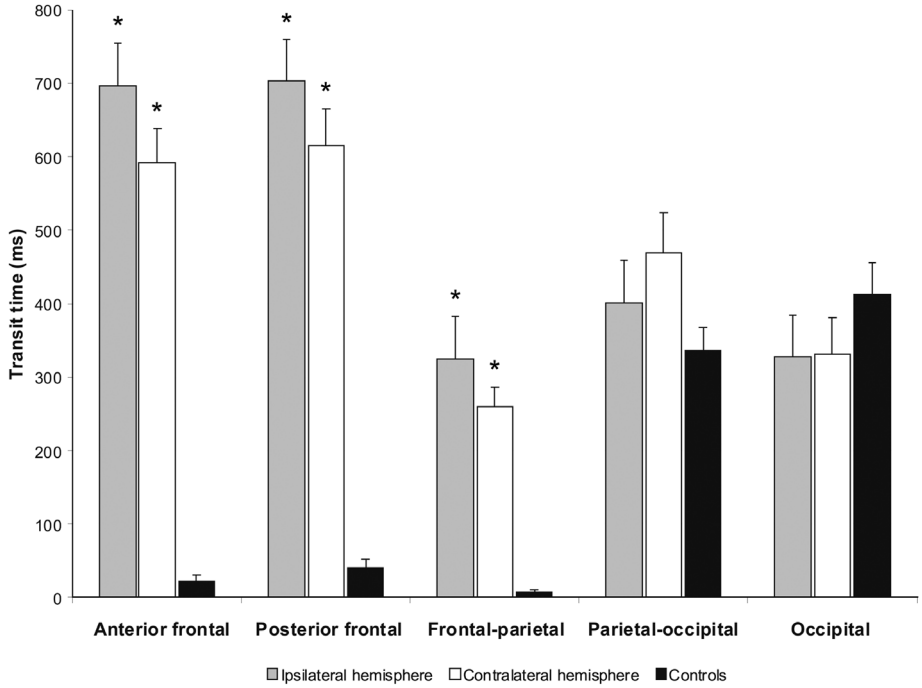

Figure 3. Transit times (mean ± SEM) in the regions of the hemisphere ipsi- and contralateral to the symptomatic ICA stenosis and those of the control group.

* indicates a significant difference between the indicated hemisphere and the control subjects.

frontal (2398 ± 161 vs 1781 ± 155 ms), fronto-parietal (1836 ± 96 vs 1169 ± 84 ms) and parieto-occipital (2371 ± 147 vs 1819 ± 113 ms) regions. No significant differences in CBF and transit times were found between the ipsi- and contralateral hemispheres in these patients.

The hemodynamic parameters in the hemisphere ipsilateral to the symptomatic stenosis in relation to the collateral pathways through the circle of Willis are presented in Table 1. TOF and phase-contrast MR angiography demonstrated collateral flow via the anterior collateral pathways in nine patients and reversed flow in the posterior collateral pathway in eleven patients. The presence or absence of collateral flow via the anterior or posterior collateral pathways did not affect CBF, transit times, or trailing edge times.

Discussion

The most important finding of our study was that delays in the arrival of arterial blood to the brain can be assessed with ASL MR imaging at multiple delay times in

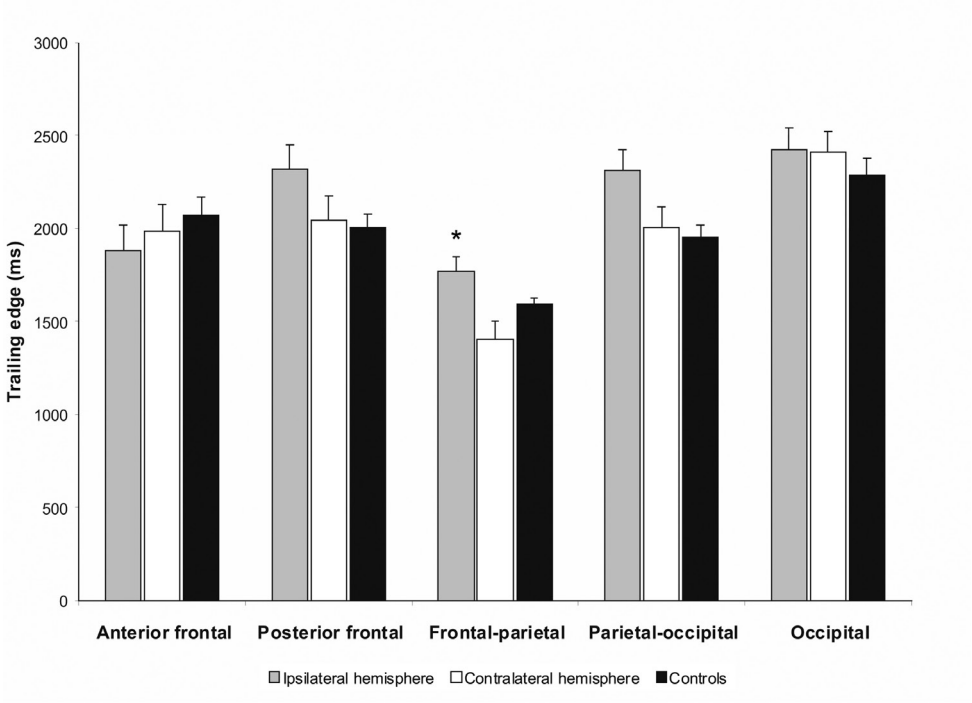

Figure 4. Trailing edge times (mean ± SEM) in the regions of the hemisphere ipsi- and contralateral to the symptomatic ICA stenosis, and those of the control group.

* significant difference between the hemisphere ipsilateral to the ICA stenosis and the control subjects.

patients with a symptomatic ICA stenosis. In patients with a unilateral ICA stenosis, trailing edge times were longer in the ipsilateral hemisphere than in the contralateral hemisphere, whereas no differences were found in patients with a contralateral stenosis ≥ 50%.

Our findings of reduced CBF and prolonged transit and trailing edge times in the flow territory distal to an ICA stenosis correspond with previous contrast-enhanced CT and MR imaging studies, in which increased arrival times of the arterial blood distal to an ICA stenosis have been demonstrated.[7-9] With ASL MR imaging of the arterial transit times, the times needed for the labeled blood bolus to reach the vascular exchange site are assessed. In general, an increase in both transit and trailing edge times will occur in case of either longer blood flow routes or lower flow velocities.[6,25] In patients with a unilateral ICA stenosis, ASL MRI timing parameters were longer in the ipsilateral hemisphere than in the contralateral hemisphere. No differences in arterial timing parameters were found between the ipsi and contralateral hemisphere in patients with an asymptomatic contralateral ICA stenosis ≥ 50%. This indicates that the arrival times of arterial blood measured with ASL MR imaging are not only prolonged in symptomatic hemispheres. Although

Table 1. Hemodynamic parameters of the hemisphere ipsilateral to the symptomatic ICA stenosis in relation to the primary collateral pathways.

	Anterior collateral flow		**Posterior collateral flow**	
	Absent (n=35)	**Present** (n=9)	**Absent** (n = 33)	**Present** (n = 11)
CBF (ml/min/100gr)				
Anterior frontal	30 ± 2	36 ± 5	32 ± 2	29 ± 6
Posterior frontal	39 ± 4	37 ± 6	39 ± 3	36 ± 8
Fronto-parietal	51 ± 3	53 ± 5	53 ± 3	46 ± 8
Parieto-occipital	36 ± 4	33 ± 5	37 ± 4	29 ± 3
Occipital	39 ± 4	36 ± 6	40 ± 4	33 ± 4
Transit time (ms)				
Anterior frontal	676 ± 58	604 ± 87	648 ± 52	701 ± 123
Posterior frontal	705 ± 60	694 ± 78	727 ± 56	631 ± 109
Fronto-parietal	330 ± 36	292 ± 74	332 ± 37	295 ± 66
Parieto-occipital	984 ± 580	418 ± 123	1063 ± 614	285 ± 100
Occipital	328 ± 61	323 ± 164	380 ± 74	169 ± 46
Trailing edge time (ms)				
Anterior frontal	1980 ± 164	1486 ± 209	1892 ± 170	1841 ± 245
Posterior frontal	2304 ± 152	2390 ± 170	2311 ± 156	2352 ± 181
Fronto-parietal	1736 ± 93	1892 ± 127	1712 ± 85	1934 ± 183
Parieto-occipital	2262 ± 124	2514 ± 212	2295 ± 136	2372 ± 152
Occipital	2398 ± 139	2537 ± 120	2538 ± 135	2089 ± 172

Patients are divided into subgroups according to recruitment of collateral pathways via the circle of Willis: no collateral flow, collateral flow via the anterior or posterior collaterals.

no asymptomatic patients were included in the present study, the increased arterial timing parameters in both the ipsi and contralateral hemisphere of the patients with a contralateral asymptomatic stenosis > 50% indicates that asymptomatic carotid artery stenosis may give rise to changes in arterial timing parameters. This underlines that interhemispheric comparisons of ASL timing parameters should be used with caution in those with a bilateral stenosis.

In this study we found several differences between CBF and transit and trailing edge times in the hemisphere ipsilateral to the symptomatic ICA stenosis and those in the control subjects. Although there was a decreased CBF in the parieto-occipital

and occipital region in the ipsilateral hemisphere, we did not find differences in ASL MRI timing parameters. This absence of delayed arrival of arterial blood is most likely caused by the contribution of the vertebrobasilar arteries to the blood supply of the posterior part of the brain.[24,26]

No association between the presence or absence of collateral flow through the circle of Willis and arterial timing parameters was found in the patients with a symptomatic ICA stenosis. This corresponds with a previous dynamic susceptibility contrast-enhanced MRI study, in which collateral flow through the circle of Willis was not found to affect CBF, time of appearance, and time to peak in twelve patients with a greater than 70% stenosis of the ICA.[27] Furthermore, collateral flow through the circle of Willis, did not affect ASL MRI timing parameters in a study of seventeen patients with a symptomatic ICA occlusion.[28] Although recruitment of blood via collateral pathways may lead to longer arterial blood flow routes, we hypothesize that the collateral flow routes via the circle of Willis, i.e. the anterior communicating artery and the posterior communicating artery, are only short detours and therefore do not result in measurable differences in ASL MRI timing parameters. Using a dynamic MRA sequence based on ASL that is capable of visualizing intracranial flow comparable to conventional angiography, it has been showed that the speed of collateral flow through the circle of Willis is < 50 ms.[29]

In this study, we used an ASL technique with image acquisition at multiple delay times. With ASL MRI it is possible to non-invasively assess the cerebral perfusion within five minutes by using magnetically labeled blood as an endogenous contrast agent. Because of concerns regarding the use of ionizing radiation and the use of contrast in patients with renal insufficiency,[30,31] ASL may be a powerful non-invasive alternative for the *in-vivo* assessment of the cerebral hemodynamics. The utility of this method has been demonstrated for epilepsy, central nervous system neoplasms, and a variety of neurodegenerative and vascular diseases.[32-34] As the availability of ASL on clinical MRI scanners is increasing rapidly, ASL can provide valuable information for clinicians when incorporated in standard neuro-imaging protocols.[33,34] Because guidelines for the treatment of carotid artery stenosis are based mainly on the results of large randomized clinical trials in which cerebral perfusion was not assessed, the decision to perform surgery or stenting does currently not depend on the presence or absence of cerebral hemodynamic impairment.[35] However, observational studies have strongly suggested that the risk of ischemic stroke is higher in patients with an impaired perfusion in the hemisphere ipsilateral to the stenosis than those with a normal perfusion,[4,5] possibly because a decreased perfusion and reduced collateral blood flow may diminish the clearance of thromboemboli that have entered the vascular bed.[36,37] For this reason, assessment of the cerebral perfusion with ASL blood flow and arterial timing parameters could be used in future studies to select those patients who are at the highest risk of stroke and may therefore benefit most from carotid revascularization.[38] Because

of the reduced clearance of emboli in patients with an impaired perfusion, this technique could not only be useful to identify patients at risk of hemodynamic events, but also be predictive of embolic stroke.

Our study had limitations. A general drawback of ASL MR perfusion imaging is the intrinsic low signal-to-noise ratio, which is caused by subtraction of the unlabeled from the labeled images to obtain the perfusion-weighted images.[39] Furthermore, the acquisition strategy with image acquisitions at multiple delay times may have caused an additional loss of signal because of the multiple small flip angles gradient echo acquisition strategy. Both the saturation effect of the multiple flip angles and the low flip angle used to reduce this saturation will result in less signal as compared with an ASL MRI technique at a single delay time and a flip angle of 90 degrees. However, an important advantage of the labeling strategy with acquisition at multiple delay times is that it can correct for delayed arrival of the arterial blood at the brain tissue.[14,40]

Conclusion

ASL MR perfusion imaging with image acquisition at multiple delay times can be used to non-invasively assess delays in the arrival of arterial blood to the brain. ASL MR perfusion imaging may provide valuable information on the quality of perfusion to the brain in cerebrovascular disease.

References

1. The European Carotid Surgery Trialists Collaborative Group. Randomised trial of endarterectomy for recently symptomatic carotid stenosis: final results of the MRC European Carotid Surgery Trial (ECST). Lancet 1998;351:1379-1387.
2. Barnett HJ, Taylor DW, Eliasziw M, et al. Benefit of carotid endarterectomy in patients with symptomatic moderate or severe stenosis. North American Symptomatic Carotid Endarterectomy Trial Collaborators. N Engl J Med 1998;339:1415-1425.
3. Derdeyn CP, Videen TO, Yundt KD, et al. Variability of cerebral blood volume and oxygen extraction: stages of cerebral haemodynamic impairment revisited. Brain 2002;125:595-607.
4. Markus H, Cullinane M. Severely impaired cerebrovascular reactivity predicts stroke and TIA risk in patients with carotid artery stenosis and occlusion. Brain 2001;124:457-467.
5. Blaser T, Hofmann K, Buerger T, et al. Risk of stroke, transient ischemic attack, and vessel occlusion before endarterectomy in patients with symptomatic severe carotid stenosis. Stroke 2002;33:1057-1062.
6. Liebeskind DS. Collaterals in acute stroke: beyond the clot. Neuroimaging Clin N Am 2005;15:553-573.
7. Kluytmans M, van der Grond J, Viergever MA. Gray matter and white matter perfusion imaging in patients with severe carotid artery lesions. Radiology 1998;209:675-682.
8. Lu J, Li K, Zhang M, et al. Dynamic susceptibility contrast perfusion magnetic resonance imaging in patients with symptomatic unilateral middle cerebral artery stenosis or occlusion. Acta Radiol 2007;48:335-340.
9. Trivedi RA, Green HA, King-Im J, et al. Cerebral haemodynamic disturbances in patients with moderate carotid artery stenosis. Eur J Vasc Endovasc Surg 2005;29:52-57.
10. Detre JA, Alsop DC, Vives LR, et al. Noninvasive MRI evaluation of cerebral blood flow in cerebrovascular disease. Neurology 1998;50:633-641.
11. Wolf RL, Alsop DC, McGarvey ML, et al. Susceptibility contrast and arterial spin labeled perfusion MRI in cerebrovascular disease. J Neuroimaging 2003;13:17-27.
12. Chalela JA, Alsop DC, Gonzalez-Atavales JB, et al. Magnetic resonance perfusion imaging in acute ischemic stroke using continuous arterial spin labeling. Stroke 2000;31:680-687.
13. Ances BM, McGarvey ML, Abrahams JM, et al. Continuous arterial spin labeled perfusion magnetic resonance imaging in patients before and after carotid endarterectomy. J Neuroimaging 2004;14:133-138.
14. Golay X, Hendrikse J, Lim TC. Perfusion imaging using arterial spin labeling. Top Magn Reson Imaging 2004;15:10-27.
15. Buxton RB, Frank LR, Wong EC, et al. A general kinetic model for quantitative perfusion imaging with arterial spin labeling. Magn Reson Med 1998;40:383-396.
16. Featherstone RL, Brown MM, Coward LJ. International carotid stenting study: protocol for a randomised clinical trial comparing carotid stenting with endarterectomy in symptomatic carotid artery stenosis. Cerebrovasc Dis 2004;18:69-74.
17. Simons PC, Algra A, van de Laak MF, et al. Second manifestations of ARTerial disease (SMART) study: rationale and design. Eur J Epidemiol 1999;15:773-781.
18. Hendrikse J, Lu H, van der Grond J, et al. Measurements of cerebral perfusion and arterial hemodynamics during visual stimulation using TURBO-TILT. Magn Reson Med 2003;50:429-433.
19. Keilholz-George SD, Knight-Scott J, Berr SS. Theoretical analysis of the effect of imperfect slice profiles on tagging schemes for pulsed arterial spin labeling MRI. Magn Reson Med 2001;46:141-148.
20. Gunther M, Bock M, Schad LR. Arterial spin labeling in combination with a look-locker sampling strategy: inflow turbo-sampling EPI-FAIR (ITS-FAIR). Magn Reson Med 2001;46:974-984.

21. Barth M, Moser E. Proton NMR relaxation times of human blood samples at 1.5 T and implications for functional MRI. Cell Mol Biol (Noisy -le-grand) 1997;43:783-791.
22. Herscovitch P, Raichle ME. What is the correct value for the brain--blood partition coefficient for water? J Cereb Blood Flow Metab 1985;5:65-69.
23. Rutgers DR, Klijn CJ, Kappelle LJ, et al. A longitudinal study of collateral flow patterns in the circle of Willis and the ophthalmic artery in patients with a symptomatic internal carotid artery occlusion. Stroke 2000;31:1913-1920.
24. Tatu L, Moulin T, Bogousslavsky J, et al. Arterial territories of the human brain: cerebral hemispheres. Neurology 1998;50:1699-1708.
25. Yang Y, Engelien W, Xu S, et al. Transit time, trailing time, and cerebral blood flow during brain activation: measurement using multislice, pulsed spin-labeling perfusion imaging. Magn Reson Med 2000;44:680-685.
26. van Laar PJ, Hendrikse J, Golay X, et al. In vivo flow territory mapping of major brain feeding arteries. Neuroimage 2006;29:136-144.
27. Kluytmans M, van der Grond J, van Everdingen KJ, et al. Cerebral hemodynamics in relation to patterns of collateral flow. Stroke 1999;30:1432-1439.
28. Bokkers RP, van Laar PJ, van de Ven KC, et al. Arterial spin-labeling MR imaging measurements of timing parameters in patients with a carotid artery occlusion. AJNR Am J Neuroradiol 2008;29:1698-1703.
29. Sallustio F, Kern R, Gunther M, et al. Assessment of intracranial collateral flow by using dynamic arterial spin labeling MRA and transcranial color-coded duplex ultrasound. Stroke 2008;39:1894-1897.
30. Penfield JG, Reilly RF, Jr. What nephrologists need to know about gadolinium. Nat Clin Pract Nephrol 2007;3:654-668.
31. Sadowski EA, Bennett LK, Chan MR, et al. Nephrogenic systemic fibrosis: risk factors and incidence estimation. Radiology 2007;243:148-157.
32. Wolf RL, Detre JA. Clinical neuroimaging using arterial spin-labeled perfusion magnetic resonance imaging. Neurotherapeutics 2007;4:346-359.
33. Deibler AR, Pollock JM, Kraft RA, et al. Arterial spin-labeling in routine clinical practice, part 2: hypoperfusion patterns. AJNR Am J Neuroradiol 2008;29:1235-1241.
34. Deibler AR, Pollock JM, Kraft RA, et al. Arterial spin-labeling in routine clinical practice, part 3: hyperperfusion patterns. AJNR Am J Neuroradiol 2008;29:1428-1435.
35. Sacco RL, Adams R, Albers G, et al. Guidelines for prevention of stroke in patients with ischemic stroke or transient ischemic attack: a statement for healthcare professionals from the American Heart Association/American Stroke Association Council on Stroke: co-sponsored by the Council on Cardiovascular Radiology and Intervention: the American Academy of Neurology affirms the value of this guideline. Stroke 2006;37:577-617.
36. Caplan LR, Hennerici M. Impaired clearance of emboli (washout) is an important link between hypoperfusion, embolism, and ischemic stroke. Arch Neurol 1998;55:1475-1482.
37. Forster A, Szabo K, Hennerici MG. Pathophysiological concepts of stroke in hemodynamic risk zones--do hypoperfusion and embolism interact? Nat Clin Pract Neurol 2008;4:216-225.
38. Barnett HJ, Meldrum HE. Endarterectomy for carotid stenosis: new approaches in patient selection. Cerebrovasc Dis 2001;11 Suppl 1:105-111.
39. Petersen ET, Zimine I, Ho YC, et al. Non-invasive measurement of perfusion: a critical review of arterial spin labelling techniques. Br J Radiol 2006;79:688-701.
40. Petersen ET, Lim T, Golay X. Model-free arterial spin labeling quantification approach for perfusion MRI. Magn Reson Med 2006;55:219-232.

CHAPTER 5

Reinoud P.H. Bokkers
Peter Jan van Laar
Kim C.C. van de Ven
L. Jaap Kappelle
Catharina J.M. Klijn
Jeroen Hendrikse

PERFUSION IMAGING OF ARTERIAL SPIN LABELING TIMING PARAMETERS IN PATIENTS WITH A CAROTID ARTERY OCCLUSION

Background and purpose: Arterial spin labeling (ASL) with image acquisition at multiple delay times can be exploited in perfusion MRI imaging to visualize and quantify the temporal dynamics of arterial blood inflow. In this study, we investigated the consequences of an internal carotid artery (ICA) occlusion and collateral blood flow on regional timing parameters.

Methods: Seventeen functionally independent patients with a symptomatic ICA occlusion (15 male and 2 women; mean age, 57±8 years) and 29 sex and age-matched control subjects were investigated. ASL at multiple delay times was used to quantify regional cerebral blood flow (CBF) and the transit and trailing edge times (arterial timing parameters reflecting, respectively, the beginning and end of the labelled bolus. Intra-arterial digital subtraction angiography and MR angiography were used to grade collaterals.

Results: In the hemisphere ipsilateral to the ICA occlusion the CBF was lower in the anterior frontal (31±4 versus 47±3 ml/min/100gr; p<0.01), posterior frontal (39±4 versus 55±2 ml/min/100gr; p<0.01) and frontal-parietal region (49±3 versus 61±3 ml/min/100gr; p=0.04) than in control subjects. The trailing edge of the frontal-parietal region was longer in the hemisphere ipsilateral to the ICA occlusion compared to control subjects (2225±167 versus 1593±35 ms; p<0.01). In patients with leptomeningeal collateral flow the trailing edge was longer in the anterior frontal region (2436±275 versus 1648±201 ms; p=0.03) and shorter in the occipital region (1815±128 versus 2388±203 ms; p=0.04) compared to patients without leptomeningeal collaterals.

Conclusion: Regional assessment of timing parameters with ASL may provide valuable information on the cerebral hemodynamic status. In patients with leptomeningeal collaterals the most impaired territory was found in the frontal lobe.

AJNR Am J Neuroradiol 2008;29(9):1698-703

Introduction

An obstructive lesion in the internal carotid artery (ICA) causes a reduction of the perfusion pressure in the cerebral circulation. As the cerebral perfusion pressure decreases, pressure is initially maintained by a compensatory vasodilation of the arterioles, followed by an increase in the oxygen extraction fraction.[1] Regionally the cerebral hemodynamic status depends not only on the degree of carotid obstruction, but also on other factors, such as the contribution of collateral pathways.[2,3]

The collateral circulation can provide alternative routes for oxygenated blood to reach the brain tissue, either through the primary pathways via the circle of Willis or the secondary pathways via leptomeningeal and ophthalmic collaterals.[4] The combination of a decreased cerebral perfusion pressure and an insufficient primary collateral blood supply may lead to hemodynamic impairment, which eventually can result in a limited clearance of emboli and ischemia.[5,6] Recruitment of the secondary collaterals is associated with further impairment and its presence may be considered a marker of inadequacy of the primary collateral pathways.[7,8] As the recruitment of collateral perfusion in patients with an ICA occlusion will lead to longer blood flow routes and a delayed arrival time of the blood, regional knowledge of the arrival times of arterial blood may provide additional information to characterize the collateral flow and may potentially be used to identify hemodynamically impaired regions. The most widely used methods to measure arrival times of blood use dynamic sampling of an injected bolus of contrast agent. However, due to the current concerns regarding contrast use in patients with poor renal function and ionizing radiation, an alternative without detrimental effects would be of great benefit.[9]

Recently, arterial spin labeling was introduced as a non-invasive method capable of assessing cerebral perfusion and the temporal dynamics of arterial blood inflow.[10] The purpose of our study was, first, to investigate hemodynamic parameters in different areas of the brain in patients with an occlusion of the ICA, and second, to evaluate the effect of collateral flow upon regional hemodynamics. We used an arterial spin labeling (ASL) magnetic resonance imaging (MRI) technique with image acquisition at multiple delay times to regionally quantify CBF and arterial timing parameters (transit and trailing edge times).

Methods

The institutional ethical standards committee approved the study protocol and written informed consent was obtained from all participants.

Patients

Seventeen functionally independent patients (15 male and 2 women; mean ±

standard deviation (SD), age, 57 ± 8 years) with an ICA occlusion, 11 were included in the study. All patients had transient or minor-disabling neurological deficits (modified Rankin score of 0 - 2) on the side of the occlusion [11] and were referred to the department of Radiology by vascular surgeons or neurologists for diagnosis and grading of the ICA obstruction. Patients who had experienced a severe stroke causing major disability (modified Rankin score of 3 – 5) in the past were not included. Diagnosis of the ICA obstruction was performed with intra-arterial DSA and the presence of a contralateral obstruction was graded in accordance to the North American Symptomatic Carotid Endarterectomy Trial criteria.[12] In eleven patients the ICA occlusion was located on the right side and in six patients on the left side.

The presence of collateral flow was assessed with intra-arterial DSA and MR-angiography (MRA). The direction of blood flow in the circle of Willis was assessed, according to a previously published imaging protocol,[13] with two consecutive two-dimensional phase contrast MRI measurements of which one was phase encoded in the left-right direction and one in the anteroposterior direction. Anterior collateral flow was defined as flow across the anterior communicating artery with retrograde flow in the pre-communicating part (A1 segment) of the anterior cerebral artery (ACA). Posterior to anterior flow in the posterior communicating artery was considered to represent posterior collateral flow. Leptomeningeal collaterals were judged as present if intra-arterial DSA showed cortical branches extending from the posterior cerebral artery that supplied the flow territory of the middle cerebral artery (MCA) or ACA.

The control group consisted of twenty-nine volunteers (25 male and 4 female; mean ± SD age, 57 ± 9 years) without a history of neurological disease, vascular pathology on T_1- or T_2-weighted MRI or MR angiography scans, or an ICA stenosis of more than 30%. The control subjects were matched to the patient group for sex and age. All control subjects were recruited from a vascular screening MRI imaging study involving subjects with symptomatic atherosclerosis or risk factors for atherosclerosis.[14]

MR imaging

Imaging was performed on a clinical 1.5 Tesla MRI scanner (Gyroscan ACS-NT, Philips Medical Systems, Best, The Netherlands). A quadrature head coil was used for radiofrequency transmission and signal reception. For perfusion MRI a pulsed ASL transfer insensitive labeling technique was used.[15] A single perfusion imaging slice was planned just above the ventricles through the centrum semiovale and aligned parallel to the orbitomeatal angle (Figure 1). Labeling was achieved by applying two consecutive slice-selective 90° radiofrequency pulses in a 140 mm thick labeling slab 10 mm proximal to the imaging slice. For image acquisition a series of thirteen 35° excitation pulses were applied, with increasing delay times from 200 to 2600 ms with a constant interval of 200 ms, followed by single shot gradient echo-planar-

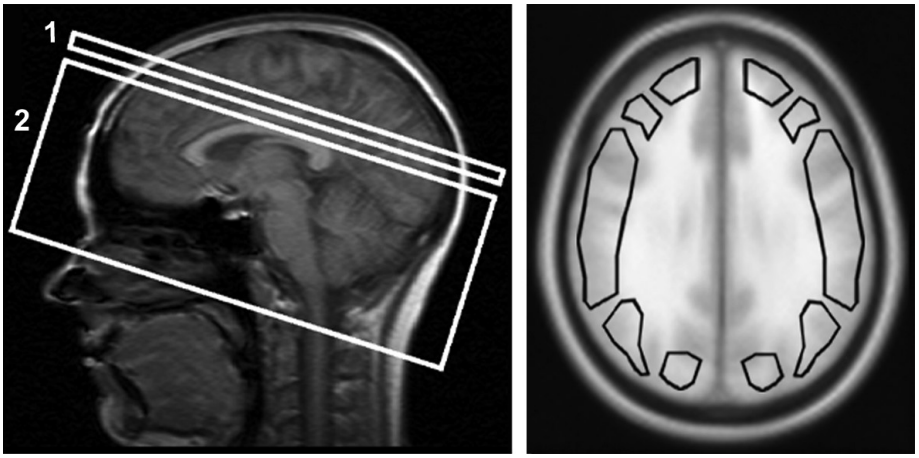

Figure 1: Left: sagittal orientation image illustrating the planning of the imaging slice (1) and the arterial spin labeling slab (2) parallel to the orbito-meatal angle. Right: regions of interest used for quantification of the hemodynamic parameters. In each hemisphere two regions of interests were drawn in the frontal lobe, and one in the frontal-parietal, parietal-occipital and occipital region.

Table 1. Patient characteristics.

Case	Age	Sex	Symptoms	Side of occlusion	Contralateral side	Collaterals flow pathways
1	44	V	Stroke	R	30 %	P + L
2	55	M	TIA	R	-	P
3	55	M	Stroke	R	-	A + P
4	48	M	TIA	R	-	A + P + L
5	53	M	Stroke	L	-	A + P
6	65	M	Stroke	R	-	A + L
7	77	M	AF	R	-	A + P
8	56	M	TIA	L	-	A + P
9	47	V	Stroke	R	-	P
10	55	M	Stroke	L	90 %	A + L
11	68	M	TIA	L	70 %	L
12	58	M	Stroke	R	30 %	A
13	53	M	TIA	R	30 %	A + P + L
14	65	M	TIA	R	-	A + L
15	60	M	Stroke	L	30 %	A + P
16	53	M	Stroke	R	-	A + L
17	58	M	Stroke	L	50 %	P + L

TIA indicates transient ischemic attack; AF, amaurosis fugax; A, anterior collateral pathway; P, posterior collateral pathway; L, leptomeningeal vessels.

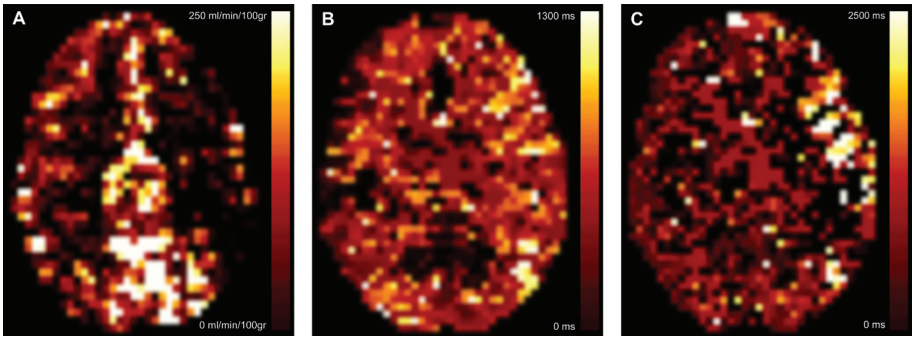

Figure 2: Transverse ASL perfusion MR images of a 76 year old man with a unilateral left-sided ICA occlusion. The images show the absolute CBF in ml/min/100gr (a), transit time in ms (b) and trailing edge in ms (c). Decreased CBF, increased transit time and increased trailing edge can be appreciated in the left hemisphere. *For color figure see page 156.*

imaging readout. ASL signal was corrected for imperfections in slice profiles.[16] Other MRI parameters for perfusion imaging were: TR 3000 ms; TE 5.6 ms; 62% partial Fourier acquisition; averages 50; field-of-view, 240 × 240 mm; 64 x 64 matrix; scan time, 5 min.

Cerebral blood flow, transit and trailing edge quantification

Perfusion-weighed images were obtained by subtracting the labeled images from the control images. In addition to quantifying CBF, ASL can also be used for the measurement of arterial timing parameters. By acquiring a series of perfusion images it is possible to follow the inflow of labeled blood into the vascular exchange site. The obtained kinetic data of blood inflow can be used to calculate the transit

Table 2. Hemodynamic values for the hemisphere ipsilateral to the occlusion in the patients with (n = 9) and with leptomeningeal collateral vessels.

	Leptomeningeal vessels present			No leptomeningeal vessels		
	CBF	Transit time	Trailing edge	CBF	Transit time	Trailing edge
Anterior frontal	31 ± 9	83 ± 46	2436 ± 275 *	31 ± 2	25 ± 15	1648 ± 201
Posterior frontal	29 ± 5 *	196 ± 103	2700 ± 469	47 ± 6	85 ± 32	1598 ± 348
Frontal-parietal	45 ± 4	228 ± 53	2362 ± 208	52 ± 6	97 ± 76	2103 ± 259
Parietal-occipital	41 ± 11	529 ± 163	2089 ± 285	33 ± 10	411 ± 106	2185 ± 271
Occipital	54 ± 13	381 ± 138	1815 ± 128 *	47 ± 5	359 ± 94	2388 ± 203

CBF values are given in ml/min/100gr and transit and trailing edge time in ms.
* significant difference between the patients with and without leptomeningeal vessels.

time and trailing edge times. These are physiological parameters that reflect the time needed for the labeled arterial blood to reach the brain tissue. Transit time is the duration between labeling and the first arrival of the magnetized blood into the imaging voxel. The trailing edge time is the duration needed for the end of the labeled bolus to reach the imaging voxel.

To quantify CBF, transit and trailing edge time, the perfusion signal (ΔM) at varying delay times (t) was fitted to the kinetic perfusion model of Buxton et al,[17] with the adaptations as proposed by Gunther et al [18]:

$$\Delta M(t) = 0 \qquad 0 < t < \tau_a \qquad [1]$$

$$\Delta M(t) = \frac{-2 \cdot M_{a,0} \cdot f}{\delta R} e^{-R_{1a} \cdot t} (1 - e^{\delta R \cdot (t - \tau_a)}) \qquad \tau_a \le t \le \tau_d \qquad [2]$$

$$\Delta M(t) = \frac{-2 \cdot M_{a,0} \cdot f}{\delta R} e^{-R_{1a} \cdot t_d} (1 - e^{\delta R \cdot (t - \tau_d)}) \cdot e^{-R_{1app,eff} \cdot (t - \tau_d)} \qquad t \ge \tau_d \qquad [3]$$

where f is the perfusion value CBF in ml/min/100gr, τ_a is the transit time, τ_d is the trailing edge time, $\delta R = R_{1a} - R_{1app,eff}$ and $R_{1app,eff} = R_1 + f/\lambda - \ln(\cos\alpha/\Delta TI)$, λ is the brain/blood partition coefficient, α is the flip angle, ΔTI is the time between consecutive readouts, R_{1a} is the longitudinal relaxation rate of arterial blood, R_1 is the longitudinal relaxation rate of tissue and $M_{a,0}$ is the equilibrium magnetization in a blood filled voxel, estimated by fitting the unlabeled signal in the sagittal sinus to a saturation-recovery curve. The following physical constants were obtained from literature: R_1, 1000 ms; R_{1a}, 1400 ms; λ (brain/blood partition coefficient of water), 0.9 mL/g.[19,20]

Data and statistical analysis

Data were analyzed with mathematic software (MATLAB, The Mathworks, Natick, Mass). Based on the ASL control images, regions of interests (ROIs) were drawn according to a standardized template symmetrically in both hemispheres, in distinct areas of gray matter (see Figure 1 for the locations of the ROIs).

SPSS (SPSS Inc., Chicago, Illinois, U.S.A.) for Windows, version 12.0.1, was used for statistical analysis. Mean CBF, transit and trailing edge times were calculated over all ROIs in the hemisphere on the side of the symptomatic and contralateral asymptomatic hemisphere. Because no differences were found in CBF, transit and trailing edge times between the left and right hemisphere in control subjects, values for both hemispheres were averaged for analysis. Differences in CBF, transit and trailing edge ROI measurements between the hemispheres ipsi and contra-lateral to the ICA occlusion, and the control group were evaluated using a one-way ANOVA with Bonferroni correction for multiple comparisons. To examine the influence of collateral flow patterns, differences between CBF, transit and trailing edge times in

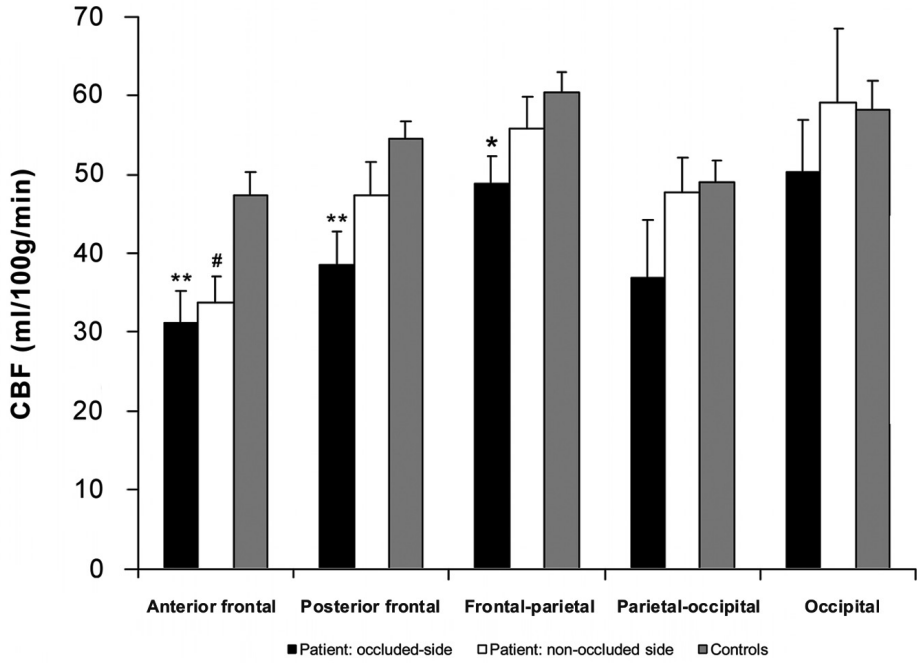

Figure 3: CBF (mean ± SEM) in the regions of the hemisphere ipsi and contra-lateral to the occlusion, and of the control group.

* significant difference ($p < 0.05$) between the hemisphere ipsilateral to the occlusion and the controls
** significant difference ($p < 0.01$) between the hemisphere ipsilateral to the occlusion and the controls
# significant difference ($p < 0.05$) between the hemisphere contralateral to the occlusion and the controls

the hemisphere ipsilateral to the ICA occlusion were evaluated using Student's t test. A p value of less than 0.05 was considered to indicate a statistically significant difference. Values are expressed as mean ± standard error of the mean (SEM).

Results

The baseline characteristics of the patients are given in Table 1. An example of an ASL MRI investigation of a patient with a symptomatic left-sided ICA occlusion is shown in Figure 2. Decreased CBF and increased timing parameters, resulting from a delayed arrival of the magnetically labeled bolus, can be appreciated in the left hemisphere.

Regional quantification of CBF, transit and trailing edge time

In the hemisphere ipsilateral to the ICA occlusion, the CBF was significantly lower than in the control subjects in the anterior frontal region (31 ± 4 versus 47 ± 3 ml/

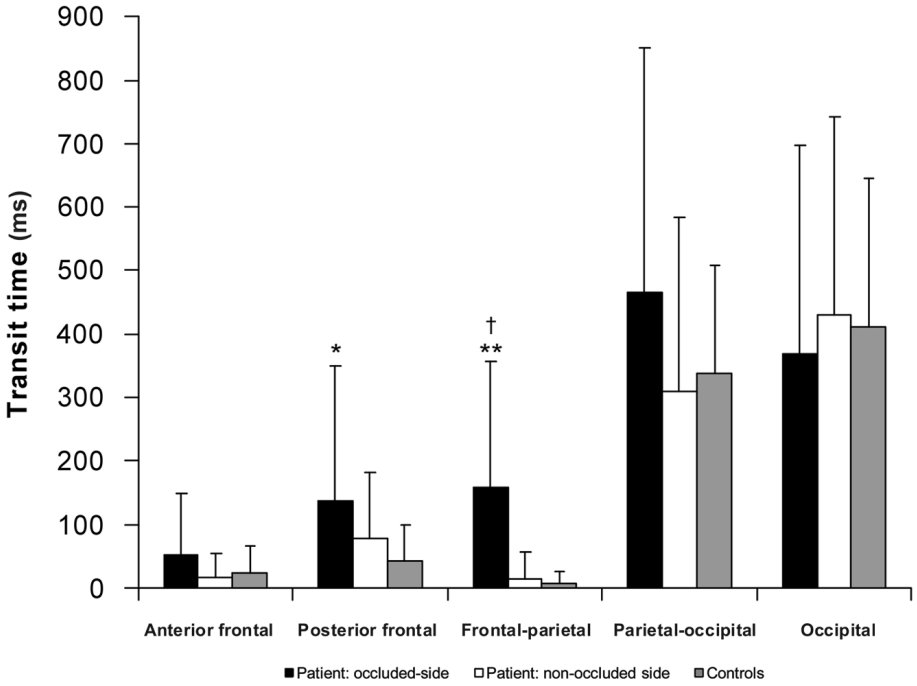

Figure 4: Transit time (mean ± SEM) in the regions of the hemisphere ipsi and contralateral to the occlusion, and of the control group.

* significant difference ($p < 0.05$) between the hemisphere ipsilateral to the occlusion and controls

** significant difference ($p < 0.01$) between the hemisphere ipsilateral to the occlusion and controls subjects

† significant difference ($p < 0.01$) between the hemisphere ipsi and contralateral to the ICA occlusion

min/100gr; $p < 0.01$), posterior frontal region (39 ± 4 versus 55 ± 2 ml/min/100gr; $p < 0.01$), and in the frontal-parietal region (49 ± 3 versus 61 ± 3 ml/min/100gr; $p = 0.04$) (Figure 3). In the hemisphere contralateral to the ICA occlusion, CBF in patients was significantly lower in the anterior frontal region than in control subjects (34 ± 3 versus 47 ± 3 ml/min/100gr; $p = 0.02$).

The transit time in the posterior frontal region ipsilateral to the ICA occlusion was prolonged (138 ± 52 ms; $p = 0.03$) compared to the control group (41 ± 11 ms) (Figure 4). In the frontal-parietal region ipsilateral to the ICA occlusion, the transit time (158 ± 49, $p < 0.01$) and the trailing edge (2225 ± 167, $p < 0.01$) were prolonged compared with the control subjects (respectively, 7 ± 4 ms and 1593 ± 35 ms) (Figure 5). In the hemisphere contralateral to the ICA occlusion, the trailing edge of the occipital region was significantly shorter in patients than in control subjects (1859 ± 122 ms versus 2289 ± 89 ms, $p = 0.02$).

Patients with leptomeningeal collateral flow (53%, n = 9) had a lower CBF in the posterior frontal region (29 ± 5 ml/min/100gr) than patients without leptomeningeal

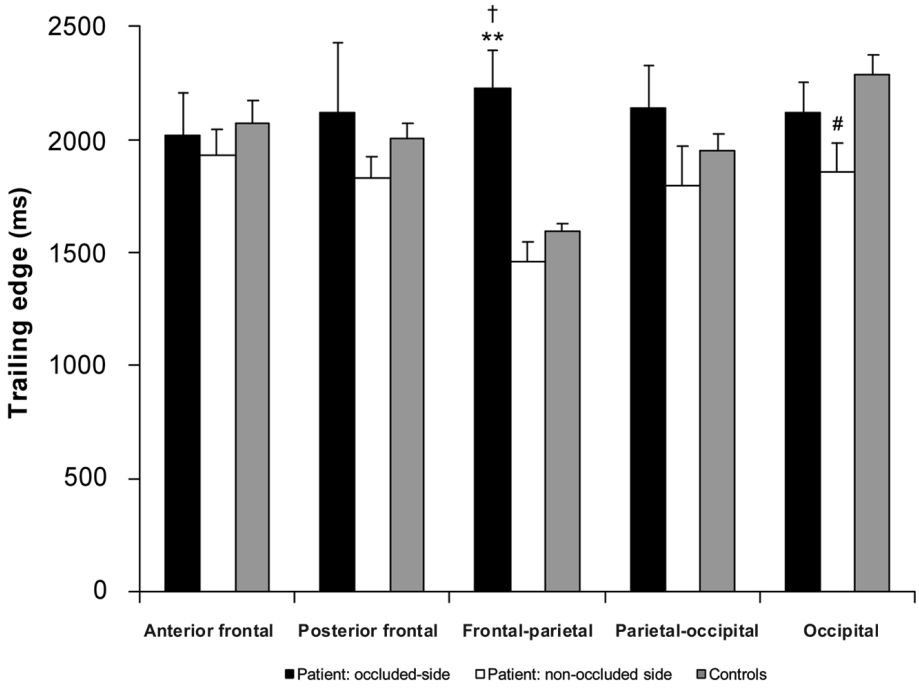

Figure 5: Trailing edge time (mean ± SEM) in the regions of the hemisphere ipsi and contralateral to the occlusion, and of the control group.

** significant difference ($p < 0.01$) between the hemisphere ipsilateral to the occlusion and controls subjects
# significant difference ($p < 0.05$) between the hemisphere contralateral to the occlusion and controls subjects
† significant difference ($p < 0.01$) between the hemisphere ipsi and contralateral to the ICA occlusion

collaterals (47 ± 6 ml/min/100gr, p = 0.04) in the hemisphere ipsilateral to the ICA occlusion. Furthermore, the trailing edge was longer in the anterior frontal region (2436 ± 275 versus 1648 ± 201 ms; p = 0.03) and shorter in the occipital region (1815 ± 128 versus 2388 ± 203 ms; p = 0.04) than in patients without leptomeningeal collateral flow. No differences in hemodynamic parameters were found for the presence or absence of collateral flow via the anterior (71%, n = 12) or posterior (65%, n = 11) collateral pathways.

Discussion

The most important findings of our study are twofold. Firstly, we found significant heterogeneity of regional cerebral hemodynamics in patients with a symptomatic ICA occlusion, with decreased CBF and increased timing parameters in the hemisphere ipsilateral to the occlusion. Secondly, in patients with leptomeningeal collateral flow there was a prolonged trailing edge in the anterior and a decreased CBF in the

posterior frontal region ipsilateral to the occlusion in comparison to patients without leptomeningeal collateral flow. Most of the modalities that can assess cerebral blood flow in patients are invasive and require the injection of a radioactive tracer or contrast agent.[21] ASL MRI has been developed to measure cerebral perfusion non-invasively by using magnetically labeled blood as an endogenous contrast agent.[10]

Most current ASL approaches acquire the imaging at a single inversion time point, which in healthy volunteers is sufficient for an adequate exchange of the label with the brain tissue water. However, in patients with an occlusion of the ICA collateral blood flow recruitment may result in increased transit times of the labeled blood to the brain tissue,[22] resulting in an underestimation of CBF.[23,24] By performing multiple ASL experiments at various delay times all labeled spin contribute to the perfusion signal and no prior knowledge of individuals transit times are needed. An additional advantage of this acquisition method is that it can be used to visualize and quantify the temporal dynamics of blood inflow and tissue perfusion.[18,25] While previous studies have demonstrated the ability of ASL at multiple delay time to measure timing parameters and the effect of brain activation on timing parameters,[15,26-28] this is the first study to investigate the consequences of an occlusion of the ICA and collateral blood flow patterns on regional ASL timing parameters and CBF.

In this study, we found a significant decreased CBF in both frontal and the frontal-parietal regions in the hemisphere ipsilateral to the ICA occlusion, which is in agreement with previous positron emission tomography (PET), ^{133}Xenon inhalation, and MRI based studies.[29-33] Furthermore, we demonstrated that the time needed for the labeled bolus to travel to the affected hemisphere is increased in patients with a symptomatic ICA occlusion, in regions corresponding to the anterior borderzone and the flow territory of the middle cerebral artery. In previous studies, researchers have found similar regional heterogeneity in hemodynamic parameters with ASL.[25] Roughly comparable measures to the ASL timing parameters are the arrival time and time to peak in dynamic contrast enhanced MR and CT perfusion imaging. In contrast enhanced perfusion studies of patients with an ICA occlusion, researchers have demonstrated increased time to peak times and reduced CBF in the gray and white-matter of the affected hemisphere,[34-36] which was thought to be caused by decreased flow in the arteries and increased dispersion in the microvasculature. This corresponds with our findings of a delayed arrival of arterial blood in the hemisphere ipsilateral to the ICA occlusion.

With the ten millimetre gap between the imaging and labeling slice, the time needed for the blood from the upper site of the labeled volume to travel to the brain tissue will depend on the vascular pathways distal to the circle of Willis. In contrast, the lower edge of the labeling volume is below the level of the circle of Willis. Therefore the trailing edge time will depend both on the vascular pathways proximal and distal to the circle of Willis. In the evaluation of the impact of collateral flow on the delay of arterial blood, the trailing edge will consequently be the most informative

parameter of the two. Furthermore, the transit and trailing edge times do not necessarily have to show a combined increase in patients with a vascular obstruction because the increase of timing parameters may, for instance, mainly depend on the rerouting of the labelled arterial blood proximal from the circle of Willis.

In our analysis of the role of collateral blood flow, we found that neither flow via the anterior or posterior collateral pathways had an effect on regional hemodynamic parameters in patients with ICA occlusion. Previous studies have indicated that hemodynamic and metabolic changes are more severe in patients without primary collaterals than in patients with primary collaterals,[3,37] and that the presence of secondary collateral flow is associated with an impaired hemodynamic status.[38,39] In this study, we found that patients with leptomeningeal collaterals and an occlusion of the ICA had a lower CBF and a prolonged trailing edge in the frontal lobe. No differences were found in symptoms between patients with and without leptomeningeal flow. Although the CBF measured in the frontal regions was low, it is above the value of 20 ml/min/100gr which is considered to indicated tissue at risk.[40] We hypothesize that the increased trailing edge time reflects the elongated path that the bolus of magnetically labeled blood has to travel through the leptomeningeal collaterals from the posterior circulation to the frontal lobe.

A disadvantage of using ASL at multiple delay times is the longer scan duration compared to single delay experiments. In this study we used a Look-Locker-Like sampling strategy to acquire the series of perfusion images at increasing delay times to decrease scan time. Although this makes it more practical for clinical use in patients, the train of small flip angle gradient echoes decreases the perfusion signal. Due to this signal loss, and additionally the decrease of signal due to the natural T^1 decay of the magnetised blood, we were not able to use crusher gradients. Therefore, a limitation of this study is that due to the presence of magnetic label within the vasculature, there may possibly be a regional overestimation of CBF. Although this is a well recognized problem of ASL, both the CBF values found in the patient group and the control subjects were within the reported range of previous PET studies.[1,30] In the present study, two of the seventeen patients with an occlusion of the ICA had a contralateral stenosis of 70% or larger which could have affected the hemodynamic measurements in the contralateral hemisphere. Furthermore, the DSA examinations, which were used to judge the presence of leptomeningeal collaterals, were not specifically performed to visualize leptomeningeal collaterals. Therefore, an underestimation of the prevalence of leptomeningeal collaterals is possible. In our study, nine of the seventeen patients (53%) had collateral flow through leptomeningeal vessels. Although there is a large interindividual variability in the number and size of leptomeningeal anastomoses, this is in accordance with previous reported prevalences.[41]

Conclusion

ASL with image acquisition at multiple delay times can be used to quantify the temporal dynamics of arterial blood inflow and identify brain regions with impaired hemodynamics. In this study we found significant heterogeneity of regional cerebral hemodynamics in patients with a symptomatic ICA occlusion. In patients with leptomeningeal collaterals the most impaired region is found in the frontal lobe.

References

1. Derdeyn CP, Videen TO, Yundt KD, et al. Variability of cerebral blood volume and oxygen extraction: stages of cerebral haemodynamic impairment revisited. Brain 2002;125:595-607.
2. Powers WJ, Press GA, Grubb RL, Jr. The effect of hemodynamically significant carotid artery disease on the hemodynamic status of the cerebral circulation. Ann Intern Med 1987;106:27-35.
3. Vernieri F, Pasqualetti P, Matteis M, et al. Effect of collateral blood flow and cerebral vasomotor reactivity on the outcome of carotid artery occlusion. Stroke 2001;32:1552-1558.
4. Powers WJ. Cerebral hemodynamics in ischemic cerebrovascular disease. Ann Neurol 1991;29:231-240.
5. Caplan LR, Hennerici M. Impaired clearance of emboli (washout) is an important link between hypoperfusion, embolism, and ischemic stroke. Arch Neurol 1998;55:1475-1482.
6. Schomer DF, Marks MP, Steinberg GK, et al. The anatomy of the posterior communicating artery as a risk factor for ischemic cerebral infarction. N Engl J Med 1994;330:1565-1570.
7. Liebeskind DS. Collateral Circulation. Stroke 2003;34:2279-2284.
8. Hofmeijer J, Klijn CJ, Kappelle LJ, et al. Collateral circulation via the ophthalmic artery or leptomeningeal vessels is associated with impaired cerebral vasoreactivity in patients with symptomatic carotid artery occlusion. Cerebrovasc Dis 2002;14:22-26.
9. Penfield JG, Reilly RF, Jr. What nephrologists need to know about gadolinium. Nat Clin Pract Nephrol 2007;3:654-668.
10. Golay X, Hendrikse J, Lim TC. Perfusion imaging using arterial spin labeling. Top Magn Reson Imaging 2004;15:10-27.
11. Bamford JM, Sandercock PAG, Warlow CP, et al. Interobserver agreement for the assessment of handicap in stroke patients. Stroke 1989;20:828.
12. Fox AJ. How to measure carotid stenosis. Radiology 1993;186:316-318.
13. Rutgers DR, Klijn CJ, Kappelle LJ, et al. A longitudinal study of collateral flow patterns in the circle of Willis and the ophthalmic artery in patients with a symptomatic internal carotid artery occlusion. Stroke 2000;31:1913-1920.
14. Simons PC, Algra A, van de Laak MF, et al. Second manifestations of ARTerial disease (SMART) study: rationale and design. Eur J Epidemiol 1999;15:773-781.
15. Hendrikse J, Lu H, van der Grond J, et al. Measurements of cerebral perfusion and arterial hemodynamics during visual stimulation using TURBO-TILT. Magn Reson Med 2003;50:429-433.
16. Keilholz-George SD, Knight-Scott J, Berr SS. Theoretical analysis of the effect of imperfect slice profiles on tagging schemes for pulsed arterial spin labeling MRI. Magn Reson Med 2001;46:141-148.
17. Buxton RB, Frank LR, Wong EC, et al. A general kinetic model for quantitative perfusion imaging with arterial spin labeling. Magn Reson Med 1998;40:383-396.
18. Gunther M, Bock M, Schad LR. Arterial spin labeling in combination with a look-locker sampling strategy: inflow turbo-sampling EPI-FAIR (ITS-FAIR). Magn Reson Med 2001;46:974-984.
19. Barth M, Moser E. Proton NMR relaxation times of human blood samples at 1.5 T and implications for functional MRI. Cell Mol Biol (Noisy -le-grand) 1997;43:783-791.
20. Herscovitch P, Raichle ME. What is the correct value for the brain--blood partition coefficient for water? J Cereb Blood Flow Metab 1985;5:65-69.
21. Wintermark M, Sesay M, Barbier E, et al. Comparative overview of brain perfusion imaging techniques. Stroke 2005;36:e83-e99.
22. Gibbs JM, Wise RJ, Leenders KL, et al. Evaluation of cerebral perfusion reserve in patients with carotid-artery occlusion. Lancet 1984;1:310-314.
23. Calamante F, Williams SR, van Bruggen N, et al. A model for quantification of perfusion in pulsed labelling techniques. NMR Biomed 1996;9:79-83.

24. Alsop DC, Detre JA. Reduced transit-time sensitivity in noninvasive magnetic resonance imaging of human cerebral blood flow. J Cereb Blood Flow Metab 1996;16:1236-1249.
25. Hendrikse J, Petersen ET, van Laar PJ, et al. Cerebral border zones between distal end branches of intracranial arteries: MR imaging. Radiology 2008;246:572-580.
26. Rao H, Wang J, Tang K, et al. Imaging brain activity during natural vision using CASL perfusion fMRI. Hum Brain Mapp 2007;28:593-601.
27. Gonzalez-At JB, Alsop DC, Detre JA. Cerebral perfusion and arterial transit time changes during task activation determined with continuous arterial spin labeling. Magn Reson Med 2000;43:739-746.
28. Yang Y, Engelien W, Xu S, et al. Transit time, trailing time, and cerebral blood flow during brain activation: measurement using multislice, pulsed spin-labeling perfusion imaging. Magn Reson Med 2000;44:680-685.
29. Norrving B, Nilsson B, Risberg J. rCBF in patients with carotid occlusion. Resting and hypercapnic flow related to collateral pattern. Stroke 1982;13:155-162.
30. Yamauchi H, Fukuyama H, Kimura J, et al. Hemodynamics in internal carotid artery occlusion examined by positron emission tomography. Stroke 1990;21:1400-1406.
31. Leblanc R, Yamamoto YL, Tyler JL, et al. Borderzone ischemia. Ann Neurol 1987;22:707-713.
32. Roc AC, Wang J, Ances BM, et al. Altered hemodynamics and regional cerebral blood flow in patients with hemodynamically significant stenoses. Stroke 2006;37:382-387.
33. Hendrikse J, van Osch MJ, Rutgers DR, et al. Internal carotid artery occlusion assessed at pulsed arterial spin-labeling perfusion MR imaging at multiple delay times. Radiology 2004;233:899-904.
34. Apruzzese A, Silvestrini M, Floris R, et al. Cerebral hemodynamics in asymptomatic patients with internal carotid artery occlusion: a dynamic susceptibility contrast MR and transcranial Doppler study. AJNR Am J Neuroradiol 2001;22:1062-1067.
35. van Osch MJ, Rutgers DR, Vonken EP, et al. Quantitative cerebral perfusion MRI and CO2 reactivity measurements in patients with symptomatic internal carotid artery occlusion. Neuroimage 2002;17:469-478.
36. Kluytmans M, van der Grond J, Viergever MA. Gray matter and white matter perfusion imaging in patients with severe carotid artery lesions. Radiology 1998;209:675-682.
37. Kluytmans M, van der Grond J, van Everdingen KJ, et al. Cerebral hemodynamics in relation to patterns of collateral flow. Stroke 1999;30:1432-1439.
38. Muller M, Schimrigk K. Vasomotor reactivity and pattern of collateral blood flow in severe occlusive carotid artery disease. Stroke 1996;27:296-299.
39. Tatemichi TK, Chamorro A, Petty GW, et al. Hemodynamic role of ophthalmic artery collateral in internal carotid artery occlusion. Neurology 1990;40:461-464.
40. Muir KW, Buchan A, von KR, et al. Imaging of acute stroke. Lancet Neurol 2006;5:755-768.
41. Brozici M, van der Zwan A, Hillen B. Anatomy and functionality of leptomeningeal anastomoses: a review. Stroke 2003;34:2750-2762.

.

PART 2
Cerebral autoregulation

CHAPTER 6

Reinoud P.H. Bokkers
Matthias J.P. van Osch
H. Bart van der Worp
Gert J. de Borst
Willem P.Th.M. Mali
Jeroen Hendrikse

CEREBRAL AUTOREGULATIVE IMPAIRMENT IN PATIENTS WITH A SYMPTOMATIC CAROTID ARTERY STENOSIS

Purpose: to measure the cerebral autoregulatory status of the brain tissue supplied by the individual brain feeding arteries in patients with symptomatic internal carotid artery (ICA) stenosis using arterial spin labeling (ASL) MRI and to compare this to healthy controls.

Methods: Institutional review board approval and informed consent were obtained. Twenty-three patients (69.3±8.0 years) with a unilateral symptomatic ICA stenosis and 20 healthy controls (66.8±6.3 years) underwent perfusion and flow-territory selective ASL MRI before and after intravenous acetazolamide administration. The cerebrovascular reactivity was measured throughout the brain in the gray matter supplied by the individual ICAs and the basilar artery. Data were analyzed using paired and unpaired *t*-tests.

Results: In patients with a symptomatic ICA stenosis, the flow territory of the symptomatic carotid artery was smaller than that of the asymptomatic carotid artery. After administration of acetazolamide, a statically significant increase in CBF at the brain tissue level was measured in both controls and patients in all perfusion territories. The cerebrovascular reactivity was 35.9±3.0% and 44.6±3.5% in the flow territories of the symptomatic and asymptomatic ICA, respectively, and 47.9±3.1% in the control subjects. The cerebrovascular reactivity was lower in the flow territory of the symptomatic ICA when compared to control subjects (mean difference, -12.0%; 95% confidence interval, -20.7 – -3.3).

Conclusion: The results of this study show that in patients with symptomatic ICA stenoses the vasodilatory capacity in the flow territories of the major cerebral arteries can be visualized and quantified at the brain tissue level with ASL MRI.

Radiology 2010;256(1):201-208

Introduction

Patients with symptomatic stenosis of the carotid artery have a high risk of ischemic stroke.[1,2] In these patients, impairment of the vasodilatory capacity of the cerebral vasculature is an important measure of the degree of hemodynamic compromise.[3] Autoregulatory vasodilatation of the terminal arterioles occurs in order to sustain normal perfusion by reducing the vascular resistance to arterial inflow.[4,5] In patients with a recent cerebral ischemic event, the vasodilatory capacity, or cerebrovascular reactivity, is reduced compared to patients without symptoms.[6] Ischemic events occur more frequently in patients with both high-grade stenoses and impaired cerebrovascular reactivity than in those with high-grade stenosis but normal reactivity.[7-11]

There are two basic strategies for measuring cerebral vasodilatory capacity. In the first strategy, the flow velocity in a major cerebral artery is measured before and after a vasodilatory stimulus. The increase in blood flow reflects the dilatory capacity of the vasculature distal to the artery.[12] The second strategy measures cerebral perfusion at the brain tissue level before and after a vasodilatory challenge with techniques such as positron emission tomography (PET), computed tomography (CT), single photon emission tomography (SPECT) or dynamic susceptibility contrast magnetic resonance imaging (MRI).[13,14] A disadvantage of these imaging methods is that they are invasive and require ionizing radiation and / or contrast agents. Furthermore, a steno-occlusive lesion in one of the brain feeding arteries may lead to a shift in the perfusion territories of these arteries,[15,16] making it difficult to measure vasodilatory capacity in the complete territory of an individual artery.

Arterial spin labeling (ASL) is an MRI technique for measuring cerebral blood flow (CBF) at the brain tissue level. It uses radiofrequency pulses to non-invasively label water protons in blood.[17-19] In conjunction with a vascular challenge, ASL MRI can measure the vasodilatory capacity throughout the brain at high spatial resolution.[20,21] Furthermore, with the recent introduction of flow territory-selective ASL techniques, it is also possible to visualize the perfusion territories of the individual brain feeding arteries.[22,23] By combining quantitative perfusion with flow territory-selective ASL, it is possible to simultaneously assess both the cerebral hemodynamic status at the brain tissue level and the flow territories of the major brain feeding arteries.

The aim of our study was to measure the cerebral autoregulatory status of the brain tissue supplied by the individual brain feeding arteries in patients with symptomatic internal carotid artery (ICA) stenosis using arterial spin labeling (ASL) MRI and to compare this to healthy controls.

Methods

The institutional ethical standards committee approved the study protocol and written informed consent was obtained from all participants.

Subjects

Twenty-three patients (13 men and 10 women; mean age ± standard deviation (SD), 69.3 ± 8.0 years) with a recently symptomatic unilateral ICA stenosis ≥ 50% referred to the Department of Radiology at the University Medical Center Utrecht for diagnosis and grading of the ICA stenosis were prospectively included in this study between January 2008 and February 2009. All patients had suffered a transient ischemic attack (TIA) or non-disabling ischemic stroke ipsilateral to the ICA stenosis. Patients were excluded from the study if they had diabetes mellitus, severe renal or liver dysfunction, or had experienced a severe stroke causing major disability (score on the modified Rankin scale of 3 – 5).[24] Grading of the ICA stenosis was performed with duplex ultrasonography. The control group consisted of 20 healthy volunteers (12 men and 8 women; mean age ± SD, 66.8 ± 6.3 years). All control subjects were recruited through local media advertisements and did not have a history of neurological disease or vascular pathology on MRI or MR angiography of the brain. The demographic and clinical characteristics of the participants are outlined in Table 1.

Table 1. Demographic and clinical characteristics of the study population.

	Healthy controls (n = 20)	**Patients** (n = 23)
Male, %	12 (60%)	13 (57%)
Age, mean years ± SD	66.8 ± 6.3	69.3 ± 8.0
Male	67.6 ± 6.2	69.1 ± 7.5
Female	66.9 ± 6.3	69.6 ± 9.0
Degree of symptomatic ICA stenosis		
0 – 49%	20	0
50 – 69%	0	2
70 – 99 %	0	21
Occluded	0	0
Presenting events, n		
Transient ischemic attack	0	13
Ischemic stroke	0	6
Amaurosis fugax	0	4

Unless otherwise specified, data are number of patients.

MR imaging

All MRI investigations were performed on a 3 Tesla MRI scanner (Achieva, Philips Medical Systems, Best, The Netherlands) equipped with an eight-channel head coil and locally developed software to enable ASL MR imaging. Both patients and volunteers underwent ASL perfusion MRI before and 15 minutes after intravenous administration of 14 mg/kg acetazolamide (Goldshield Pharmaceuticals, Croydon Surrey, UK). A T_1-weighted spin-echo sequence was obtained in the sagittal plane for positioning of the imaging section. Perfusion imaging was performed with a pseudo-continuous ASL sequence.[25] Labeling was performed by employing a train of 18 degrees, 0.5 ms, Hanning-shaped radiofrequency pulses at an interpulse pause of 0.5 ms, for a duration of 1650 ms, in combination with a balanced gradient scheme.[26,27] The control situation, without labeling of arterial blood, was achieved by adding 180° to the phase of all even RF pulses. Imaging was performed with single-shot echo planar imaging in combination with parallel imaging (SENSE factor, 2.5) 1525 ms after the labeling stopped. ASL MR imaging was performed in combination with background suppression, which consisted of a saturation pulse immediately before labeling and inversion pulses at 1680 and 2830 ms after the saturation pulse.[28] The perfusion images, consisting of seventeen 7 mm slices aligned parallel to the orbito-meatal angle, were acquired in ascending fashion with an in-plane resolution of 3 x 3 mm^2. The other ASL MRI parameters were: TR, 4000 ms; TE, 14 ms; pairs of control/label, 38; FOV, 240 x 240 x 119 mm; matrix, 80 x 79; scanning time 5 minutes.

For determination of the flow territories of the ICAs and the basilar artery, flow territory-specific perfusion images were acquired with selective ASL, according to a previously published protocol.[29,30] Selective labeling was accomplished by spatial manipulation of the labeling efficiency within the labeling plane, by applying additional gradients between the labeling pulses in sets of 5 dynamics as shown in Figure 1. The flow territories of the left ICA, right ICA and basilar artery were identified by means of k-means clustering.[31] An inversion-recovery sequence was acquired for measurement of the magnetization of arterial blood (M_0) and for segmentation purposes. Both the flow territory-selective ASL and inversion-recovery images were acquired with the same geometry and resolution as the quantitative perfusion ASL images. T_2weighted fluid attenuated inversion recovery images were acquired for detecting areas with tissue infarction using the following parameters: TR, 11000ms; TE, 125 ms; inversion time, 2800 ms; matrix size 240 x 240 with 24 slices; slice thickness 2mm.

Data analysis

Data were analyzed with MATLAB (The MathWorks, Natick, Mass, version 7.5) and SPM5 (Wellcome Trust Centre for Neuroimaging, Oxford, United Kingdom).

Cerebral blood flow ($mL{\cdot}100mL^{-1}{\cdot}min^{-1}$) was calculated from the ASL MR images according to a previously published model.[32] The T_2^* transversal relaxation

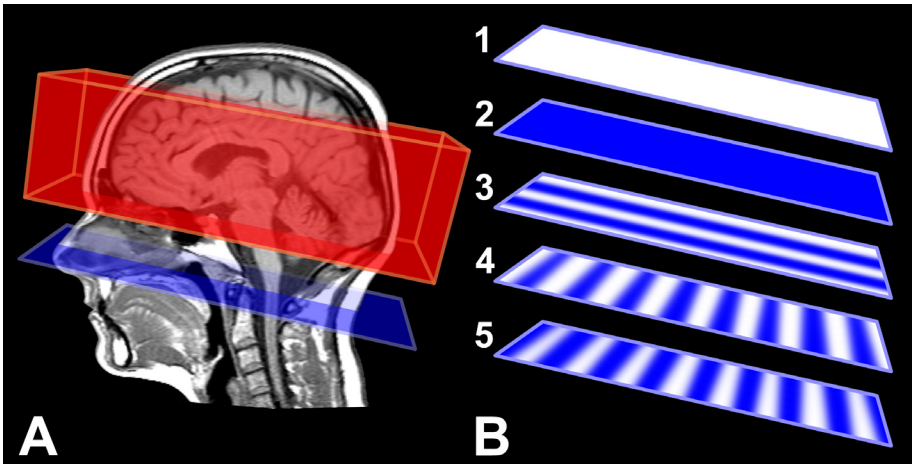

Figure 1. Sagittal T1 weighted image illustrating the imaging volume aligned parallel to the orbito-meatal angle and the labeling plane of the flow territory-specific perfusion selective ASL imaging (A). Labeling efficiency was spatially manipulated within the labeling plane in sets of five dynamics, in which: 1) no labeling applied (control), 2) non-selective labeling applied (globally perfusion weighted), 3) labeling varied in right-left (RL) direction (distance of 50 mm between full label and control situation), 4) labeling varied in anterior-posterior (AP1) direction (distance of 18 mm between full label and control situation), and 5) labeling varied in anterior-posterior direction (AP2, similar to AP1, but shifted 9 mm in posterior direction compared to the previous dynamic). *For color figure see page 157.*

rate of arterial blood and T_1 of blood were assumed to be 50 ms and 1680 ms, respectively.[33,34] The water content of blood was assumed to be 0.76 ml per milliliter of arterial blood.[35] The mean resting magnetization of the blood in all volunteers was determined by selecting a region of interest in the cerebrospinal fluid and iteratively fitting the inversion recovery data according to a previously outlined procedure.[35]

Cerebrovascular reactivity was defined as the percentage of increase in CBF after administration of acetazolamide. The CBF of the white and gray matter of the individual perfusion territories of the ICAs and basilar artery were measured before and after acetazolamide administration. For the placement of the regions of interest throughout all slices, three preprocessing steps were performed (Figure 2). First, a surrogate T_1-weighted image was calculated from the inversion recovery sequence by calculating the reciprocal of the quantitative T_1 and subsequently segmented with SPM into gray and white matter probability maps. Thresholding was applied to avoid partial voluming of white and gray matter. Secondly, the flow territories of the individuals ICAs and the basilar artery were defined. This was done by manually segmenting the perfusion territories of the individual arteries as determined with the flow territory-selective ASL sequence with the clustering algorithm. On all 17 slices, the flow territory border of the RPI image was delineated by one observer as shown in Figure 2. The final step was to combine the gray matter mask and

Table 2. CBF in mL·100mL^{-1}·min^{-1} and cerebrovascular reactivity (percent of CBF increase) before and after acetazolamide.

	Pre (mL·100mL^{-1}·min^{-1})	Post (mL·100mL^{-1}·min^{-1})	Reactivity (%)
Healthy controls			
ICA	52.2 ± 1.8	77.4 ± 3.2 *	47.9 ± 3.1
Basilar artery	48.7 ± 2.6	82.6 ± 4.8 *	69.9 ± 4.8
Patients			
Symptomatic ICA	44.7 ± 1.9	60.9 ± 3.0 *	35.9 ± 3.0 ** †
Asymptomatic ICA	43.1 ± 2.4	61.5 ± 3.1 *	44.6 ± 3.5
Basilar artery	42.9 ± 2.5	66.5 ± 3.7 *	56.7 ± 3.9

* Significant increase in CBF after administration of acetazolamide (paired *t* test).
** Significant difference in between patients and control subjects (unpaired *t* test).
† Significant difference in between the symptomatic and asymptomatic ICA flow territory (unpaired *t* test).

flow territory masks. Areas of hyperintensities on the FLAIR MR images, depicting areas of infarction, were manually excluded from the ROI. To correct for motion, all images pre- and post acetazolamide were coregistered, with SPM, to the baseline CBF map using a least squares approach and a six-parameter (rigid body) spatial transformation.

Flow territory maps of the individual brain feeding arteries in the patients with ICA stenoses and healthy control subjects were produced by normalizing the selective ASL images with SPM to a standardized PET brain template. The segmentations of the flow territories were then pooled and projected on a standardized T_1-weighted anatomical image. The combined flow territory maps were color coded to produce probability maps: 100% indicates that all subjects demonstrated perfusion in that area of the brain; 0% indicates that no subject demonstrated perfusion in that region. The flow territory maps of patients with a right-sided ICA stenosis were mirrored in the midline, whereas flow territory maps of patients with a left-sided stenosis remained unchanged. All images are displayed in radiologic coordinates.

Statistical analyses

SPSS (SPSS Inc., Chicago, Illinois, U.S.A.) for Windows, version 15.0.1, and MATLAB were used for statistical analysis. Descriptive statistical analyses were preformed to summarize patient characteristics. Differences between pre- and post acetazolamide CBF measurements and between the cerebrovascular reactivity measurements of the flow territory of the symptomatic and contralateral, asymptomatic ICA, were assessed using a paired *t* test. To compare the CBF and cerebrovascular reactivity measurements in the hemispheres ipsilateral and contralateral to the ICA stenosis

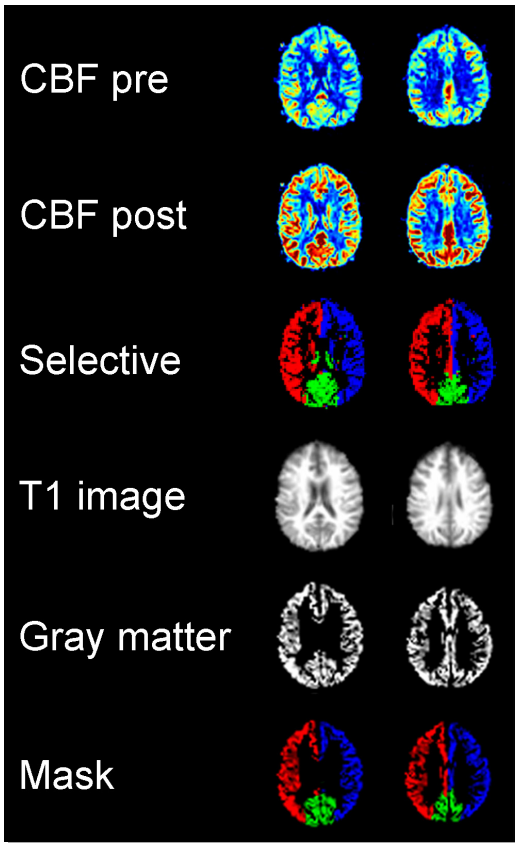

Figure 2. Pictorial description of the post-processing steps shows two of 17 slices in a 56-year old female. First shown are transverse CBF maps in mL·100mL^{-1}·min^{-1} before *(CBF pre)* and after administration *(CBF post)* administration of acetazolamide. Selective ASL images *(Selective)* show the perfusion territory of the right ICA (red), left ICA (blue) and basilar artery (green). T_1-weighted image was segmented into a gray-matter probability map. By combining the gray-matter map with the cerebral flow territory information from the selective ASL image, a gray-matter mask was obtained of both carotid arteries and the basilar artery. *For color figure see page 158.*

to those of the healthy control subjects an unpaired *t* test was used. Values were considered significantly different if the 95% confidence interval (CI) did not include zero.[36] Because no differences were found in CBF or cerebrovascular reactivity between the left and right ICAs in the control subjects (paired *t* test), values for both arteries were averaged for analysis. When patients were compared to controls, the data for controls was represented for each subject as an average over hemispheres. Voxel-based χ^2 testing with Bonferroni correction (corrected for the number of brain voxels in the flow territory sections) was performed to analyze differences in the extent of the flow territories between the symptomatic and asymptomatic ICA in patients, and control subjects. Values are expressed as mean ± SEM unless otherwise specified.

Results

Figure 3 shows CBF maps before and after acetazolamide administration in a 69-year-

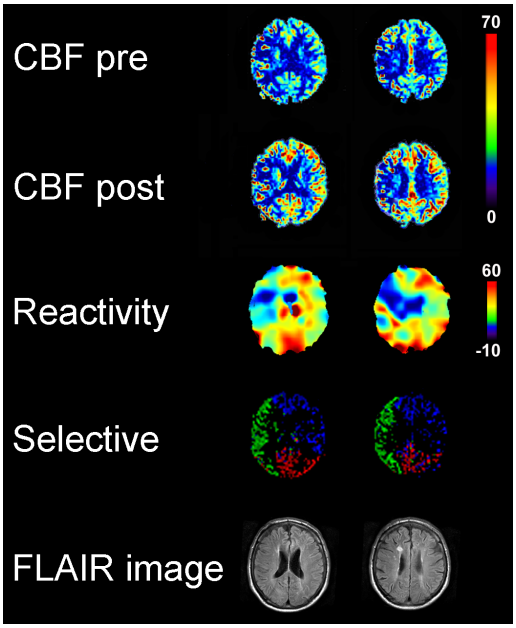

Figure 3. Transverse CBF maps in mL·100mL^{-1}·min^{-1} before *(CBF pre)* and after *(CBF post)* administration of acetazolamide of a 69-year old man with a symptomatic stenosis of the right ICA. CBF and a decreased cerebrovascular reactivity (percentage CBF increase) can are decreased, especially in the top slices, in the flow territory of the affected right ICA. For selective ASL image, green = right ICA territory; blue, left ICA territory; red, basilar artery territory; *FLAIR image,* fluid-attenuated inversion-recovery MR image. *For color figure see page 159.*

old man with a symptomatic stenosis of the right carotid artery. Figure 4 shows the segmented flow territory maps of the ICAs and the basilar artery, projected on a standardized brain template, for all patients with symptomatic ICA stenoses and for the healthy control subjects. The flow territory of the stenosed ICA was significantly smaller in size than that in the healthy control subjects. No changes in flow territory, indicative of intracranial steal, were observed after administration of acetazolamide in the patients with symptomatic ICA stenoses.

Comparisons of the extent of the flow territories of the symptomatic ICA with the asymptomatic ICA and the ICA territories in control subjects, demonstrated a significantly smaller flow territory on the symptomatic ICA. Table 2 summarizes the CBF values before and after administration of acetazolamide in the flow territories of the ICAs ipsilateral and contralateral to the symptomatic stenosis, and of the basilar artery. There was a significant ($p < 0.01$) increase in CBF at brain tissue level in all perfusion territories in both healthy controls and patients. In all flow territories, CBF was lower in patients than in the control group, but a reduced cerebrovascular reactivity as compared to controls was observed only in the territory of the symptomatic ICA (mean difference, -12.0%; 95% CI, -20.7 – -3.3). In the perfusion-territory of the symptomatic ICA, the cerebrovascular reactivity was non-significantly lower in the patients who had experiences stroke (n = 6; 34.8 ± 15.5%) than in the patients who had experienced a TIA (n = 13; 36.6 ± 15.8%; mean difference, 1.8; 95% CI, -14.6 – 18.2) or amaurosis fugax (n = 4; 35.3 ± 10.0%; mean difference, 0.5; 95% CI, -20.0 – 20.9). The cerebrovascular reactivity was

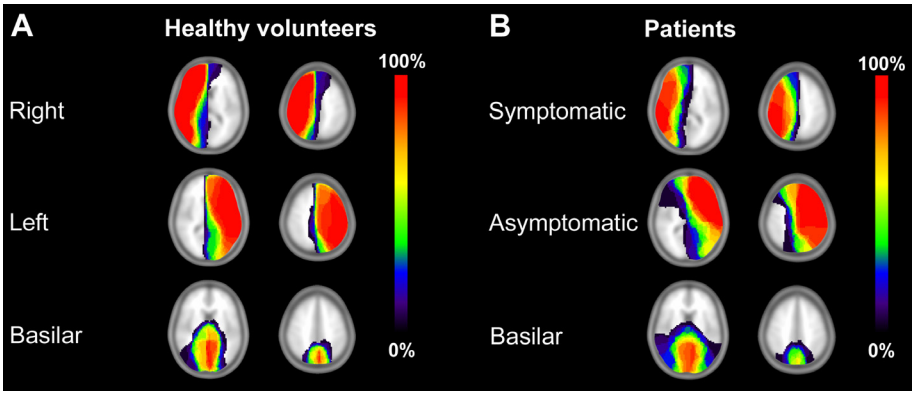

Figure 4. Transverse perfusion territory maps projected on a standardized brain template for right ICA, left ICA and basilar artery in **(a)** healthy control subjects (n = 20) and **(b)** patients with symptomatic ICA stenosis (n = 23). Scale indicates percentage of individuals in the group who had perfusion in that area. *For color figure see page 160.*

lower ($p < 0.01$) in the flow territory of the symptomatic ICA when compared to the contralateral asymptomatic ICA (mean difference, - 8.7%; 95% CI, -12.5 – -4.8). No difference in reactivity was observed between the asymptomatic ICA and healthy controls (mean difference, 4.7%; 95% CI, -12.9 – 6.3).

Discussion

In the present study, we were able to assess the hemodynamic status in the individual flow territories of the major brain feeding arteries. Patients with symptomatic ICA stenoses had decreased cerebral vasodilatory capacity measured with ASL in the brain tissue supplied by the symptomatic ICA when compared to the contralateral ICA and healthy control subjects. We also found that the flow territory of the symptomatic ICA was smaller than that of the asymptomatic, contralateral carotid artery.

Our results are in line with those of studies that have investigated reactivity by measuring the increase in flow velocity with transcranial Doppler in the major cerebral arteries,[37-39] and with studies that assessed reactivity at the brain tissue level in patients with a symptomatic carotid artery stenosis.[40-42] In previous studies measuring reactivity at the tissue level, regions of interest were selected based on traditional flow territory maps. However, a steno-occlusive lesion in the ICA can lead to a considerable shift in the flow territories of the brain feeding arteries,[43] affecting the reliability of these maps. The only cerebrovascular reactivity studies that have assessed the autoregulatory status of the efferent vasculature of the stenosed carotid are those with transcranial Doppler.[37-39] A disadvantage of this technique

is that this is based on measuring the global increase in blood flow velocity in a major cerebral artery, and does not assess perfusion changes at the tissue level. By combining quantitative perfusion with flow territory-selective ASL we were able to non-invasively assess the hemodynamic status at the brain tissue level and simultaneously visualize the perfusion territories of the major brain feeding arteries. Our finding of a smaller ICA flow territory ipsilateral to the stenosis indicates that the affected hemisphere is supplied with blood via collaterals from the contralateral ICA and vertebrobasilar arteries.

One study has previously assessed cerebrovascular reactivity with ASL MRI in patients with cerebrovascular disease.[20] In twelve patients with a symptomatic, anterior circulation, large artery stenosis cerebrovascular reactivity was measured using a continuous ASL approach at 1.5 Tesla. Varying patterns of CBF changes after administration of acetazolamide were observed, varying from focal and diffuse vasodilatory failure to normal autoregulation. In the present study, we included a healthy control group to avoid potential effects of generalized atherosclerosis. Furthermore, at 3 Tesla ASL benefits from an increased T^1 decay and higher signal to noise relative to 1.5 Tesla. And with the introduction of pseudo-continuous labeling schemes and background suppression, ASL image quality has improved significantly, which is especially of importance for reactivity measurements where differences in perfusion before and after a challenge are measured.

The decision to perform carotid endarterectomy or stenting in patients with a carotid artery stenosis is currently not dependent on the presence and severity of cerebral hemodynamic impairment.[44] Guidelines for the treatment of carotid stenosis are based primarily on large randomized clinical trials in which cerebral perfusion and hemodynamic reserve capacity were not taken into account. However, observational studies have strongly suggested that the risk of ischemic stroke is higher in patients with impaired cerebrovascular reactivity in the hemisphere ipsilateral to a symptomatic or asymptomatic carotid stenosis than those with a normal perfusion.[11,45] Assessment of the cerebrovascular reactivity at the brain tissue level with ASL MRI may therefore be used in future studies to non-invasively select those patients at the highest risk of stroke and who may benefit most from revascularization.

A limitation of the pulsed continuous ASL technique used in the present study is that the labeling of the arterial water spins is flow dependent. With an increase in flow velocity in the brain feeding arteries, as a result of administration of acetazolamide, the efficiency of labeling may decrease, leading to a reduction in the amount of blood that is labeled and subsequently to a lower CBF and vascular reactivity. However, this effect will be present in all arteries. Furthermore, with this ASL technique the images are made 1525 ms after labeling. It is possible that due to the increase in blood flow after administration of acetazolamide, the blood flows faster from the supplying arteries to the brain tissue, leading to an earlier

arrival of the magnetic bolus at the brain tissue and therefore to an earlier washout of the labeled blood. However, the parameters for the pulsed continuous ASL sequence were chosen such that this effect was minimized. Because only a single perfusion measurement was made after administration of acetazolamide, it is possible that due to variation in the time-response curve, the maximal response of CBF was not reached. However, perfusion measurements were obtained after 15 minutes, which previous studies have indicated to be within the plateau phase of maximal response.[46,47] Both an advantage and a limitation of the present study is that the mean cerebrovascular reactivity of the complete flow territory was measured, possibly resulting in the dilution of the effects of small areas with a severely decreased reactivity. Furthermore, it is possible that due to hemodynamic steal there has been a shift of the flow territories of the brain feeding arteries in individual patients.

Conclusion

In this study we used a quantitative perfusion and flow territory-selective ASL to measure the vasodilatory capacity. The results of this study show that in patients with a symptomatic ICA stenosis, the vasodilatory capacity in the flow territories of the major cerebral arteries can be visualized and quantified at the brain tissue level with ASL MRI. Decreased vasodilatory capacity was measured in the brain tissue supplied by the symptomatic ICA. With further testing and validation, reactivity measurements with ASL MR imaging may be used as a diagnostic tool to evaluate cerebral autoregulation.

References

1. The European Stroke Prevention Study (ESPS). Principal end-points. The ESPS Group. Lancet 1987;2:1351-1354.
2. Barnett HJM, Taylor DW, Eliasziw M, et al. Benefit of carotid endarterectomy in patients with symptomatic moderate or severe stenosis. N Eng J Med 1998;339:1415-1425.
3. Derdeyn CP, Videen TO, Yundt KD, et al. Variability of cerebral blood volume and oxygen extraction: stages of cerebral haemodynamic impairment revisited. Brain 2002;125:595-607.
4. Lassen NA. Cerebral blood flow and oxygen consumption in man. Physiol Rev 1959;39:183-238.
5. MacKenzie ET, Farrar JK, Fitch W, Graham DI, Gregory PC, Harper AM. Effects of hemorrhagic hypotension on the cerebral circulation. I. Cerebral blood flow and pial arteriolar caliber. Stroke 1979;10:711-718.
6. Kleiser B, Widder B. Course of carotid artery occlusions with impaired cerebrovascular reactivity. Stroke 1992;23:171-174.
7. Silvestrini M, Vernieri F, Pasqualetti P, et al. Impaired cerebral vasoreactivity and risk of stroke in patients with asymptomatic carotid artery stenosis. JAMA 2000;283:2122-2127.
8. Powers WJ. Cerebral hemodynamics in ischemic cerebrovascular disease. Ann Neurol 1991;29:231-240.
9. Yonas H, Smith HA, Durham SR, Pentheny SL, Johnson DW. Increased stroke risk predicted by compromised cerebral blood flow reactivity. J Neurosurg 1993;79:483-489.
10. Gur AY, Bova I, Bornstein NM. Is impaired cerebral vasoreactivity a predictive factor of stroke in asymptomatic patients. Stroke 1996;27:2188-2190.
11. Markus H, Cullinane M. Severely impaired cerebrovascular reactivity predicts stroke and TIA risk in patients with carotid artery stenosis and occlusion. Brain 2001;124:457-467.
12. Aaslid R, Markwalder TM, Nornes H. Noninvasive transcranial Doppler ultrasound recording of flow velocity in basal cerebral arteries. J Neurosurg 1982;57:769-774.
13. Eskey CJ, Sanelli PC. Perfusion imaging of cerebrovascular reserve. Neuroimaging Clin N Am 2005;15:367-381.
14. Derdeyn CP, Grubb RLJ, Powers WJ. Cerebral hemodynamic impairment: methods of measurement and association with stroke risk. Neurology 1999;53:251-259.
15. van der Zwan A, Hillen B, Tulleken CAF, Dujovny M, Dragovic L. Variability of the territories of the major cerebral arteries. J Neurosurg 1992;77:927-940.
16. van Laar PJ, Hendrikse J, Golay X, Lu H, van Osch MJ, van der Grond J. In vivo flow territory mapping of major brain feeding arteries. Neuroimage 2006;29:136-144.
17. Williams DS, Detre JA, Leigh JS, Koretsky AP. Magnetic resonance imaging of perfusion using spin inversion of arterial water. Proc Natl Acad Sci U S A 1992;89:212-216.
18. Detre JA, Leigh JS, Williams DS, Koretsky AP. Perfusion imaging. Magn Reson Med 1992;23:37-45.
19. Edelman RR, Siewert B, Darby DG, et al. Qualitative mapping of cerebral blood flow and functional localization with echo-planar MR imaging and signal targeting with alternating radio frequency. Radiology 1994;192:513-520.
20. Detre JA, Samuels OB, Alsop DC, Gonzalez-At JB, Kasner SE, Raps EC. Noninvasive magnetic resonance imaging evaluation of cerebral blood flow with acetazolamide challenge in patients with cerebrovascular stenosis. J Magn Reson Imaging 1999;10:870-875.
21. Zhao P, Alsop DC, Abduljalil A, et al. Vasoreactivity and peri-infarct hyperintensities in stroke. Neurology 2009;72:643-649.
22. Paiva FF, Tannus A, Silva AC. Measurement of cerebral perfusion territories using arterial spin labelling. NMR Biomed 2007;20:633:642.
23. van Laar PJ, van der Grond J, Hendrikse J. Brain perfusion territory imaging: methods and clinical applications of selective arterial spin-labeling MR imaging. Radiology 2008;246:354-364.

24. Bamford JM, Sandercock PAG, Warlow CP, Slattery J. Interobserver agreement for the assessment of handicap in stroke patients. Stroke 1989;20:828.
25. Dai W, Garcia D, de Bazelaire C, Alsop DC. Continuous flow-driven inversion for arterial spin labeling using pulsed radio frequency and gradient fields. Magn Reson Med 2008;60:1488-1497.
26. Garcia DM, de Bazelaire C, Alsop DC. Pseudo-continuous Flow Driven Adiabatic Inversion for Arterial Spin Labeling. Proceedings 13th Scientific Meeting, ISMRM 2005:37.
27. Wu WC, Fernandez-Seara M, Detre JA, Wehrli FW, Wang J. A theoretical and experimental investigation of the tagging efficiency of pseudocontinuous arterial spin labeling. Magn Reson Med 2007;58:1020-1027.
28. Ye FQ, Frank JA, Weinberger DR, McLaughlin AC. Noise reduction in 3D perfusion imaging by attenuating the static signal in arterial spin tagging (ASSIST). Magn Reson Med 2000;44:92-100.
29. Gevers S, Nederveen A, Bokkers RP, et al. Reproducibility of flow territories defined by plannings-free vessel encoded pseudo-continuous arterial spin labeling. Proceedings 17th Scientific Meeting, ISMRM 2009:1524.
30. Wong EC. Vessel-encoded arterial spin-labeling using pseudocontinuous tagging. Magn Reson Med 2007;58:1086-1091.
31. Wong EC, Kansagra AP. Mapping Middle Cerebral Artery Branch Territories with Vessel Encoded Pseudo-Continuous ASL: Sine/Cosine Tag Modulation and Data Clustering in Tagging Efficiency Space. Proceedings 16th Scientific Meeting, ISMRM 2008:182.
32. Alsop DC, Detre JA. Reduced transit-time sensitivity in noninvasive magnetic resonance imaging of human cerebral blood flow. J Cereb Blood Flow Metab 1996;16:1236-1249.
33. Golay X, Petersen ET, Hui F. Pulsed star labeling of arterial regions (PULSAR): a robust regional perfusion technique for high field imaging. Magn Reson Med 2005;53:15-21.
34. St Lawrence KS, Wang J. Effects of the apparent transverse relaxation time on cerebral blood flow measurements obtained by arterial spin labeling. Magn Reson Med 2005;53:425-433.
35. Chalela JA, Alsop DC, Gonzalez-Atavales JB, Maldjian JA, Kasner SE, Detre JA. Magnetic resonance perfusion imaging in acute ischemic stroke using continuous arterial spin labeling. Stroke 2000;31:680-687.
36. Gardner MJ, Altman DG. Confidence intervals rather than P values: estimation rather than hypothesis testing. Br Med J (Clin Res Ed) 1986;292:746-750.
37. Silvestrini M, Troisi E, Matteis M, Cupini LM, Caltagirone C. Transcranial Doppler assessment of cerebrovascular reactivity in symptomatic and asymptomatic severe carotid stenosis. Stroke 1996;27:1970-1973.
38. Soinne L, Helenius J, Tatlisumak T, et al. Cerebral hemodynamics in asymptomatic and symptomatic patients with high-grade carotid stenosis undergoing carotid endarterectomy. Stroke 2003;34:1655-1661.
39. Telman G, Kouperberg E, Nitecki S, et al. Cerebral hemodynamics in symptomatic and asymptomatic patients with severe unilateral carotid stenosis before and after carotid endarterectomy. Eur J Vasc Endovasc Surg 2006;32:375-378.
40. Chen A, Shyr MH, Chen TY, Lai HY, Lin CC, Yen PS. Dynamic CT perfusion imaging with acetazolamide challenge for evaluation of patients with unilateral cerebrovascular steno-occlusive disease. AJNR Am J Neuroradiol 2006;27:1876-1881.
41. Bisdas S, Nemitz O, Berding G, et al. Correlative assessment of cerebral blood flow obtained with perfusion CT and positron emission tomography in symptomatic stenotic carotid disease. Eur Radiol 2006;16:2220-2228.
42. Hasegawa Y, Yamaguchi T, Tsuchiya T, Minematsu K, Nishimura T. Sequental change of hemodynamic reserve in patients with major cerebral artery occlusion or severe stenosis. Neuroloradiology 1992;34:15-21.

43. van Laar PJ, Hendrikse J, Mali WP, et al. Altered flow territories after carotid stenting and carotid endarterectomy. J Vasc Surg 2007;45:1155-1161.
44. Sacco RL, Adams R, Albers G, et al. Guidelines for prevention of stroke in patients with ischemic stroke or transient ischemic attack: a statement for healthcare professionals from the American Heart Association/American Stroke Association Council on Stroke: co-sponsored by the Council on Cardiovascular Radiology and Intervention: the American Academy of Neurology affirms the value of this guideline. Stroke 2006;37:577-617.
45. Blaser T, Hofmann K, Buerger T, Effenberger O, Wallesch CW, Goertler M. Risk of stroke, transient ischemic attack, and vessel occlusion before endarterectomy in patients with symptomatic severe carotid stenosis. Stroke 2002;33:1057-1062.
46. Dahl A, Russell D, Rootwelt K, Nyberg-Hansen R, Kerty E. Cerebral vasoreactivity assessed with transcranial Doppler and regional cerebral blood flow measurements. Dose, serum concentration, and time course of the response to acetazolamide. Stroke 1995;26:2302-2306.
47. Grossmann WM, Koeberle B. The dose-response relationship of acetazolamide on the cerebral blood flow in normal subjects. Cerebrovasc Dis 2000;10:65-69.

CHAPTER 7

Reinoud P.H. Bokkers
Matthias J.P. van Osch
Catharina J.M. Klijn
L. Jaap Kappelle
Jeroen Hendrikse

CEREBRAL AUTOREGULATIVE IMPAIRMENT WITHIN PERFUSION TERRITORIES IN PATIENTS WITH A SYMPTOMATIC CAROTID ARTERY OCCLUSION

Background and purpose: Arterial spin labeling (ASL) is a magnetic resonance imaging technique for measuring perfusion at brain tissue level. The aim of our study was to investigate cerebrovascular reactivity (CVR) at brain tissue level in patients with an internal carotid artery (ICA) occlusion by combining ASL-MRI with a vascular challenge, and determine whether the CVR varies within the perfusion-territory of the brain feeding arteries.

Methods: Sixteen patients with a symptomatic ICA occlusion and 16 age-matched healthy control subjects underwent perfusion and perfusion-territory selective ASL-MRI before and after acetazolamide administration. CVR was assessed throughout the brain in the gray-matter supplied by the unaffected asymptomatic ICA and the basilar artery.

Results: Cerebral blood flow increased ($p<0.01$) in all perfusion-territories after acetazolamide in the patients and controls. In the tissue supplied by the unaffected contralateral ICA, CVR was lower in the tissue supplied by the unaffected contralateral ICA in the patients when compared to the controls (22.8±16.1 vs. 54.2±13.1%; mean difference, -31.5%; 95% confidence interval (CI), -42.1–-20.8). Within the perfusion-territory of the unaffected ICA, the CVR was lower in the brain tissue on the side of the occluded ICA than on the side of the unaffected ICA (13.5±20.4 vs. 26.2±16.0%; paired mean difference, -12.5%; 95% CI, -20.3–-4.7).

Conclusion: ASL-MRI can assess impaired cerebrovascular reactivity at brain tissue level in patients with a symptomatic ICA occlusion. Assessment of CVR with ASL-MRI may possibly help identify the tissue most at risk for future stroke and as such may guide medical treatment.

J Neurol Neurosurg Psychiatry 2011 Mar 8. Ahead of print.

Introduction

Patients with a symptomatic internal carotid artery (ICA) occlusion have an annual risk of 5 - 6% for recurring stroke.[1] This risk is raised to 9 - 18% per year in patients with compromised cerebral hemodynamics and poor collateral blood flow.[2-4] A large, international randomized trial in 1985 showed that extracranial to intracranial (EC/IC) bypass surgery does not prevent stroke in patients with symptomatic ICA occlusion.[5] Additional studies have however suggested that patients with hemodynamic compromise of the brain perfusion, may benefit from bypass surgery.[6]

Hemodynamic compromise occurs when the compensatory responses of the brain to a decrease in the perfusion pressure are exhausted and adequate cerebral blood flow cannot be maintained.[7] With a steno-occlusive lesion in one or more brain feeding arteries, additional flow is initially recruited through collateral pathways.[8] When this flow is not sufficient, resistance arterioles dilate in order to reduce the vascular resistance to arterial inflow. The vasodilatory capacity, or cerebrovascular reactivity, can be assessed indirectly by measuring the dilatory response after a vascular challenge. This can be measured either at brain tissue level with techniques like positron emission tomography (PET) and single photon emission tomography, or by measuring the increase in flow-velocity in the middle cerebral artery with transcranial Doppler (TCD).[2,3,9] Both approaches have limitations. The measurements at brain tissue level are non-specific to the route of blood supply and flow-velocity measurements are limited to single brain feeding arteries. In patients with a steno-occlusive lesion in one of the ICAs this is especially problematic as additional blood is recruited through collateral pathways and there is a shift in the perfusion-territories of the brain feeding arteries.[10,11]

Arterial spin labeling perfusion magnetic resonance imaging (ASL-MRI), in combination with a vascular challenge, has been introduced as an alternative technique for measuring cerebrovascular reactivity at brain tissue level.[12,13] ASL-MRI uses radiofrequency pulses to magnetically label blood and does not require gadolinium-based contrast agents. With the recent introduction of perfusion-territory selective labeling techniques, ASL-MRI can also visualize the individual contribution of the cerebral arteries and collateral vessels to the brain.[14,15]

The objective of this study was to assess cerebrovascular reactivity at brain tissue level with ASL-MRI in patients with an ICA occlusion and in healthy controls, and determine whether cerebrovascular reactivity varies within the perfusion-territories of the brain feeding arteries of patients with an ICA occlusion.

Methods

The institutional ethical standards committee approved the study protocol and written informed consent was obtained from all participants.

Table 1. Demographic and clinical characteristics of the study population.

	Controls (n=16)	**Patients** (n=16)
Age, mean years ± SD	56.5 ± 5.7	56.3 ± 13.8
Male, y	5 (31.3%)	12 (75%)
Degree of contralateral ICA stenosis		
0–49%	0	10
50–69%	0	4
70–99%	0	2
Occluded	0	0
Presenting events		
Transient ischemic attack	0	10
Ischemic stroke	0	5
Amaurosis fugax	0	1

Unless otherwise specified, data are number of patients.

Subjects

Sixteen patients (mean age ± standard deviation (SD), 56.3 years ± 13.8) with a recently symptomatic atherosclerotic ICA occlusion and 16 age-matched healthy control volunteers (mean ± SD age, 56.5 ± 5.7) were prospectively included into the study. All patients were admitted to our hospital because of a transient ischemic attack (TIA) or non-disabling stroke on the side of the ICA occlusion. Imaging was performed within three months of symptom onset. Patients were excluded from the study if they had diabetes mellitus, severe renal or liver dysfunction, or had experienced a stroke causing major disability (modified Rankin score of 3 – 5) in the past.[16] Diagnosis of the ICA occlusion was performed with either computed tomography or MR angiography. The healthy control volunteers were recruited through local media advertisements and were without a history of neurological disease or vascular pathology on MRI or MR angiography. The demographic and clinical characteristics of the subjects are outlined in Table 1.

MR imaging

All MRI investigations were performed on a clinical 3 Tesla MRI scanner (Achieva, Philips Medical Systems, Best, The Netherlands). Perfusion images were obtained before and 15 minutes after administration of a bolus of 14 mg/kg, with a maximum dose of 1200 mg, acetazolamide (Goldshield Pharmaceuticals, Croydon, UK). Perfusion imaging was performed with a pseudo-continuous ASL sequence in combination with background suppression.[17] For positioning of the imaging section a low-resolution T_1-weighted spin-echo sequence was obtained in the sagittal plane.

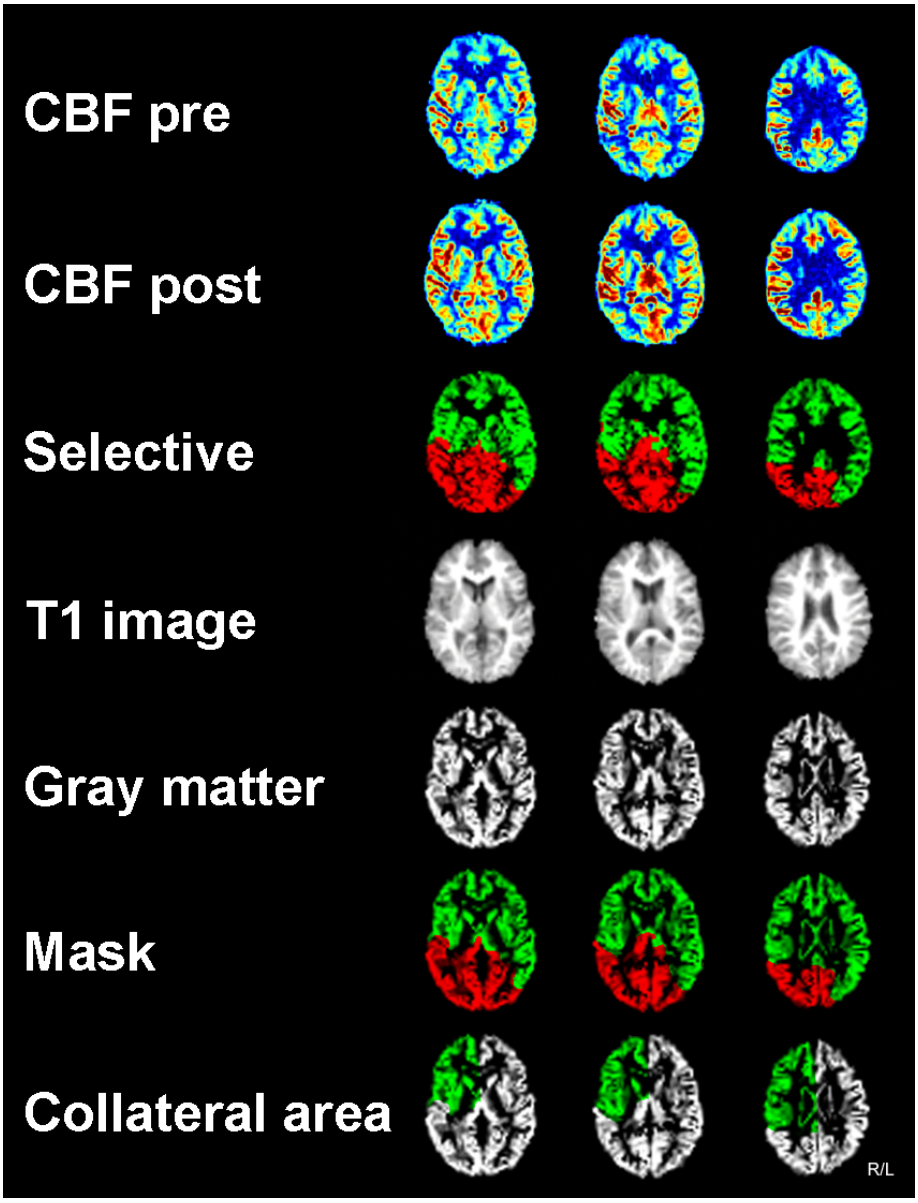

Figure 1: Pictorial description of the preprocessing steps in 3 of the 17 slices in a patient with an occluded right ICA. First shown are transverse CBF maps in mL·100mL^{-1}·min^{-1} before *(CBF pre)* and after administration *(CBF post)* administration of acetazolamide. Selective ASL images *(Selective)* show the perfusion territory of the ICA (green) and basilar artery (red). T_1-weighted image was segmented into a gray-matter probability map. By combining the segmented gray matter map with the perfusion-territory information, a gray-matter mask was obtained of the ICA, basilar artery and collateral pathways originating from the unaffected contralateral ICA. *For color figure see page 161.*

The perfusion images consisted of seventeen 7 mm slices aligned parallel to the orbitomeatal angle, acquired in ascending fashion with an in-plane resolution of 3 x 3 mm (true acquisition resolution). The other ASL-MRI parameters were: repetition time (TR), 4000 ms; echo time (TE), 14 ms; pairs of control/label, 38; post-labeling delay, 1525 ms; field-of-view (FOV), 240 x 240 x 119 mm^2; matrix, 80 x 79; SENSE factor, 2.5; scan time, 5 minutes.

The perfusion-territories of the carotid arteries and the basilar artery were assessed with a perfusion-territory selective ASL sequence using pseudo-continuous tagging, according to a previously published protocol.[18] Selective ASL labeling (same labeling settings and geometry as the ASL perfusion scan) was accomplished through manipulating the spatial labeling efficiency by applying additional gradients between the labeling pulses (Chapter 6, Figure 1). The additional gradients were applied in sets of 5 dynamics: no labeling applied (control), non-selective labeling applied (globally perfusion weighted), labeling varied in right-left (RL) direction (distance of 50 mm between full label and control situation), labeling varied in anterior-posterior (AP1) direction (distance of 18 mm between full label and control situation) and labeling varied in AP direction (AP2, similar to AP1, but shifted 9 mm in posterior direction compared to the previous dynamic).

An inversion recovery sequence was acquired prior to the perfusion scans to measure the magnetization of arterial blood, the M0 which is needed to quantitatively calculate cerebral blood flow in $mL{\cdot}100mL^{-1}{\cdot}min^{-1}$, and to segment brain tissue into gray and white matter. Both the perfusion-territory selective ASL and inversion recovery sequence were acquired with echo planar imaging with the same geometry and resolution as the ASL images. T_2-weighted FLAIR images and a three-dimensional time-of-flight MR angiography with subsequent maximum-intensity projection reconstruction were acquired with standard imaging sequences provided by the MRI vendor.

The presence of collateral flow routes in the circle of Willis were assessed with a three-dimensional time-of-flight MR angiography sequence with subsequent maximal intensity projection reconstruction (TR/TE, 23/3.5 ms; flip angle, 18°; FOV, 200 x 200 mm^2; matrix, 304 x 200; 100 slices; slice thickness, 1.2 mm with 0.6 mm overlap; scan time, three minutes). The direction of blood flow in these collaterals was determined according to a previously published imaging protocol with two consecutive two-dimensional phase-contrast MR imaging measurements, of which one was phase-encoded in the left-right direction and one in the antero-posterior direction (TR/TE, 9.4/5.9 ms; flip angle, 7.5°; FOV, 250 x 188 mm; matrix, 256 x 134; eight averages; slice thickness, 13 mm; velocity sensitivity, 40 cm/s, scan time, 20 sec).[19] Anterior collateral flow was defined as flow across the anterior communicating artery with retrograde flow in the precommunicating part of the anterior cerebral artery (A1 segment). Posterior-to-anterior flow in the posterior communicating artery was considered to represent posterior collateral flow.

Table 2. CBF in mL·100mL^{-1}·min^{-1} and cerebrovascular reactivity (percent of CBF increase) before and after acetazolamide.

	CBF pre-acetazolamide *(mL·100mL^{-1}·min^{-1})*	**CBF post-acetazolamide** *(mL·100mL^{-1}·min^{-1})*	**Cerebrovascular reactivity** *(%)*
Controls			
ICA	51.8 ± 8.1 *	78.6 ± 12.4	54.2 ± 13.1
Basilar artery	48.8 ± 12.1 *	83.4 ± 20.3	73.7 ± 23.7
Patients			
ICA			
Complete territory	44.7 ± 6.0 *	54.7 ± 9.3	22.8 ± 16.1 †
Side of occlusion	41.1 ± 13.0 *	47.2 ± 17.5	13.5 ± 20.4 †#
Unaffected side	47.4 ± 4.3 *	59.6 ± 7.7	26.2 ± 16.0 †
Basilar artery	45.4 ± 11.1 *	59.5 ± 16.0	32.3 ± 16.6 †

* Significant difference pre and post-acetazolamide (paired t-test).
† Significant difference between patients and control subjects (independent-samples t-test).
# Significant difference between the side of the occlusion and the unaffected side (paired t-test).

Data analysis

Data were analyzed with MATLAB (The MathWorks, Mass, version 7.5) and SPM5 (Wellcome Trust Centre for Neuroimaging, Oxford, United Kingdom).

Cerebral blood flow (CBF) images in mL·100mL^{-1}·min^{-1} were calculated from the ASL-MR images according to a previously published model.[20] The T_2^* transversal relaxation rate and T_1 of arterial blood at 3T were assumed to be, respectively, 50 ms and 1680 ms.[21,22] The water content of blood was assumed to be 0.76%.[23] The blood magnetization at thermal equilibrium (M0) for all volunteers was determined by selecting a region of interest in the cerebral spinal fluid and iteratively fitting the inversion recovery data by a non-linear least-square method.[23]

The CBF of the gray matter of the perfusion-territories of the basilar and ICA was measured before and after administration of acetazolamide. Cerebrovascular reactivity was defined as the percentage of CBF increase after administration of acetazolamide. For the placement of the regions of interest in the gray matter throughout all seventeen slices, three preprocessing steps were performed (Figure 1). First, to avoid partial voluming of white matter, a surrogate T_1-weighted image was calculated from the inversion recovery sequence by calculating the reciprocal of the quantitative T_1. This was segmented into gray and white matter probability maps with SPM and corrective thresholding was subsequently applied to ensure maximal exclusion of all white matter. Secondly, the perfusion-territories of the basilar and ICA were identified by means of a k-means clustering algorithm.[24] The individual perfusion-territories were then manually drawn on the output images

of the clustering algorithm. Two additional regions of interest (ROIs) were drawn within the perfusion-territory of the contralateral ICA; one on the unaffected side and one in the affected hemisphere on the side of the occlusion. This ROI represents the brain tissue supplied through collateral pathways originating from the asymptomatic ICA. For this, the perfusion-territory crossing over the midline of the brain into the hemisphere with the ICA occlusion was delineated (Figure 1). The final step was to combine the gray matter masks with the segmented perfusion-territory masks. Areas of hyperintensities on FLAIR, depicting areas of infarction, were manually excluded from the ROI. To correct for motion, all images pre and post-acetazolamide were first coregistered with SPM to the baseline CBF map using the normalized mutual information and a rigid body transformation.

Statistical analysis

SPSS (SPSS Inc., Chicago, Illinois, U.S.A. version 15) was used for statistical analysis. Differences between pre and post-acetazolamide CBF measurements, and between the perfusion-territories within the healthy control subject, were assessed using a paired t-test. Because no differences were found in the CBF or cerebrovascular reactivity between the left and right ICAs in the healthy control subjects, values for both perfusion-territories were averaged for further comparisons. To compare the cerebrovascular reactivity measurements in the patients with the healthy control subjects an independent-samples t-test was used. A paired t-test was used to compare cerebrovascular reactivity measurements of the perfusion-territories in patients. The mean differences in cerebrovascular reactivity with the 95% confidence intervals (CI) were calculated and considered significantly different if the 95% CI did not include zero. Values are expressed as mean ± standard deviation.

Results

Figure 2 shows CBF maps pre and post-acetazolamide of a 47-year old man with a symptomatic occlusion of the left ICA and collateral blood flow from the unaffected contralateral ICA. Figure 3 shows CBF maps of a 51-year old man with a symptomatic occlusion of the right ICA and collateral blood flow from the posterior circulation. Both patients had decreased CBF and cerebrovascular reactivity on the side of the occluded ICA.

Table 2 summarizes the CBF measurements before and after acetazolamide, and the cerebrovascular reactivity measurements. CBF increased ($p < 0.01$) in all perfusion-territories after administration of acetazolamide. In the patients with an ICA occlusion, the cerebrovascular reactivity was lower in the tissue fed by the unaffected ICA (22.8 ± 16.1%) when compared to the healthy control subjects (54.2 ± 13.1%; mean difference, -31.5%; 95% CI, -42.1 to -20.8). The cerebrovascular reactivity was also lower in the brain tissue fed by the basilar artery (32.2 ± 16.6%)

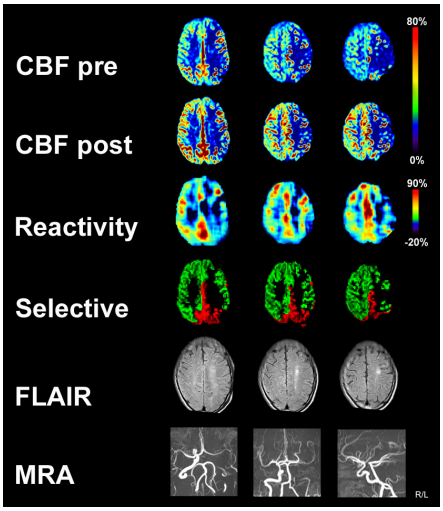

Figure 2: Transverse CBF maps in mL·100mL^{-1}·min^{-1} before *(CBF pre)* and after *(CBF post)* administration of acetazolamide of a 47-year old man with a symptomatic occlusion of the left ICA and collateral flow from unaffected contralateral ICA (green on Selective ASL image). CBF and cerebrovascular reactivity (percentage CBF increase) are decreased in the left hemisphere. On the anatomical fluid-attenuated inversion recovery (FLAIR) image, multiple hyperintensities are present in the left hemisphere. MRA, MR angiography. *For color figure see page 162.*

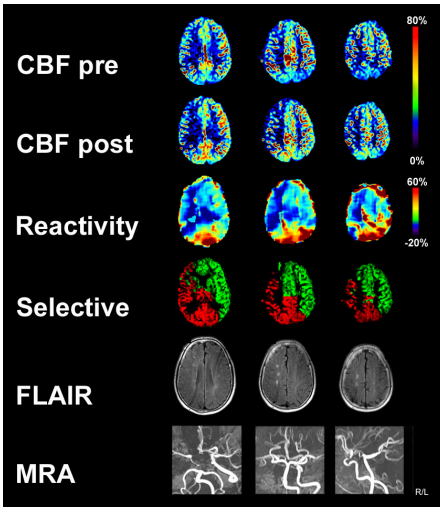

Figure 3: Transverse CBF maps in mL·100mL^{-1}·min^{-1} before *(CBF pre)* and after *(CBF post)* administration of acetazolamide of a 51-year old man with a symptomatic occlusion of the right ICA and collateral flow from the posterior circulation (red on Selective ASL image). CBF and cerebrovascular reactivity (percentage CBF increase) are decreased in the in the right hemisphere. On the anatomical fluid-attenuated inversion recovery (FLAIR) image, multiple hyperintensities are present in the right hemisphere. MRA, MR angiography. *For color figure see page 163.*

when compared to the healthy control subjects (73.7 ± 23.7%; mean difference -40%; 95% CI, -55 to -25).

When compared to the healthy control subjects, in patients the cerebrovascular reactivity was lower within the perfusion-territory of the unaffected ICA; both in the hemisphere ipsilateral to the ICA occlusion 13.5 ± 20.4 vs. 54.2 ± 13.1%; mean difference, -40.7%; 95% CI, -53.2 to -28.2 and in the hemisphere ipsilateral to the unaffected side 26.2 ± 16.0 vs. 54.2 ± 13.1%; mean difference, -28.0; 95% CI, -38.6 to -17.5. Within the perfusion-territory, the cerebrovascular reactivity was lower in the brain tissue on the side of the occlusion (13.5 ± 20.4%) than on the side of the unaffected ICA (26.2 ± 16.0%; paired mean difference, -12.5%; 95% CI, -20.3 to -4.7). And 9 of the 16 patients had severely decreased cerebrovascular reactivity (< 20%) in the hemisphere ipsilateral to the ICA occlusion (3.7 ± 6.6 vs. 28.3 ± 25.6%; mean difference, 24.6%; 95% CI, 5.5 to 43.7). In 4 of the 16 patients cerebral blood flow

decreased in the brain tissue on the side of the occlusion after acetazolamide (-6.0 ± 9.9 vs. 20.6 ± 18.6%; mean difference, 26.7%; 95% CI, 5.3 to 48.0).

Time-of-flight and phase-contrast angiography demonstrated anterior collateral flow in 3 patients, posterior collateral flow in 6 patients and a combination of both in 4 patients. In 3 patients it could not be defined due to incorrect planning of the imaging section. The presence or absence of anterior or posterior collateral flow did not affect CBF or the vascular reactivity in the hemisphere with the ICA occlusion.

Discussion

We investigated the cerebrovascular reactivity of the brain feeding arteries at the level of the brain tissue by combining quantitative and perfusion-territory selective ASL-MRI with a vascular challenge. Our study shows that the cerebrovascular reactivity is decreased throughout the brain in patients with a symptomatic ICA occlusion and varies within the perfusion-territory of the unaffected contralateral ICA. Cerebrovascular reactivity on the side of the ICA occlusion fed by the unaffected contralateral ICA is the most impaired.

Previous studies have shown that the presence of primary and secondary collaterals is associated with decreased cerebrovascular reactivity.[25,26] Primary collaterals are the anterior and posterior communicating arteries of the circle of Willis, and the ophthalmic artery and leptomeningeal vessels are considered to be secondary collaterals.[11] A fully developed collateral network however has also been reported to be associated with normal cerebrovascular reactivity and a lower risk of future stroke when compared to patients without collateral or with only primary collaterals.[27] This discrepancy could possibly be explained by the techniques used to evaluate the contribution of collaterals. The efficiency of the collateral vasculature cannot be evaluated by merely determining the presence of certain collateral pathways, but should ideally be evaluated by measuring the hemodynamic status in tissue fed by these collaterals as well. Our results show that the cerebrovascular reactivity is the most impaired on the side of the ICA occlusion in tissue that is fed by collaterals originating from the unaffected contralateral ICA.

Although there are no previous studies validating ASL-MRI perfusion reactivity measurements by comparing to other established techniques, our finding of impaired cerebrovascular reactivity in patients with a symptomatic ICA occlusion is in agreement with other studies that have used either TCD to measure cerebrovascular reactivity in the intracranial arteries or use techniques such as PET and SPECT to measure cerebrovascular reactivity at the brain tissue level.[28,29] ASL-MRI has previously been used to assess cerebrovascular reactivity in patients with large artery cerebrovascular stenosis of the anterior circulation.[12] With a continuous ASL-MRI sequence at 1.5T in combination with acetazolamide, a varying pattern of cerebrovascular reactivity was observed, ranging from normal to focal and diffuse

hemodynamic impairment. In a test-retest reproducibility study, Yen *et al* have furthermore shown that cerebrovascular reactivity measurements performed with a flow sensitive alternating inversion recovery ASL technique at 1.5T has a good reproducibility and is sensitive to small changes related to disease or treatment.[30] The advantage of the currently used pseudo-continuous ASL sequence at 3T is the higher signal-to-noise ratio when used in combination with background suppression. For cerebrovascular reactivity measurements this is of particular importance as a relatively small increase in signal has to be measured. Furthermore, by adding perfusion-territory selective ASL, we were able to assess the perfusion-territories of the cerebral arteries. We were therefore able to assess cerebrovascular reactivity within the perfusion-territories of the brain feeding arteries and evaluate the tissue fed through collaterals. The slightly lower cerebrovascular reactivity measured in the hemisphere contralateral to the ICA occlusion when compared to the healthy control subjects might potentially be explained by the presence of a contralateral ICA stenosis in some of the patients or decreased cerebrovascular reactivity due to generalized atherosclerosis.

For patients with a symptomatic occlusion of the ICA the best management is yet to be defined.[31] EC/IC bypass surgery has been largely abandoned since the EC-IC study has shown that it does not prevent stroke.[32] It has however been suggested that EC/IC bypass surgery may be effective in a subgroup of patients with severely impaired cerebral hemodynamics.[6,33] In the carotid occlusion surgery study, efficacy of the EC/IC bypass has been studied in patients with increased oxygen extraction fraction as measured by PET.[34] A drawback of PET however, is that it is only available in a limited number of institutions. ASL-MRI can simultaneously assess the cerebrovascular reactivity and the shifts in the perfusion-territories of the brain feeding arteries at tissue level on MRI scanners widely available in a clinical setting. It may therefore help depict the brain tissue most at risk for future stroke and define which patients would benefit most from revascularization operations such as EC/IC bypass or carotid endarterectomy of a severe contralateral ICA stenosis. With further studies, this could be either a certain cerebrovascular reactivity threshold or the occurrence of steal, where blood is redistributed to more healthy tissue and CBF decreases.

A limitation of this study is that in patients with an ICA occlusion, collateralization may lead to a delayed arrival of the bolus of magnetically labeled blood spins. As the perfusion-weighted images are acquired after a fixed amount of time in ASL-MRI, this could potentially lead to an underestimation of the perfusion. And in healthy tissue with uncompromised cerebrovascular reactivity the blood may flow faster from the supplying arteries to the brain tissue, resulting in complete arrival of labeled spins during imaging and thus a stronger ASL signal when compared to impaired tissue. During the acetazolamide challenge, these transit times might decrease due to faster flow, leading to a relative less severe underestimation of

ASL-signal and an overestimation of cerebrovascular reactivity. To minimize these effects, we employed a delay time of 1525 ms in this study, where the protons that have been labeled directly after the start of the labeling have an effective delay time of more than 3 seconds. Furthermore, these transit time effects would lead to an overestimation of the cerebrovascular reactivity ipsilateral to the occlusion, whereas in this study we observed a statistically decreased reactivity in the patients. Collateral flow from the posterior circulation was not evaluated in this study as the brain tissue that is supplied through collaterals originating from the vertebrobasilar arteries could not be reliably differentiated from normal variations in the perfusion territories of the posterior circulation. Perfusion-territory selective ASL-MRI can visualize the extent of the perfusion-territory of the vertebrobasilar artery, however the boundary between tissue natively being perfused by the basilar artery and tissue supplied through collaterals (posterior communicating artery or leptomeningeals) cannot be accurately determined. Finally, two patients were included with a contralateral stenosis ≥ 70%. Although this may have decreased the cerebrovascular reactivity measurements in the unaffected contralateral ICA, we still found that the cerebrovascular reactivity varies within the perfusion-territory of the unaffected artery.

Conclusion

ASL-MRI can assess impaired cerebrovascular reactivity at brain tissue level in patients with a symptomatic ICA occlusion. Impairment of the hemodynamic status of the brain is associated with increased risk of stroke. With further research, cerebrovascular reactivity assessment with ASL-MRI may possibly help identify the brain tissue most at risk for future stroke and as such may guide medical treatment.

References

1. Klijn CJ, Kappelle LJ, Algra A, et al. Outcome in patients with symptomatic occlusion of the internal carotid artery or intracranial arterial lesions: a meta-analysis of the role of baseline characteristics and type of antithrombotic treatment. Cerebrovasc Dis 2001;12:228-234.
2. Vernieri F, Pasqualetti P, Passarelli F, et al. Outcome of carotid artery occlusion is predicted by cerebrovascular reactivity. Stroke 1999;30:593-598.
3. Grubb RL, Jr., Derdeyn CP, Fritsch SM, et al. Importance of hemodynamic factors in the prognosis of symptomatic carotid occlusion. JAMA 1998;280:1055-1060.
4. Klijn CJ, Kappelle LJ, van Huffelen AC, et al. Recurrent ischemia in symptomatic carotid occlusion: prognostic value of hemodynamic factors. Neurology 2000;55:1806-1812.
5. The EC/IC bypass study group. Failure of extracranial-intracranial arterial bypass to reduce the risk of ischemic stroke. Results of an international randomized trial. N Engl J Med 1985;313:1191-1200.
6. Adams HP, Jr. Occlusion of the internal carotid artery: reopening a closed door? JAMA 1998;280:1093-1094.
7. Derdeyn CP, Videen TO, Yundt KD, et al. Variability of cerebral blood volume and oxygen extraction: stages of cerebral haemodynamic impairment revisited. Brain 2002;125:595-607.
8. Powers WJ. Cerebral hemodynamics in ischemic cerebrovascular disease. Ann Neurol 1991;29:231-240.
9. Hirano T, Minematsu K, Hasegawa Y, et al. Acetazolamide reactivity on 123I-IMP single photon emission computed tomography in patients with major cerebral artery occlusive disease: correlation with positron emission tomography parameters. J Cereb Blood Flow Metab 1994;14:763-770.
10. van Laar PJ, Hendrikse J, Klijn CJ, et al. Symptomatic carotid artery occlusion: flow territories of major brain-feeding arteries. Radiology 2007;242:526-534.
11. Liebeskind DS. Collateral Circulation. Stroke 2003;34:2279-2284.
12. Detre JA, Samuels OB, Alsop DC, et al. Noninvasive magnetic resonance imaging evaluation of cerebral blood flow with acetazolamide challenge in patients with cerebrovascular stenosis. J Magn Reson Imaging 1999;10:870-875.
13. Yen YF, Field AS, Martin EM, et al. Test-retest reproducibility of quantitative CBF measurements using FAIR perfusion MRI and acetazolamide challenge. Magn Reson Med 2002;47:921-928.
14. Paiva FF, Tannus A, Silva AC. Measurement of cerebral perfusion territories using arterial spin labelling. NMR Biomed 2007;20:633-642.
15. van Laar PJ, van der Grond J, Hendrikse J. Brain perfusion territory imaging: methods and clinical applications of selective arterial spin-labeling MR imaging. Radiology 2008;246:354-364.
16. Bamford JM, Sandercock PAG, Warlow CP, et al. Interobserver agreement for the assessment of handicap in stroke patients. Stroke 1989;20:828.
17. Dai W, Garcia D, de BC, et al. Continuous flow-driven inversion for arterial spin labeling using pulsed radio frequency and gradient fields. Magn Reson Med 2008;60:1488-1497.
18. Gevers S, Nederveen A, Bokkers RP, et al. Reproducibility of flow territories defined by plannings-free vessel encoded pseudo-continuous arterial spin labeling. Proceedings 17th Scientific Meeting, ISMRM 2009;1524.
19. Rutgers DR, Klijn CJ, Kappelle LJ, et al. A longitudinal study of collateral flow patterns in the circle of Willis and the ophthalmic artery in patients with a symptomatic internal carotid artery occlusion. Stroke 2000;31:1913-1920.
20. Alsop DC, Detre JA. Reduced transit-time sensitivity in noninvasive magnetic resonance imaging of human cerebral blood flow. J Cereb Blood Flow Metab 1996;16:1236-1249.

21. Golay X, Petersen ET, Hui F. Pulsed star labeling of arterial regions (PULSAR): a robust regional perfusion technique for high field imaging. Magn Reson Med 2005;53:15-21.
22. St Lawrence KS, Wang J. Effects of the apparent transverse relaxation time on cerebral blood flow measurements obtained by arterial spin labeling. Magn Reson Med 2005;53:425-433.
23. Chalela JA, Alsop DC, Gonzalez-Atavales JB, et al. Magnetic resonance perfusion imaging in acute ischemic stroke using continuous arterial spin labeling. Stroke 2000;31:680-687.
24. Wong EC, Kansagra AP. Mapping Middle Cerebral Artery Branch Territories with Vessel Encoded Pseudo-Continuous ASL: Sine/Cosine Tag Modulation and Data Clustering in Tagging Efficiency Space. Proceedings 16th Scientific Meeting , ISMRM 2008:182.
25. Norrving B, Nilsson B, Risberg J. rCBF in patients with carotid occlusion. Resting and hypercapnic flow related to collateral pattern. Stroke 1982;13:155-162.
26. Muller M, Schimrigk K. Vasomotor reactivity and pattern of collateral blood flow in severe occlusive carotid artery disease. Stroke 1996;27:296-299.
27. Vernieri F, Pasqualetti P, Matteis M, et al. Effect of collateral blood flow and cerebral vasomotor reactivity on the outcome of carotid artery occlusion. Stroke 2001;32:1552-1558.
28. Imaizumi M, Kitagawa K, Hashikawa K, et al. Detection of misery perfusion with split-dose 123I-iodoamphetamine single-photon emission computed tomography in patients with carotid occlusive diseases. Stroke 2002;33:2217-2223.
29. Ogasawara K, Ogawa A, Yoshimoto T. Cerebrovascular reactivity to acetazolamide and outcome in patients with symptomatic internal carotid or middle cerebral artery occlusion: a xenon-133 single-photon emission computed tomography study. Stroke 2002;33:1857-1862.
30. Yen YF, Field AS, Martin EM, et al. Test-retest reproducibility of quantitative CBF measurements using FAIR perfusion MRI and acetazolamide challenge. Magn Reson Med 2002;47:921-928.
31. Flemming KD, Brown RD, Jr., Petty GW, et al. Evaluation and management of transient ischemic attack and minor cerebral infarction. Mayo Clin Proc 2004;79:1071-1086.
32. Caplan LR, Piepgras DG, Quest DO, et al. EC-IC bypass 10 years later: is it valuable? Surg Neurol 1996;46:416-423.
33. Derdeyn CP, Grubb RLJ, Powers WJ. Cerebral hemodynamic impairment: methods of measurement and association with stroke risk. Neurology 1999;53:251-259.
34. Grubb RL, Jr., Powers WJ, Derdeyn CP, et al. The Carotid Occlusion Surgery Study. Neurosurg Focus 2003;14:e9.

CHAPTER 8

Reinoud P.H. Bokkers
Jeroen Hendrikse
Nolan S. Hartkamp
Catharina J.M. Klijn
Matthias J.P. van Osch

WHITE MATTER HEMODYNAMIC EFFECT OF LARGE VESSEL DISEASE AND WHITE MATTER LESIONS

Background and purpose: Ischemia in the white matter is classically associated with thickened vessel walls, endothelial dysfunction and hemodynamic impairment. The aim of our study was to assess the effect of white matter lesions and large vessel disease on white matter hemodynamics by assessing cerebral blood flow (CBF) and the autoregulatory capacity with arterial spin labeling (ASL) perfusion MRI in combination with a vasodilatory challenge in patients with a steno-occlusive lesion in one of the internal carotid arteries.

Methods: We studied 20 age and sex-matched healthy control subjects and 32 patients with a unilateral symptomatic steno-occlusive ICA lesion; 17 with a stenosis >50% and 15 with an occlusion. White matter CBF and CVR was assessed within the white and gray matter with ASL-MRI before and after acetazolamide administration. White matter lesions were graded according to the Fazekas classification scheme.

Results: In both patients with an ICA stenosis and occlusion, CVR was lower in the white matter on the side of the symptomatic ICA when compared to healthy control subjects. Patients with Fazekas grade 2 and 3 abnormalities had a lower CVR in the white matter when compared to those without, and CVR was lower in these patients in the white matter of the symptomatic hemisphere when compared to the asymptomatic hemisphere.

Conclusion: Our study indicates that both large vessel disease and white matter lesions have an effect upon white matter hemodynamics. With further research, cerebrovascular reactivity assessment with ASL-MRI may possibly help understand the pathogenesis underlying white matter lesions and the roll of large vessel disease on white matter perfusion.

Introduction

Ischemia in the white matter is classically associated with thickened vessel walls (lipohyalinosis), endothelial dysfunction and hemodynamic impairment.[1,2] Patients with extensive ischemic white matter changes, leukoaraiosis, have a poor prognosis in terms of death, stroke and myocardial infarction.[3] These white matter lesions have further been associated with dementia and cognitive decline.[4-6]

The autoregulatory capacity of the cerebral vasculature is an important marker of the hemodynamic status of the brain. In the model of hemodynamic impairment in ischemic cerebrovascular disease, introduced by Powers and Derdeyn, there are two stages of hemodynamic impairment.[7,8] Stage I is characterized by compensatory autoregulative vasodilatation of the cerebral resistance arterioles and leads to increased cerebral blood volume and decreased cerebrovascular reactivity (CVR). In stage II, the vasodilatory capacity is overcome, cerebral blood flow decreases and the oxygen extraction fraction increases to sustain oxygen metabolism. In patients with atherosclerosis represented by a stenosis or occlusion of the internal carotid artery (ICA), the vasodilatory capacity may be decreased by both reduced perfusion pressure distal to the steno-occlusive lesion and lipohyalinosis with endothelial dysfunction of the deep arterial perforators. Both may result in impairment of the cerebral autoregulation in a early stage before tissue damage has yet occurred.

Arterial spin labeling (ASL) is a noninvasive MR perfusion technique for imaging whole brain cerebral perfusion that uses radiofrequency pulses to magnetically label arterial blood without ionizing radiation or contrast agents. In combination with a vascular challenge it can also assess the hemodynamic status at brain tissue level by measuring the cerebrovascular reactivity (CVR).[9-11] Recently developed ASL methods which combine pseudo-continuous ASL labeling pulses, background suppression and an MRI field strength of 3.0 Tesla have shown that also smaller and less perfused brain regions such as the basal ganglia and white matter can be assessed.[12]

The aim of our study was to assess the effect of white matter lesions and large vessel disease on white matter hemodynamics by assessing cerebral blood flow (CBF) and the autoregulatory capacity with pseudo-continuous ASL perfusion MRI in combination with a vasodilatory challenge.

Materials and methods

The institutional ethical standards committee approved the study protocol and written informed consent was obtained from all participants.

Subjects

Thirty-two functionally independent patients (19 males and 13 females; mean age ± SD, 63.4 ± 12.6 years) with a symptomatic unilateral stenosis > 50% or occlusion

Table 1. Demographic and clinical characteristics of patients and healthy controls.

	Patients with ICA stenosis (n = 17)	**Patients with ICA occlusion** (n = 15)	**Healthy controls** (n = 20)
Age, y	69 ± 9	58 ± 14	64 ± 8
Male, n	8 (53%)	11 (73%)	12 (60%)
Degree of contralateral ICA stenosis, n			
0 – 49%	17	12	20
50 – 69%	0	2	0
70 – 99 %	0	1	0
Occluded	0	0	0
Presenting events			
Amaurosis fugax	2	1	0
Transient hemispheric ischemic attack	10	9	0
Ischemic stroke	5	5	0

Unless otherwise specified, data are number of patients.

of the ICA and 20 age and sex-matched healthy volunteers (12 males and 8 females; mean age ± SD, 63.6 ± 7.8 years) were prospectively included. Seventeen of the 32 patients had an ICA stenosis > 50% and 15 an ICA occlusion. All patients had been admitted to the University Medical Center Utrecht with a transient ischemic attack (TIA) or non-disabling stroke on the side of the ICA stenosis of occlusion in the three months preceding inclusion into this study. The degree of stenosis was assessed by computed tomography or MR angiography in accordance to the North American Symptomatic Carotid Endarterectomy Trial criteria.[13]

The control group of healthy volunteers were recruited through local media advertisements. None of the control subjects had a history of neurological disease or vascular pathology on MRI or MR angiography of the brain. Each volunteer underwent ASL MR perfusion imaging before and 15 minutes after administration of an intravenous bolus of 14 mg/kg, with a maximum dose of 1200 mg, acetazolamide (Goldshield Pharmaceuticals, Croydon Surrey, UK). The characteristics of patients and healthy control volunteers are outlined in Table 1.

Imaging protocol

MR imaging was performed on a clinical 3 Tesla MRI scanner (Achieva, Philips Medical Systems, Best, The Netherlands) equipped with an eight-channel coil and locally developed software to enable ASL imaging. Perfusion imaging was performed with

a pseudo-continuous ASL sequence in combination with background suppression. Labeling was performed by employing a train of 18 degrees, 0.5 ms, Hanning shaped RF pulses at an interval of 1 ms, for a duration of 1650 ms, in combination with a balanced gradient scheme.[14,15] The control situation was achieved by adding 180° to the phase of all even RF pulses. Single shot echo planar imaging was used for image acquisition in combination with parallel imaging (SENSE factor, 2.5) 1525 ms after the labeling stopped. Background suppression consisted of a saturation pulse immediately before labeling and inversion pulses at 1680 and 2830 ms after the saturation pulse.[16] For localization of the imaging section of seventeen 7 mm slice aligned parallel to the orbito-meatal angle, a T_1 weighted spin-echo sequence was first obtained in the sagittal plane. The ASL images were acquired in ascending fashion with an in-plane resolution of 3 x 3 mm^2. An inversion recovery sequence was acquired with the same geometry and resolution for measurement of the magnetization of arterial blood (M_0) and for gray/white segmentation. The other ASL-MRI parameters were: TR, 4000 ms; TE, 14 ms; pairs of control/label, 38; FOV, 240 x 240 x 119 mm; matrix, 80 x 79; scan time, 5 minutes.

T_2 weighted FLAIR images and a three-dimensional time-of-flight MR angiography with subsequent maximum-intensity projection reconstruction were acquired for depiction of ischemic lesions and visualization of the cerebral arteries (TR/TE/flip angle, 1.1s /125 ms/120° (FLAIR) and 23 ms/3.5ms/18° (MRA); FOV, 230 x 183 mm (FLAIR) and 200 x 200 mm (MRA); matrix size, 352 x 158 (FLAIR) and 304 x 200 (MRA); slice thickness, 4 mm with a 1 mm gap (FLAIR) and 1.2 with 0.6 mm overlap (MRA); slices, 26 (FLAIR) and 50 (MRA); 2 averages (MRA).

Perfusion data analyses

Data were analyzed with MATLAB (The MathWorks, Natick, Mass, version 7.5) and SPM8 (Wellcome Trust Centre for Neuroimaging, Oxford, United Kingdom).

CBF maps in $mL \cdot 100mL^{-1} \cdot min^{-1}$ were calculated according to the perfusion model of Alsop et al:[17]

$$CBF = \frac{6000}{2 \cdot \lambda \cdot \alpha \cdot T_{1,blood}} \frac{\Delta M_{ASL}}{M_{0,CSF}} \cdot e^{(delay + slice\_time \cdot z)/T_{1,blood}} \cdot e^{TE/T_2^*}$$

where λ is the water content of blood (assumed to be 0.76 mL per mL of blood [18]), α the labeling efficiency, the T_1 of blood is assumed to be 1680 ms,[19] *delay* is the imaging delay, *z* is the number of current slice, *slice_time* is the read-out duration of a single slice, *TE* is the echo time and T_2^* is the transversal relaxation rate of arterial blood (assumed to be 50 ms).[20] The labeling efficiency was assumed to be 85% based on numerical simulations of the labeling process comparable to simulations by Wu et al.[15] The mean resting magnetization (M_0) of the blood in all volunteers was determined according to the procedure outlined by Chalela et al.[18] For this, a region

of interest was selected in the cerebral spin fluid, and the M_0 and T_1 were iteratively fitted based on the inversion recovery data.[18]

CVR was defined as the percentage CBF increase measured 15 minutes after the intravenous administration of acetazolamide. CBF was measured before and after acetazolamide in the white and gray matter throughout the brain. Two regions of interest were placed within each hemisphere; one in the white matter and one the gray matter of the middle cerebral artery flow territory. For the placement of the regions of interest throughout all seven slices, three semi-automated processing steps were followed. Fist, a surrogate T_1weighted image was calculated from the inversion recovery sequence by calculating the reciprocal of the quantitative T_1. This was then segmented into gray and white matter probability maps with SPM and corrective thresholding was subsequently applied to avoid partial voluming of white and gray matter. Regions of interest were manually drawn within the flow territory of the middle cerebral artery on the gray matter mask based on a standardized flow territory template described previously by Tatu et al.[21] To correct for motion, the T_1 weighted and post acetazolamide CBF images were coregistered to the first CBF image using a least squares approach and a six-parameter rigid body spatial transformation.

White matter lesions

The presence of white matter lesions was graded according to the Fazekas classification.[22] In grade 0 white matter lesions are absent, in grade 1 small punctuate lesions are present in the deep white matter, in grade 2 there are beginning confluences of foci and in grade 3 there are large confluent areas of white matter lesions. Irregular periventricular hyperintensities were also classified as grade 3.

Statistical analysis

Descriptive statistical analyses were performed to summarize patient characteristics. To compare the CBF and CVR measurements in the hemispheres ipsilateral and contralateral to the ICA stenosis to those of the healthy control subjects we applied an unpaired t test. Values were considered significantly different if the 95% confidence interval (CI) did not include zero. Because no differences were found in CBF or CVR between the left and right hemisphere in the control subjects (paired *t* test), values for both hemispheres were averaged for analysis. Values are expressed as mean ± standard error of the mean (SEM) unless otherwise specified. SPSS (SPSS Inc., Chicago, Illinois, U.S.A.) for Windows, version 15.0.1, was used for statistical analysis.

Table 2. Cerebral blood flow (CBF) pre and post acetazolamide, CVR in the gray and white matter.

	CBF pre-acetazolamide *(mL·100mL^{-1}·min^{-1})*	**CBF post-acetazolamide** *(mL·100mL^{-1}·min^{-1})*	**Cerebrovascular reactivity** *(%)*
Control group			
White-matter	12 ± 1	20 ± 1 *	66 ± 5
Gray-matter	52 ± 2	78 ± 3 *	51 ± 3
Stenosis patients			
White-matter			
Symptomatic side	13 ± 1	19 ± 2 *	49 ± 4 †
Asymptomatic side	12 ± 1	19 ± 2 *	53± 4
Gray-matter			
Symptomatic side	44 ± 4	58 ± 5 *	35 ± 5 †
Asymptomatic side	43 ± 4	60 ± 5 *	39 ± 5 †
Occlusion patients			
White-matter			
Symptomatic side	9 ± 2	11 ± 1 *	31 ± 25 †
Asymptomatic side	12 ± 2	15 ± 2 *	38 ± 10 †
Gray-matter			
Symptomatic side	44 ± 5	48 ± 6 *	18 ± 6 †
Asymptomatic side	45 ± 4	62 ± 4 *	27 ± 4 †

** significant difference between the pre and post-acetazolamide CBF.*
† significant difference in cerebrovascular reactivity between patients and control subjects.

Results

Figure 1 shows an example of the CBF and CVR images obtained in a 51-year-old female with a high-grade stenosis of the right ICA and Figure 2 of a 75-year-old man with an occlusion of the left ICA. Both patients had decreased CBF and CVR on the side of steno-occlusive ICA.The images are scaled towards the lower perfusion signal to optimize visualisation of the white matter perfusion.

The CBF values in mL·100mL^{-1}·min^{-1} before and after acetazolamide, and the CVR (percentage increase of CBF) of the patients and healthy control subject are summarized in table 2. There were no differences in white matter CBF between

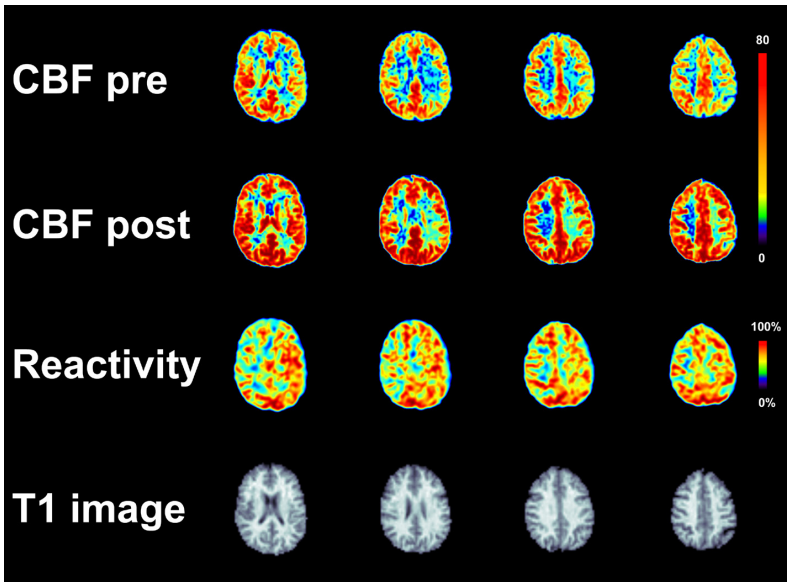

Figure 1. Clinical example of a 51-year old female with a right sided high-grade stenosis of the ICA. Decreased cerebral blood flow and cerebrovascular reactivity can be appreciated in the gray and white matter of the right hemisphere. *For color figure see page 164.*

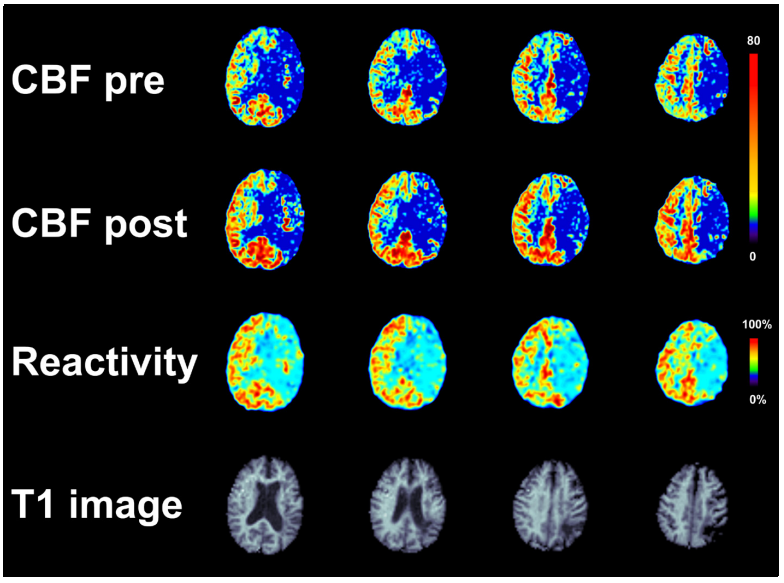

Figure 2. Clinical example of a 75-year old man with a left sided ICA occlusion. Decreased cerebral blood flow and cerebrovascular reactivity can be appreciated in the gray and white matter of the right hemisphere. *For color figure see page 165.*

the symptomatic and asymptomatic hemispheres in patients with an ICA stenosis and occlusion, or when patients were compared to the healthy control subjects. After administration of acetazolamide CBF increased significantly ($p < 0.01$) in the patients and healthy control subjects throughout the white and gray matter regions of interest. In the patients with an ICA stenosis, CVR was lower in the white matter on the side of the symptomatic ICA stenosis than in healthy control subjects (mean difference 20%; 95% confidence interval (CI), 4 – 31%). For the contralateral asymptomatic hemisphere there was no difference. In the patients with a symptomatic ICA occlusion, CVR was decreased in the white matter both on the side of the occlusion (paired mean difference, 35; 95% CI, 19 – 51%) and in the contralateral asymptomatic hemisphere (mean difference 28, 95% CI, 15 – 40%) when compared to healthy control subjects. There were no differences in CVR between the symptomatic and asymptomatic hemispheres in the stenosis and occlusion patients.

Twenty-three of the 32 patients had white matter hyperintensities. There were 8 patients with Fazekas grade 1, 11 patients with Fazekas grade 2 and 4 patients with Fazekas grade 3 abnormalities. Patients with Fazekas grade 2 and 3 abnormalities had a lower CVR (37.1 ± 4.1 vs. 48.7 ± 15.8%, paired mean difference, 11.6%; 95% confidence interval (CI), 0.12 – 23.1) in the white matter of both hemispheres when compared to those without (Fazekas grade 0 and 1). In the patients with Fazekas grade 2 and 3 white matter lesions, CVR was lower in the white matter of the symptomatic hemisphere when compared to the asymptomatic hemisphere (29.9 ± 5.4 vs. 44.5 ± 4.7%, paired mean difference, 14.6%; 95% confidence interval (CI), 1.8 – 27.3). This asymmetry between both hemispheres was more pronounced in the patients with an occlusion of the ICA (16.1 ± 6.5 vs. 37.9 ± 4.8%, paired mean difference, 21.7%; 95% CI, 2.9 – 40.6) than in those with ICA stenosis (41.9 ± 5.9 vs. 50.2 ± 7.4%, mean difference, 8.3%; 95% confidence interval (CI), -2.1 – 28.8).

Discussion

The effect of large vessel disease and white matter lesions on white matter autoregulation was investigated in the present study by combining quantitative ASL-MRI with a vascular challenge. Patients with a symptomatic ICA stenosis and occlusion had normal CBF, but decreased CVR in the white matter on the side of the symptomatic ICA when compared to healthy control subjects, and patients with white matter lesions had further decreased CVR when compared to patients without.

The effect of large vessel disease on the hemodynamic state of cortical gray matter has been widely investigated. As perfusion pressure drops due to a steno-occlusive lesion in one of the brain feeding arteries cerebral vasodilatation sustains adequate delivery of nutrients and oxygen by lowering the cerebrovascular

resistance. When this regulative mechanism falls short, CBF drops and eventually brain becomes ischemic. Studies have previously used transcranial Doppler to measure the flow-velocity in the middle cerebral artery, and methods such as positron emission tomography and single photon emission tomography to study hemodynamics at brain tissue level.[23-25] ASL has recently been shown to be able to evaluate the hemodynamic status of cortical gray matter in patients with an ICA stenosis and occlusion.[9,26] Its ability to measure white matter perfusion has, however, been under debate due to the relatively low signal-to-noise ratio of ASL-MRI.[27] By applying improved, pseudo-continuous, ASL labeling techniques in combination with background suppression it was recently demonstrated that perfusion signal could be reliably measured in white matter. We now show that in combination with a vascular challenge ASL-MRI can assess CBF and decreased cerebrovascular reactivity in patients with a stenosis and occlusion.

White matter lesions in the borderzones between the vascular territories of the major cerebral arteries have been attributed to hemodynamic failure and steno-occlusive carotid artery disease.[28,29] Our results show that patients with a stenosis and occlusion of the ICA and severe white matter damage have more severe autoregulative impairment than those without. This indicates that large vessel disease does not only affect the cortical and subcortical gray matter, but also white matter. Although the occurrence of white matter lesions are often silent, they have been shown to be associated with increased risk of stroke, dementia and mortality.[30-32]

The white matter CVR values in our study are relatively high compared to the gray matter in both patients and healthy control subjects. With pseudo-continuous ASL imaging, perfusion-weighted images are acquired 1525 milliseconds after labeling. As the time needed for blood to travel from the excitation site to the deep white matter is longer than that of to the gray matter, white matter CBF may be underestimated. After the vascular challenge there is an increase in blood flow, leading to a faster arrival of the blood and an artificially higher signal. Although our results correspond with previous studies, this could be a possible explanation of the higher overall reactivity measurements within the white matter.[33,34] With the pseudo-continuous labeling technique, protons are first labeled for 1.1 seconds, resulting in an effective delay time of more than 3 seconds. When the symptomatic and asymptomatic hemispheres are compared, we still find decreased CVR on the side of steno-occlusive lesion in the ICA indicating autoregulative impairment.

This study had limitations. After administration of acetazolamide there may be an increase in the blood flow velocity through the carotid arteries due to the peripheral vasodilatation and lower cerebrovascular resistance. This could lead to a decreased labeling efficiency, and subsequently a lower CBF and CVR. The effect however would be evenly distributed throughout the brain and when using CBF and CVR maps to depict focal areas with decreased perfusion, areas with

impaired hemodynamics should be easy to detect. A second limitation of this study is that in patients with steno-occlusive lesion in one of the brain feeding arteries, collateralization may lead to a delayed arrival of the bolus of magnetically labeled blood spins. As the perfusion-weighted images are acquired after a fixed amount of time in ASL-MRI, this could potentially lead to an underestimation of the perfusion. To minimize these effects, we employed a delay time of 1525 ms in this study, where the protons that have been labeled directly after the start of the labeling have an effective delay time of more than 3 seconds.

Conclusion

By combining pseudo-continuous ASL-MRI with a vascular challenge CBF and CVR was assessed within the white-matter in patients with an ICA stenosis and occlusion. A stenosis or occlusion in one the ICAs leads to decreased CVR in white matter, and patients with white matter lesions have further decreased CVR. Our study indicates that both large vessel disease and white matter lesions have an effect upon white matter hemodynamics. With further research, cerebrovascular reactivity assessment with ASL-MRI may possibly help understand the pathogenesis underlying white matter lesions and the roll of large vessel disease on white matter perfusion.

References

1. Bamford JM, Warlow CP. Evolution and testing of the lacunar hypothesis. Stroke 1988;19:1074-1082.
2. Wardlaw JM. What causes lacunar stroke? J Neurol Neurosurg Psychiatry 2005;76:617-619.
3. Pantoni L, Inzitari D. New clinical relevance of leukoaraiosis. European Task Force on Age-Related White Matter-Changes. Stroke 1998;29:543.
4. de Leeuw FE, de Groot JC, Achten E, et al. Prevalence of cerebral white matter lesions in elderly people: a population based magnetic resonance imaging study. The Rotterdam Scan Study. J Neurol Neurosurg Psychiatry 2001;70:9-14.
5. Scheltens P, Barkhof F, Valk J, et al. White matter lesions on magnetic resonance imaging in clinically diagnosed Alzheimer's disease. Evidence for heterogeneity. Brain 1992;115:735-748.
6. Longstreth WT, Manolio TA, Arnold A, et al. Clinical correlates of white matter findings on cranial magnetic resonance imaging of 3301 elderly people. The Cardiovascular Health Study. Stroke 1996;27:1274-1282.
7. Derdeyn CP, Videen TO, Yundt KD, et al. Variability of cerebral blood volume and oxygen extraction: stages of cerebral haemodynamic impairment revisited. Brain 2002;125:595-607.
8. Powers WJ. Cerebral hemodynamics in ischemic cerebrovascular disease. Ann Neurol 1991;29:231-240.
9. Detre JA, Samuels OB, Alsop DC, et al. Noninvasive magnetic resonance imaging evaluation of cerebral blood flow with acetazolamide challenge in patients with cerebrovascular stenosis. J Magn Reson Imaging 1999;10:870-875.
10. Zhao P, Alsop DC, Abduljalil A, et al. Vasoreactivity and peri-infarct hyperintensities in stroke. Neurology 2009;72:643-649.
11. Bokkers RP, van Osch MJ, van der Worp HB, et al. Symptomatic carotid artery stenosis: impairment of cerebral autoregulation measured at the brain tissue level with arterial spin-labeling MR imaging. Radiology 2010;256:201-208.
12. van Osch MJ, Teeuwisse WM, van Walderveen MA, et al. Can arterial spin labeling detect white matter perfusion signal? Magn Reson Med 2009;62:165-173.
13. Fox AJ. How to measure carotid stenosis. Radiology 1993;186:316-318.
14. Garcia DM, de Bazelaire CM, Alsop DC. Pseudo-continuous Flow Driven Adiabatic Inversion for Arterial Spin Labeling. Proceeding of the 13th Scientific Meeting, ISMRM 2005:37.
15. Wu WC, Fernandez-Seara M, Detre JA, et al. A theoretical and experimental investigation of the tagging efficiency of pseudocontinuous arterial spin labeling. Magn Reson Med 2007;58:1020-1027.
16. Ye FQ, Frank JA, Weinberger DR, et al. Noise reduction in 3D perfusion imaging by attenuating the static signal in arterial spin tagging (ASSIST). Magn Reson Med 2000;44:92-100.
17. Alsop DC, Detre JA. Reduced transit-time sensitivity in noninvasive magnetic resonance imaging of human cerebral blood flow. J Cereb Blood Flow Metab 1996;16:1236-1249.
18. Chalela JA, Alsop DC, Gonzalez-Atavales JB, et al. Magnetic resonance perfusion imaging in acute ischemic stroke using continuous arterial spin labeling. Stroke 2000;31:680-687.
19. St Lawrence KS, Wang J. Effects of the apparent transverse relaxation time on cerebral blood flow measurements obtained by arterial spin labeling. Magn Reson Med 2005;53:425-433.
20. Golay X, Petersen ET, Hui F. Pulsed star labeling of arterial regions (PULSAR): a robust regional perfusion technique for high field imaging. Magn Reson Med 2005;53:15-21.
21. Tatu L, Moulin T, Bogousslavsky J, et al. Arterial territories of the human brain: cerebral hemispheres. Neurology 1998;50:1699-1708.

22. Fazekas F, Niederkorn K, Schmidt R, et al. White matter signal abnormalities in normal individuals: correlation with carotid ultrasonography, cerebral blood flow measurements, and cerebrovascular risk factors. Stroke 1988;19:1285-1288.
23. Aaslid R, Markwalder TM, Nornes H. Noninvasive transcranial Doppler ultrasound recording of flow velocity in basal cerebral arteries. J Neurosurg 1982;57:769-774.
24. Eskey CJ, Sanelli PC. Perfusion imaging of cerebrovascular reserve. Neuroimaging Clin N Am 2005;15:367-381.
25. Derdeyn CP, Grubb RLJ, Powers WJ. Cerebral hemodynamic impairment: methods of measurement and association with stroke risk. Neurology 1999;53:251-259.
26. Bokkers RP, van Osch MJ, van der Worp HB, et al. Symptomatic carotid artery stenosis: impairment of cerebral autoregulation measured at the brain tissue level with arterial spin-labeling MR imaging. Radiology 2010;256:201-208.
27. van Gelderen P, de Zwart JA, Duyn JH. Pittfalls of MRI measurement of white matter perfusion based on arterial spin labeling. Magn Reson Med 2008;59:788-795.
28. Momjian-Mayor I, Baron JC. The pathophysiology of watershed infarction in internal carotid artery disease: review of cerebral perfusion studies. Stroke 2005;36:567-577.
29. Del SM, Eliasziw M, Streifler JY, et al. Internal borderzone infarction: a marker for severe stenosis in patients with symptomatic internal carotid artery disease. For the North American Symptomatic Carotid Endarterectomy (NASCET) Group. Stroke 2000;31:631-636.
30. de Jong G., Kessels F, Lodder J. Two types of lacunar infarcts: further arguments from a study on prognosis. Stroke 2002;33:2072-2076.
31. Debette S, Markus HS. The clinical importance of white matter hyperintensities on brain magnetic resonance imaging: systematic review and meta-analysis. BMJ 2010;341:3666.
32. Vermeer SE, Longstreth WT, Jr., Koudstaal PJ. Silent brain infarcts: a systematic review. Lancet Neurol 2007;6:611-619.
33. Ye FQ, Berman KF, Ellmore T, et al. H(2)(15)O PET validation of steady-state arterial spin tagging cerebral blood flow measurements in humans. Magn Reson Med 2000;44:450-456.
34. Kimura H, Kado H, Koshimoto Y, et al. Multislice continuous arterial spin-labeled perfusion MRI in patients with chronic occlusive cerebrovascular disease: a correlative study with CO2 PET validation. J Magn Reson Imaging 2005;22:189-198.

PART 3
General discussion and summary

CHAPTER 9

GENERAL DISCUSSION

General discussion

The studies in this thesis investigate the ability of arterial spin labeling (ASL) MRI to measure cerebral perfusion. The first part of this thesis focuses on applying different ASL-MRI techniques to assess brain perfusion and depict areas with reduced perfusion in patients with acute stroke and symptomatic large-vessel disease. The second part of this thesis combines ASL perfusion imaging with an intravenously administered vascular challenge, acetazolamide, to assess the cerebral autoregulatory status in patients with symptomatic large-vessel disease.

Arterial spin labeling perfusion imaging

Two different ASL perfusion imaging techniques were used in this thesis; a pulsed labeling strategy with image acquisition at multiple delay times and a pseudo-continuous labeling technique with image acquisition at a fixed inversion time. The first technique, which is used in *chapter 3 to 5*, measures the inflow of the magnetized blood bolus into the brain by acquiring multiple images of the brain at increasing inversion times with multiple small flip angle gradient echo readouts. When labeled ASL images are acquired at a fixed inversion time after the radiofrequency pulse, it is possible that the magnetic label may not have reached the imaging plane, potentially leading to an underestimation of CBF.[1,2] This is especially an issue in patients with cerebrovascular disease as blood is recruited through collaterals.[3,4] These alternative pathways of blood flow have been shown to lead to a delayed arrival of the labeled blood bolus to the brain and may result in an underestimation of CBF.[1-3] The accuracy of perfusion quantification in tissue with spatially variable tissue times can therefore be enhanced by acquiring a series of images at increasing delay times after the initial labeling.

The second advantage of using an ASL perfusion sequence with image acquisition at multiple delay times is that the kinetics of the labeled blood bolus can be used as a physiological parameter.[5] The arrival time and the duration needed for the end of the labeled bolus to reach the brain tissue can be calculated through hemodynamic modeling.[6] These hemodynamic parameters, respectively the transit and trailing edge times, are roughly comparable to the arrival time and time to peak in dynamic contrast enhanced MR and CT perfusion imaging. *Chapter 4 and 5* show that both in patients with a stenosis and occlusion of the internal carotid artery (ICA), reduced CBF and prolonged transit and trailing edge times can be found in the flow territory distal to a steno-occlusive ICA lesion. This may have been caused by either the lower flow velocities in the brain feeding arteries or longer blood flow routes due to collateral blood flow recruitment.[7,8]

Collaterals can provide the brain tissue with additional blood flow when there is an obstructive lesion in one of the brain feeding arteries through either the primary collaterals of the circle of Willis or secondary collaterals, such as the ophthalmic artery

and leptomeningeal vessels.[4] Previous studies have indicated that hemodynamic and metabolic changes are more severe in patients without primary collaterals than in patients with and that the presence of secondary collateral flow is associated with an impaired hemodynamic status.[9-12] In the analysis of the role of collateral blood flow, neither flow via the anterior or posterior collateral pathways had an effect on regional hemodynamic parameters in the patients with a stenosis or occlusion. Patients with an ICA occlusion and leptomeningeal collaterals, however, had a lower CBF and a prolonged trailing edge in the frontal lobe. The increased trailing edge time may reflect the elongated path that the bolus of magnetically labeled blood has to travel through the leptomeningeal collaterals from the posterior circulation to the frontal lobe. The collateral flow routes via the circle of Willis, i.e. the anterior communicating artery and the posterior communicating artery, are only short detours and may therefore not result in measurable differences.

A main drawback of ASL perfusion imaging at multiple delay times is the considerably longer acquisition time in comparison to a single inversion time ASL perfusion sequence. To speed up imaging, a small flip angle gradient echo sampling strategy can be used in a similar manner to the Look-Locker technique used for fast T_1 mapping.[13] A drawback of this imaging strategy is that the train of RF pulses during the readout decreases the perfusion signal. As a result of this signal loss and the natural T_1 decay of the magnetized blood, the remaining signal from the ASL label is small, resulting in low signal-to-noise and diminished spatial resolution. In *chapter 2* and the *second part* of this thesis, a pseudo-continuous ASL perfusion sequence was used in combination with background suppression. The pseudo-continuous labeling scheme has a higher labeling efficiency and enables the combined use of the body transmit coil with the multi-detector coils increasing the SNR.[14,15] The background suppression increases the SNR further by almost twofold.[16] Not only does this increase spatial resolution, but it allows for a shorter imaging time. In patients where there is limited time available, for example in the acute stroke patients in *chapter 2*, this makes fast and rapid assessment of potentially hemodynamic compromise feasible. To minimize the effect of transit times, a long delay time of 1525 ms was used, resulting in an effective delay time of more than 3 seconds for the protons that were labeled directly after the start of labeling.

Cerebral autoregulation

The degree of hemodynamic compromise distal to an obstructive lesion in one of the brain feeding arteries does not only depend on the degree of stenosis and capability of collateral vessels to provide additional blood flow, but also on the autoregulatory capacity of the brain. The cerebrovasculature is able to sustain adequate blood flow to the brain tissue when there is a drop in the cerebral perfusion pressure through vasodilatation of small arteries and arterioles.[17] Adequate cerebral perfusion is largely maintained throughout this autoregulatory range, although CBF may

decrease up to 18%. When the vasodilatory capacity is overcome, CBF will decrease passively with the decline in perfusion pressure. The oxygen fraction will then increase to its maximum in order to sustain oxygen metabolism. Further decline will inevitably lead to cellular ischemia and permanent brain tissue damage.

Guidelines for the treatment of cerebrovascular disease are currently primarily based on large, randomized clinical trials in which cerebral perfusion and hemodynamic reserve capacity were not taken into account.[18] Observational studies have however shown that in patients with an ICA stenosis the risk of ischemic stroke is higher in patients with impaired cerebral autoregulation in the hemisphere ipsilateral to a symptomatic or asymptomatic carotid stenosis than those with a normal perfusion.[19,20] And for patients with an ICA occlusion, that extracranial-intracranial (EC/IC) bypass surgery may be effective in patients with severe impaired cerebral hemodynamics.[21,22] Techniques that can assess the autoregulative status may therefore help depict the brain tissue most at risk for future stroke and define which patients would benefit most from revascularization operations.

A variety of different imaging techniques have been developed to assess hemodynamic compromise. The first stage of decline where there is only a slight CBF decrease can be measured through indirect measurements of the dilatory response after a vasodilatory challenge. This can be done at brain tissue level with techniques like $H_2{}^{15}O$ positron emission tomography (PET) and single photon emission tomography. Or by measuring the increase in flow-velocity in the middle cerebral artery with transcranial Doppler (TCD).[23-25] These approaches have limitations however. Perfusion measurement with $H_2{}^{15}O$ PET requires a cyclotron in the near vicinity and is therefore limited to only a few institutions. Measurements at brain tissue level are furthermore non-specific to the route of blood supply and flow-velocity measurements are limited to single brain feeding arteries. Especially in patients with a steno-occlusive lesion in one of the brain feeding arteries this is problematic as additional blood is recruited through collateral pathways and there is a shift in the perfusion-territories of the brain feeding arteries.[4,26]

The brains perfusion can be repetitively measured throughout a vasodilatory challenge with ASL perfusion imaging without high doses of ionizing radiation or multiple injections of contrast agents. With perfusion-territory selective labeling techniques, ASL-MRI can furthermore visualize the individual contribution of the cerebral arteries and collateral vessels to the brain.[27,28] Cerebral autoregulation and shifts in the perfusion-territories of the brain feeding arteries can therefore be assessed at brain tissue level on MRI scanners widely available in a clinical setting.

Acetazolamide was used as a vasodilatory challenge in the studies presented in this thesis investigating the vasodilatory capacity of the brain. Other methods such as breath holding or a CO_2 challenge are also available.[29] Each method has advantages and disadvantages which may, among other factors, depend on the experience of a department with a specific reactivity method. Limited studies are currently available

that perform head-to-head comparisons between the different vasodilatory challenge methods. The advantage of acetazolamide is the long duration of the effect and the relatively straightforwardness of administering acetazolamide during the MRI protocol without the requirement of a mask (CO_2 challenge) or patient compliance (breath holding). An issue of all measurements of the vasodilatory capacity is that they rely on functioning smooth muscle cells. Risk factors such as hypertension, diabetes mellitus and age may cause microvascular disease, reducing the vasodilatory capacity, and erroneously indicating hemodynamic impairment. Still, the decreased function of the smooth muscle cells in itself may also be a risk factor for the severity of atherosclerosis and future ischemic events.

In patients with hemodynamic compromise the reduction in cerebrovascular resistance in the surrounding tissue after a vascular challenge may lead to steal.[30,31] Inflowing freshly oxygenated blood may be redistributed from compromised brain tissue to more healthy tissue and inadvertently decrease CBF further and lead to temporary or permanent brain tissue ischemia. An example can be seen in Figure 3 of *Chapter 7*. This may can be caused by steal within the same hemisphere, interhemispherical or occur even earlier, at the level of the aortic arch. Occurrence of steal may potentially indicate high risk for future stroke and that more aggressive treatment options need to be considered, such as bypass surgery in patients with severe progressive atherosclerosis with occlusion of the feeding vessels.

Future perspectives

The studies in this thesis are some of the first to use ASL perfusion MR imaging in patients with acute stroke and symptomatic cerebrovascular disease. The studies are cross-sectional and show that ASL can depict perfusion deficits and autoregulatory impairment in groups of patients. Research is still ongoing to establish the role of perfusion imaging in clinical practice diagnosing ischemic stroke and to determine whether perfusion imaging can help target revascularization therapy in patients with atherosclerotic large-vessel disease. As the use of ionizing radiation required for CT increases the risk of tumor induction and contrast agents can cause nephropathy and nephrogenic systemic fibrosis, ASL-MRI may prove to be a powerful non-invasive alternative. Perfusion and cerebral reactivity imaging with ASL can help assess the extent of hemodynamic compromise and may potentially be used to customize medicinal and surgical treatment.

References

1. Calamante F, Williams SR, van Bruggen N, et al. A model for quantification of perfusion in pulsed labelling techniques. NMR Biomed 1996;9:79-83.
2. Alsop DC, Detre JA. Reduced transit-time sensitivity in noninvasive magnetic resonance imaging of human cerebral blood flow. J Cereb Blood Flow Metab 1996;16:1236-1249.
3. Gibbs JM, Wise RJ, Leenders KL, et al. Evaluation of cerebral perfusion reserve in patients with carotid-artery occlusion. Lancet 1984;1:310-314.
4. Liebeskind DS. Collateral Circulation. Stroke 2003;34:2279-2284.
5. Golay X, Hendrikse J, Lim TC. Perfusion imaging using arterial spin labeling. Top Magn Reson Imaging 2004;15:10-27.
6. Buxton RB, Frank LR, Wong EC, et al. A general kinetic model for quantitative perfusion imaging with arterial spin labeling. Magn Reson Med 1998;40:383-396.
7. Yang Y, Engelien W, Xu S, et al. Transit time, trailing time, and cerebral blood flow during brain activation: measurement using multislice, pulsed spin-labeling perfusion imaging. Magn Reson Med 2000;44:680-685.
8. Liebeskind DS. Collaterals in acute stroke: beyond the clot. Neuroimaging Clin N Am 2005;15:553-573.
9. Vernieri F, Pasqualetti P, Matteis M, et al. Effect of collateral blood flow and cerebral vasomotor reactivity on the outcome of carotid artery occlusion. Stroke 2001;32:1552-1558.
10. Kluytmans M, van der Grond J, van Everdingen KJ, et al. Cerebral hemodynamics in relation to patterns of collateral flow. Stroke 1999;30:1432-1439.
11. Muller M, Schimrigk K. Vasomotor reactivity and pattern of collateral blood flow in severe occlusive carotid artery disease. Stroke 1996;27:296-299.
12. Tatemichi TK, Chamorro A, Petty GW, et al. Hemodynamic role of ophthalmic artery collateral in internal carotid artery occlusion. Neurology 1990;40:461-464.
13. Look DC, Locker DR. Time saving measurement of NMR and EPR relaxation times. Rev.Sci.Instum 1970;41:250-251.
14. Fernandez-Seara MA, Edlow BL, Hoang A, et al. Minimizing acquisition time of arterial spin labeling at 3T. Magn Reson Med 2008;59:1467-1471.
15. Wu WC, Fernandez-Seara M, Detre JA, et al. A theoretical and experimental investigation of the tagging efficiency of pseudocontinuous arterial spin labeling. Magn Reson Med 2007;58:1020-1027.
16. Garcia DM, de Bazelaire C, Alsop DC. Pseudo-continuous Flow Driven Adiabatic Inversion for Arterial Spin Labeling. Proceedings 13th Scientific Meeting, ISMRM 2005:37.
17. Derdeyn CP, Videen TO, Yundt KD, et al. Variability of cerebral blood volume and oxygen extraction: stages of cerebral haemodynamic impairment revisited. Brain 2002;125:595-607.
18. Sacco RL, Adams R, Albers G, et al. Guidelines for prevention of stroke in patients with ischemic stroke or transient ischemic attack: a statement for healthcare professionals from the American Heart Association/American Stroke Association Council on Stroke: co-sponsored by the Council on Cardiovascular Radiology and Intervention: the American Academy of Neurology affirms the value of this guideline. Stroke 2006;37:577-617.
19. Markus H, Cullinane M. Severely impaired cerebrovascular reactivity predicts stroke and TIA risk in patients with carotid artery stenosis and occlusion. Brain 2001;124:457-467.
20. Blaser T, Hofmann K, Buerger T, et al. Risk of stroke, transient ischemic attack, and vessel occlusion before endarterectomy in patients with symptomatic severe carotid stenosis. Stroke 2002;33:1057-1062.
21. Adams HP, Jr. Occlusion of the internal carotid artery: reopening a closed door? JAMA 1998;280:1093-1094.

22. Derdeyn CP, Grubb RL, Powers WJ. Cerebral hemodynamic impairment: methods of measurement and association with stroke risk. Neurology 1999;53:251-259.
23. Vernieri F, Pasqualetti P, Passarelli F, et al. Outcome of carotid artery occlusion is predicted by cerebrovascular reactivity. Stroke 1999;30:593-598.
24. Hirano T, Minematsu K, Hasegawa Y, et al. Acetazolamide reactivity on 123I-IMP single photon emission computed tomography in patients with major cerebral artery occlusive disease: correlation with positron emission tomography parameters. J Cereb Blood Flow Metab 1994;14:763-770.
25. Grubb RL, Jr., Derdeyn CP, Fritsch SM, et al. Importance of hemodynamic factors in the prognosis of symptomatic carotid occlusion. JAMA 1998;280:1055-1060.
26. van Laar PJ, Hendrikse J, Klijn CJ, et al. Symptomatic carotid artery occlusion: flow territories of major brain-feeding arteries. Radiology 2007;242:526-534.
27. Paiva FF, Tannus A, Silva AC. Measurement of cerebral perfusion territories using arterial spin labelling. NMR Biomed 2007;20:633-642.
28. van Laar PJ, van der Grond J, Hendrikse J. Brain perfusion territory imaging: methods and clinical applications of selective arterial spin-labeling MR imaging. Radiology 2008;246:354-364.
29. Aaslid R. Cerebral autoregulation and vasomotor reactivity. Front Neurol Neurosci 2006;21:216-228.
30. Choksi V, Hughes M, Selwa L, et al. Transient neurologic deficit after acetazolamide challenge for computed tomography perfusion imaging. J Comput Assist Tomogr 2005;29:278-280.
31. Komiyama M, Nishikawa M, Yasui T, et al. Reversible pontine ischemia caused by acetazolamide challenge. AJNR Am J Neuroradiol 1997;18:1782-1784.

CHAPTER 10

SUMMARY AND NEDERLANDSE SAMENVATTING

Summary

Cerebral perfusion is the basis for the delivery of oxygen and nutrients to the brain. Brain tissue can become damaged when there is a shortage in the blood supply. Basic physiological functions such as synaptic transmission, the membrane ion pump and energy metabolism are disrupted and within minutes can lead to irreversible damage and neurological symptoms.

The aim of this thesis was to investigate the ability of arterial spin labeling (ASL) MRI to measure cerebral perfusion in patients with acute stroke and symptomatic large vessel disease of the brain feeding arteries. ASL perfusion imaging is an alternative non-invasive magnetic resonance imaging (MRI) technique for visualizing brain perfusion and quantifying cerebral blood flow that does not require injection of contrast agents. The blood flowing into the brain is used as an endogenous contrast agent by magnetically labeling the inflowing blood with radiofrequency pulses.

This thesis consists of two parts. The first part focuses on the application of different ASL-MRI techniques to assess brain perfusion. In patients with acute stroke it is shown that ASL can detect perfusion deficits and perfusion-diffusion mismatch prior to treatment comparable to gadolinium based DSC perfusion imaging *(chapter 2).* By acquiring a series of perfusion-weighted images at increasing delay times after the initial labeling, ASL is able to measure the inflow of blood into the brain. Although, when compared to $H_2{}^{15}O$ PET there was a relative systematic overestimation of cerebral blood flow *(chapter 3)*, ASL can depict the presence and extent of regions with hypoperfusion and increased transit times in patients with carotid artery disease (*chapter 4 and 5)*.

The second part of this thesis focuses on assessing the cerebrovascular reactivity by combining ASL perfusion imaging with a vascular challenge. This is a measure of the brain's capacity to sustain blood flow when perfusion pressure drops. Impairment is associated with increased stroke occurrence. Cerebrovascular reactivity is impaired in patients with a carotid artery stenosis on the side of the stenosis *(chapter 6).* By using a selective ASL technique that can visualize the flow territories of the brain feeding arteries, it was shown that cerebrovascular reactivity impairment varies throughout the brain *(chapter7).* Tissue areas fed via collaterals are the most impaired. Both large vessel disease and the occurrence of white matter lesions were furthermore found to have an effect upon white matter hemodynamics *(chapter 8).*

ASL perfusion imaging can be used to visualize the cerebral blood flow and cerebrovascular reactivity. It can be used in both patients with acute stroke and large vessel disease to detect impaired hemodynamics and be used to assess a patient's risk for future stroke. In the future, ASL may potentially be used to customize medicinal and surgical treatment to individual patient needs.

Nederlandse samenvatting

De doorbloeding van de hersenen voorziet het hersenweefsel van zuurstof en voedingstoffen. Als de bloedtoevoer gestremd wordt kan het hersenweefsel beschadigd raken en afsterven. Fysiologische basisfuncties zoals synaptische transmissie en energie metabolisme worden dan verstoord en kunnen binnen enkele minuten leiden tot onomkeerbare schade en neurologische symptomen.

In dit proefschrift wordt de hersendoorbloeding en het opsporen van verstoringen hiervan onderzocht met arteriële spin labeling (ASL) bij patiënten met een acuut herseninfarct en symptomatische vernauwingen van de halsslagader. ASL is een nieuwe magnetic resonance imaging (MRI) techniek om de hersendoorbloeding af te beelden zonder gebruik te maken van schadelijke röntgenstraling en/of contrastmiddelen. Het bloed dat naar de hersenen stroomt wordt gebruikt als natuurlijk contrastmiddel door het te labelen met radiofrequentie golven.

Dit proefschrift bestaat uit twee delen. In het eerste gedeelte worden verschillende ASL perfusie technieken gebruikt om de hersendoorbloeding af te beelden. Bij patiënten met een acuut herseninfarct wordt aangetoond dat ASL snel en op vergelijkbaar niveau met dynamic susceptibility MRI een verstoorde hersendoorbloeding kan detecteren voordat er irreversibel schade is ontstaan *(hoofdstuk 2).* Door een ASL techniek te gebruiken waarbij op verschillende momenten na het labelen beelden worden geacquireerd, kan het instromen van bloed in de hersenen worden gevolgd *(hoofdstuk 3).* Bij patiënten met halsslagadervernauwingen wordt hiermee een vertraagde aankomst van bloed vastgesteld, duidend op een ernstig verstoorde hersendoorbloeding *(hoofdstuk 4 en 5).*

In het tweede gedeelte wordt ASL gecombineerd met een vasculaire challenge om de cerebrovasculaire reactiviteit te onderzoeken. Dit is een maat van de reservecapaciteit van de hersenen om een verstoring in de bloeddoorstroming op te vangen en is bij een tekort geassocieerd met een hogere incidentie van herseninfarcten. In patiënten met een halsslagadervernauwing is deze verstoord in de hersenhelft aan de kant van de vernauwing *(hoofdstuk 6)*. Door een selectieve ASL techniek dat de stroomgebieden van de hersenvaten kan afbeelden, wordt aangetoond dat de cerebrovasculaire reactiviteit varieert binnen de verschillende stroomgebieden bij patiënten met een verstopping van de halsslagader *(hoofdstuk 7)*. Breinweefsel gevoed vanuit collaterale vaten waren het meest verstoord. Daarnaast wordt aangetoond dat de cerebrovascular reactiviteit in de witte stof door zowel een halsslagadervernauwing als witte stof laesies wordt beïnvloed *(hoofdstuk 8).*

Met ASL perfusie kan snel en zonder schadelijke bijeffecten de hersendoorbloeding en cerebrovasculaire reactiviteit in beeld gebracht worden. Bij zowel patiënten met een acuut herseninfarct als halsslagadervernauwingen kan ASL worden gebruikt om verstoringen op te sporen. Hiermee kan het risico op het krijgen van een herseninfarct worden bepaald en mogelijk, in de toekomst, op individuele basis medicamenteuze en chirurgische behandelingen worden geïndiceerd.

PART 4
Appendix

LIST OF PUBLICATIONS

List of Publications

Bokkers RP, van Osch MJ, Klijn CJ, Kappelle LJ, Mali WM, Hendrikse J. Cerebrovascular reactivity within perfusion territories in patients with an ICA Occlusion. J Neurol Neurosurg Psychiatry 2011 March 8. Ahead of print.

Bokkers RP, Wessels FJ, van der Worp HB, Mali WM, Hendrikse J. Vasodilatory capacity of the cerebrovasculature in patient with carotid artery stenosis. AJNR Am J Neuroradiol 2011 March 10. Ahead of print.

Gevers S, Bokkers RP, Hendrikse J, Majoie CB, Kies DA, Teeuwisse WM, Nederveen AJ, van Osch MJ. Robustness and reproducibility of flow territories defined by planning-free vessel-encoded pseudo-continuous arterial spin labeling. AJNR Am J Neuroradiol 2011 March 10. Ahead of print.

Gevers S, van Osch MJ, Bokkers RP, Kies DA, Teeuwisse WM, Majoie CB, Hendrikse J, Nederveen AJ. Intra- and multicenter reproducibility of pulsed, continuous and pseudo-continuous arterial spin labeling methods for measuring cerebral perfusion. J Cereb Blood Flow Metab 2011 Feb 9. Ahead of print.

Bokkers RP, van Osch MJ, van der Worp HB, de Borst GJ, Mali WP, Hendrikse J. Cerebral autoregulation impairment measured at the brain tissue level with arterial spin labeling MRI in patients with a symptomatic carotid artery stenosis. Radiology 2010;256:201-208

Bokkers RP, van Laar PJ, van der Zwan A, Mali WM, Hendrikse J. Mixed perfusion: a combined blood supply to brain tissue by multiple arteries. Journal of Neuroradiology 2010;37:201-210

Hartkamp N, Bokkers RP, van der Worp HB, van Osch MJ, Kappelle LJ, Hendrikse J. Distribution of cerebral blood flow in the caudate nucleus, lentiform nucleus and thalamus in patients with carotid artery stenosis. Eur Radiol 2010;21:875-881.

Bokkers RP, Bremmer JP, van Berckel BN, Lammertsma AA, Hendrikse J, Pluim JP, Kappelle LJ, Boellaard R, Klijn CJ. Arterial spin labeling perfusion MRI at multiple delay times: a correlative study with $H_2{}^{15}O$ positron emission tomography in patients with symptomatic carotid artery occlusion. J Cereb Blood Flow Metab 2010;30:222-229.

Bokkers RP, van der Worp HB, Mali WM, Hendrikse J. Non-invasive MR imaging of cerebral perfusion in patients with a carotid artery stenosis. Neurology 2009;15:869-875.

Bokkers RP, van Laar PJ, van de Ven KC, Kappelle LJ, Klijn CJ, Hendrikse J. Arterial spin-labeling MR imaging measurements of timing parameters in patients with a carotid artery occlusion. AJNR Am J Neuroradiol 2008;29:1698-1703.

Bokkers RP, Hendrikse J, Klijn CJ, Hartkamp NS, Kappelle LJ, van Osch MJ. White matter hemodynamic effect of large vessel disease and white matter damage. Submitted.

Bokkers RP, Hernandez DA, van Osch MJ, Mirasol RV, Hendrikse J, Merino JG, Warach S, Latour LL. Whole-brain arterial spin labeling perfusion MR imaging in patients with acute stroke. In revision.

Hartkamp NS, Hendrikse J, van der Worp HB, de Borst GJ, Bokkers RP. Repeated phase-contrast magnetic resonance angiography to assess cerebrovascular reactivity in patients with carotid artery stenosis. Submitted.

Hartkamp NS, Bokkers RP, van der Worp HB, Klijn CJ, van Osch MJ, de Borst GJ, Hendrikse J. Cerebrovascular reactivity in the caudate nucleus, lentiform nucleus and thalamus in patients with steno-occlusive carotid artery disease. Submitted.

Hernandez DA, Bokkers RP, Mirasol RV, Luby M, Henning EC, Merino JG, Warach S, Latour LL. Cerebral blood flow quantification utilizing pseudo-continuous arterial spin labeling in acute stroke patients. Submitted.

Bulder MM, Bokkers RP, Braun KP, Hendrikse J, Kappelle LJ, van Nieuwenhuizen O, Klijn CJ. Arterial spin labeling perfusion MRI in young patients with arterial ischemic stroke and a unilateral intracranial arteriopathy. In preparation.

Mirasol RV, Hernandez, DA, Bokkers RP, Warach S, Latour L. Whole brain assessment of reperfusion in acute stroke using pseudo-continuous arterial spin labeling: an alternative to gadolinium-based perfusion imaging. In preparation.

COLOR FIGURES

Chapter 2

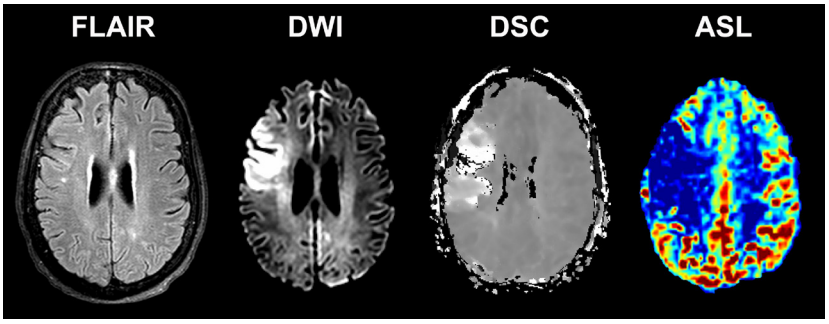

Figure 1. Transverse perfusion, diffusion and FLAIR images of a 66-year old woman presenting within 1 hour after symptom onset. Restricted diffusion and increased time-to-peak times can be appreciated in the flow territory of the right middle cerebral artery on the DWI and DSC images. The corresponding ASL image shows a corresponding decrease in perfusion.

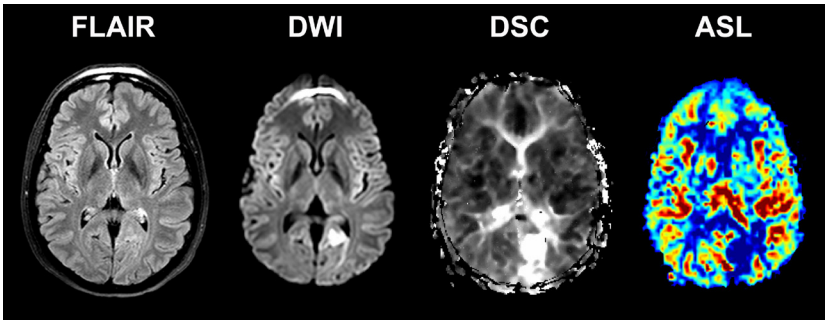

Figure 2. Transverse perfusion, diffusion and FLAIR images of a 48-year old woman presenting within 6 hours after symptom onset. Restricted diffusion and increased time-to-peak times can be appreciated in the flow territory of left posterior circulation on the DWI and DSC images. The corresponding ASL image shows a corresponding decrease in perfusion.

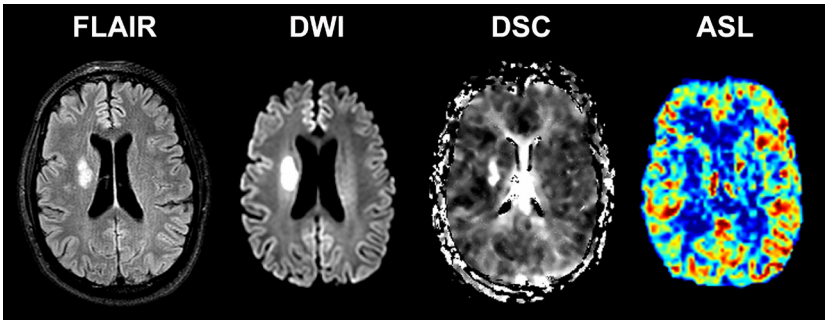

Figure 3. Transverse perfusion, diffusion and FLAIR images of a 53-year old male presenting within 10 hours after symptom onset. Restricted diffusion and increased time-to-peak times can be appreciated in the right basal ganglia on the DWI and DSC images. The perfusion deficit was however not depicted with ASL.

Chapter 3

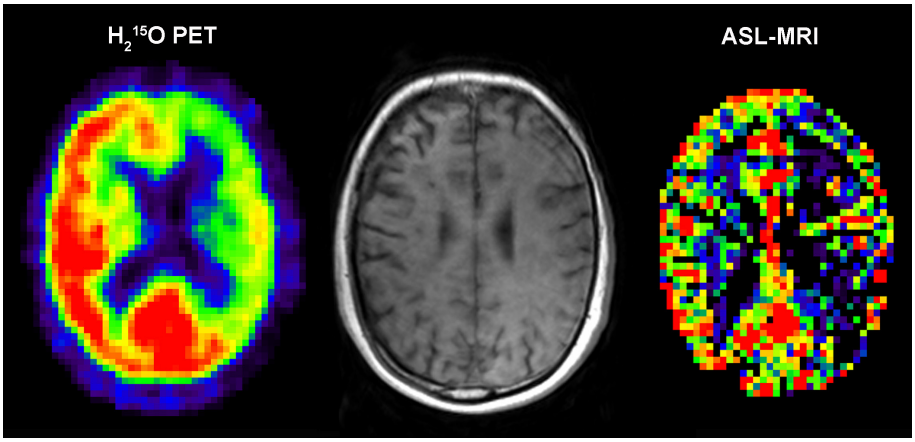

Figure 2. Transverse perfusion images in ml/min/100 g obtained with $H_2{}^{15}O$ PET (left) and ASL-MRI (right) of a 65-year-old female patient with a unilateral left-sided ICA occlusion.

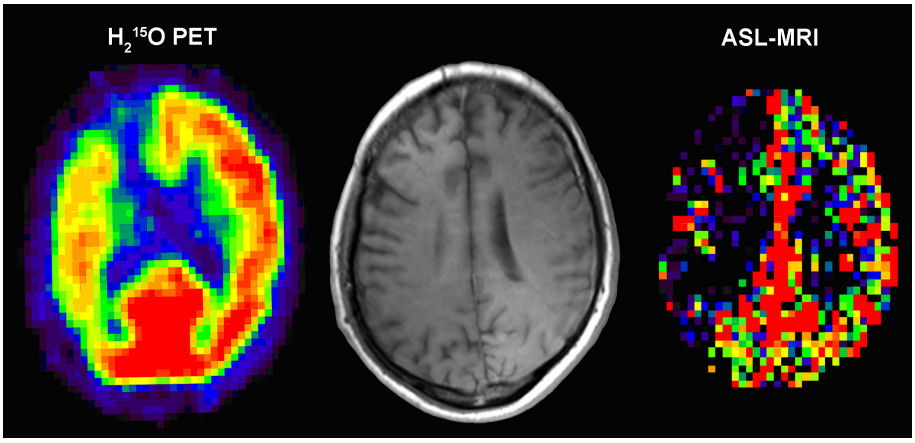

Figure 3. Transverse perfusion images in ml/min/100 g obtained with $H_2{}^{15}O$ PET (left) and ASL-MRI (right) of a 33-year-old male patient with a unilateral right-sided ICA occlusion.

Chapter 4

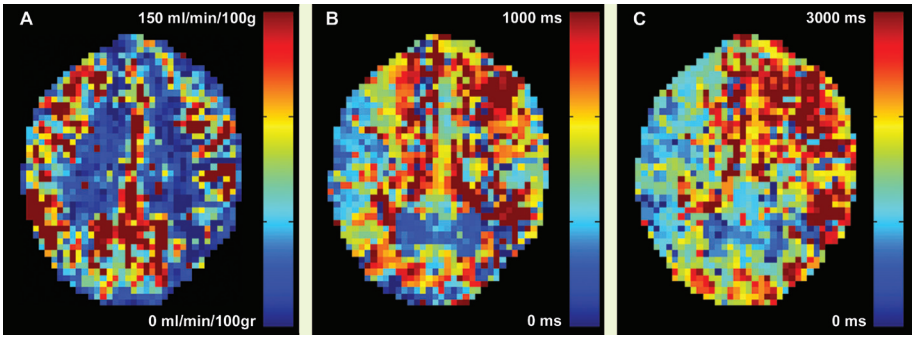

Figure 1. Transverse ASL perfusion MR images of a patient with a unilateral left-sided ICA stenosis of 90%. The images show the absolute CBF in ml/min/100gr (A), transit time in ms (B), and trailing edge time in ms (C). Decreased CBF and increasing ASL timing parameters are observed in the hemisphere ipsilateral to the internal carotid artery stenosis.

Chapter 5

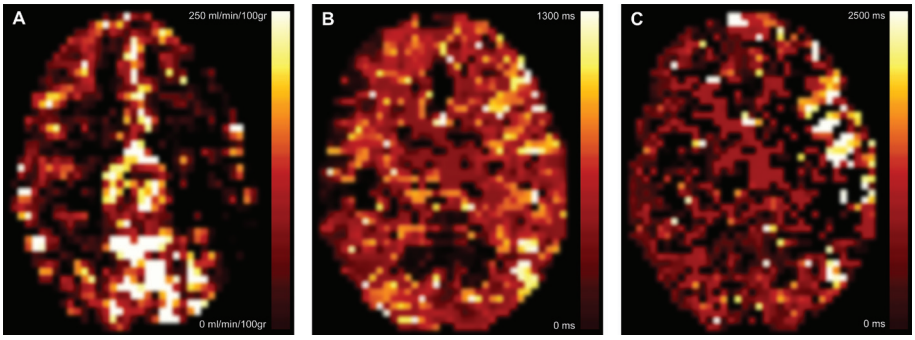

Figure 2: Transverse ASL perfusion MR images of a 76 year old man with a unilateral left-sided ICA occlusion. The images show the absolute CBF in ml/min/100gr (a), transit time in ms (b) and trailing edge in ms (c). Decreased CBF, increased transit time and increased trailing edge can be appreciated in the left hemisphere.

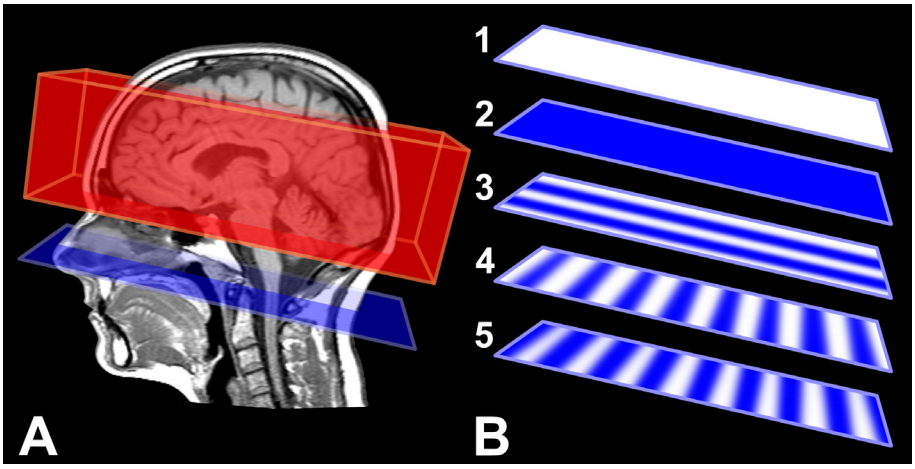

Figure 1. Sagittal T1 weighted image illustrating the imaging volume aligned parallel to the orbito-meatal angle and the labeling plane of the flow territory-specific perfusion selective ASL imaging (A). Labeling efficiency was spatially manipulated within the labeling plane in sets of five dynamics, in which: 1) no labeling applied (control), 2) non-selective labeling applied (globally perfusion weighted), 3) labeling varied in right-left (RL) direction (distance of 50 mm between full label and control situation), 4) labeling varied in anterior-posterior (AP1) direction (distance of 18 mm between full label and control situation), and 5) labeling varied in anterior-posterior direction (AP2, similar to AP1, but shifted 9 mm in posterior direction compared to the previous dynamic).

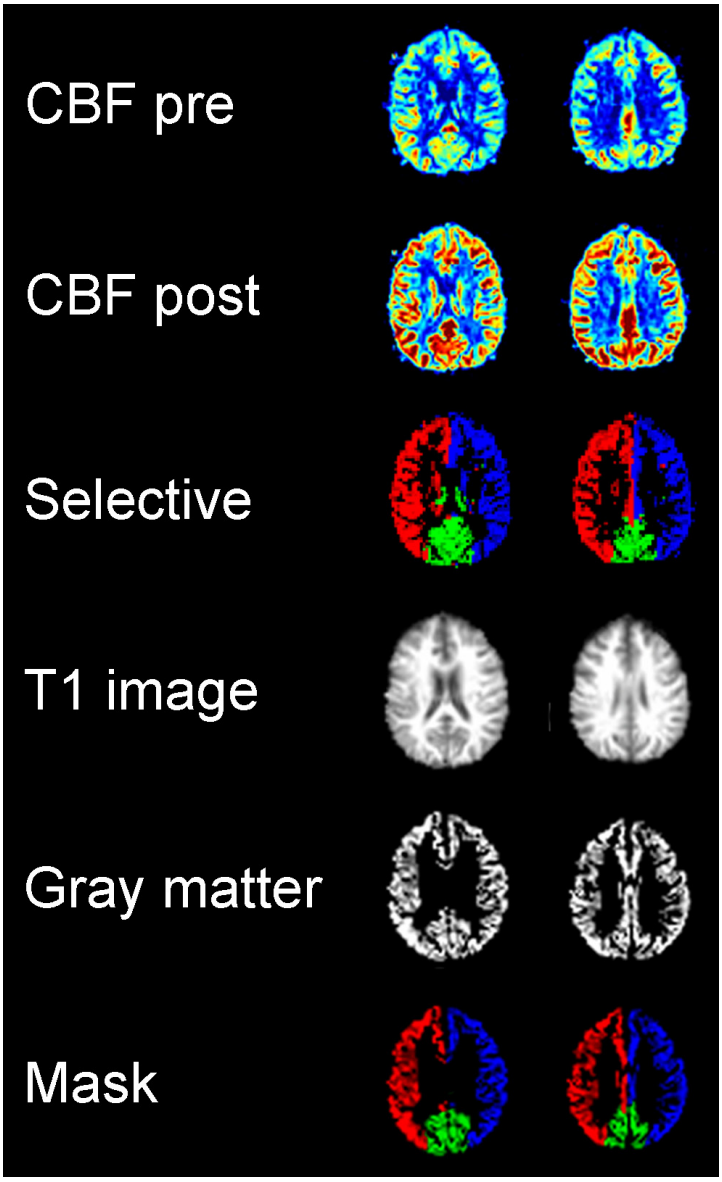

Figure 2. Pictorial description of the post-processing steps shows two of 17 slices in a 56-year old female. First shown are transverse CBF maps in mL·100mL^{-1}·min^{-1} before *(CBF pre)* and after administration *(CBF post)* administration of acetazolamide. Selective ASL images *(Selective)* show the perfusion territory of the right ICA (red), left ICA (blue) and basilar artery (green). T_1-weighted image was segmented into a gray-matter probability map. By combining the gray-matter map with the cerebral flow territory information from the selective ASL image, a gray-matter mask was obtained of both carotid arteries and the basilar artery.

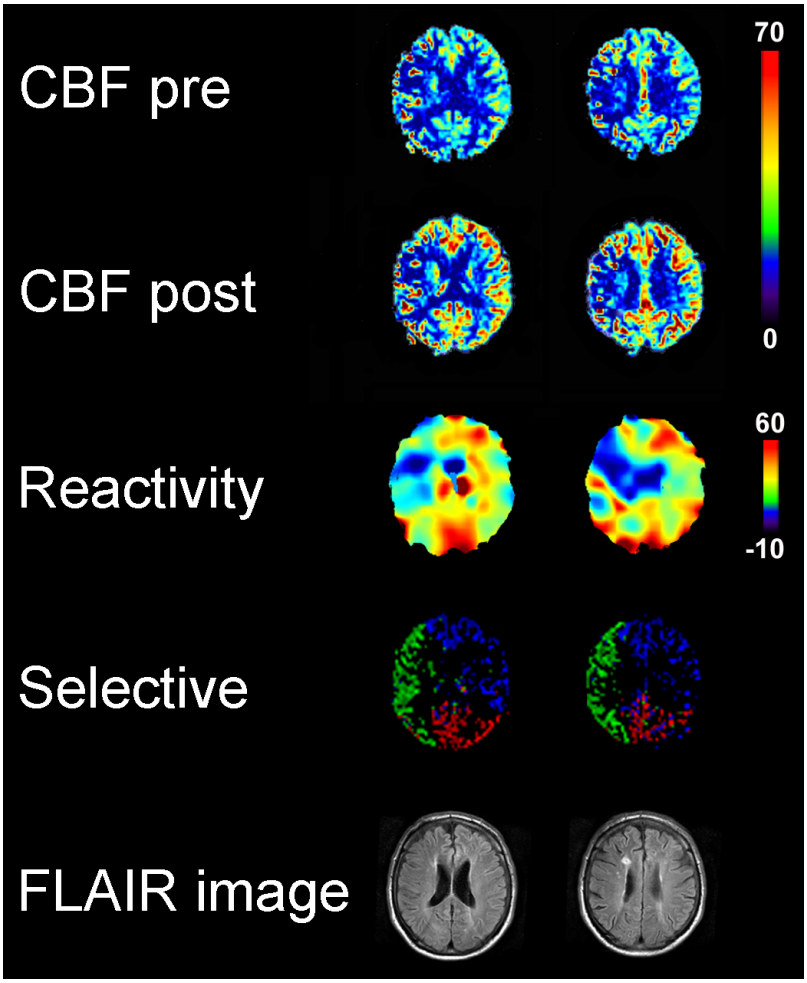

Figure 3. Transverse CBF maps in mL·100mL^{-1}·min^{-1} before *(CBF pre)* and after *(CBF post)* administration of acetazolamide of a 69-year old man with a symptomatic stenosis of the right ICA. CBF and a decreased cerebrovascular reactivity (percentage CBF increase) can are decreased, especially in the top slices, in the flow territory of the affected right ICA. For selective ASL image, green = right ICA territory; blue, left ICA territory; red, basilar artery territory; *FLAIR image,* fluid-attenuated inversion-recovery MR image.

Chapter 6

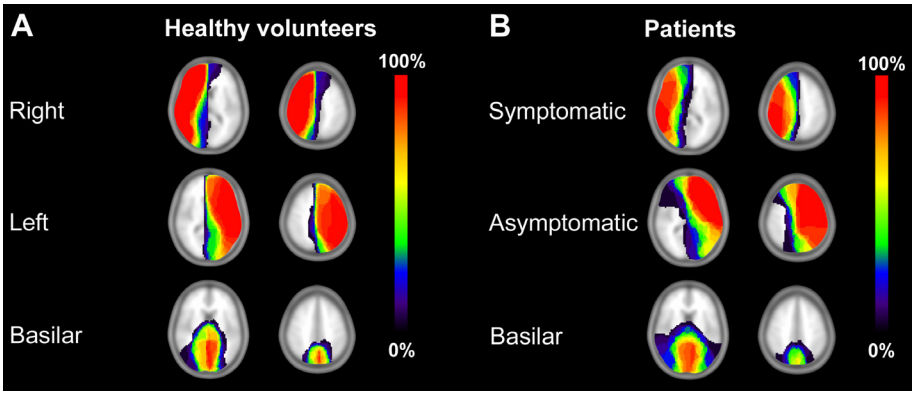

Figure 4. Transverse perfusion territory maps projected on a standardized brain template for right ICA, left ICA and basilar artery in **(a)** healthy control subjects (n = 20) and **(b)** patients with symptomatic ICA stenosis (n = 23). Scale indicates percentage of individuals in the group who had perfusion in that area.

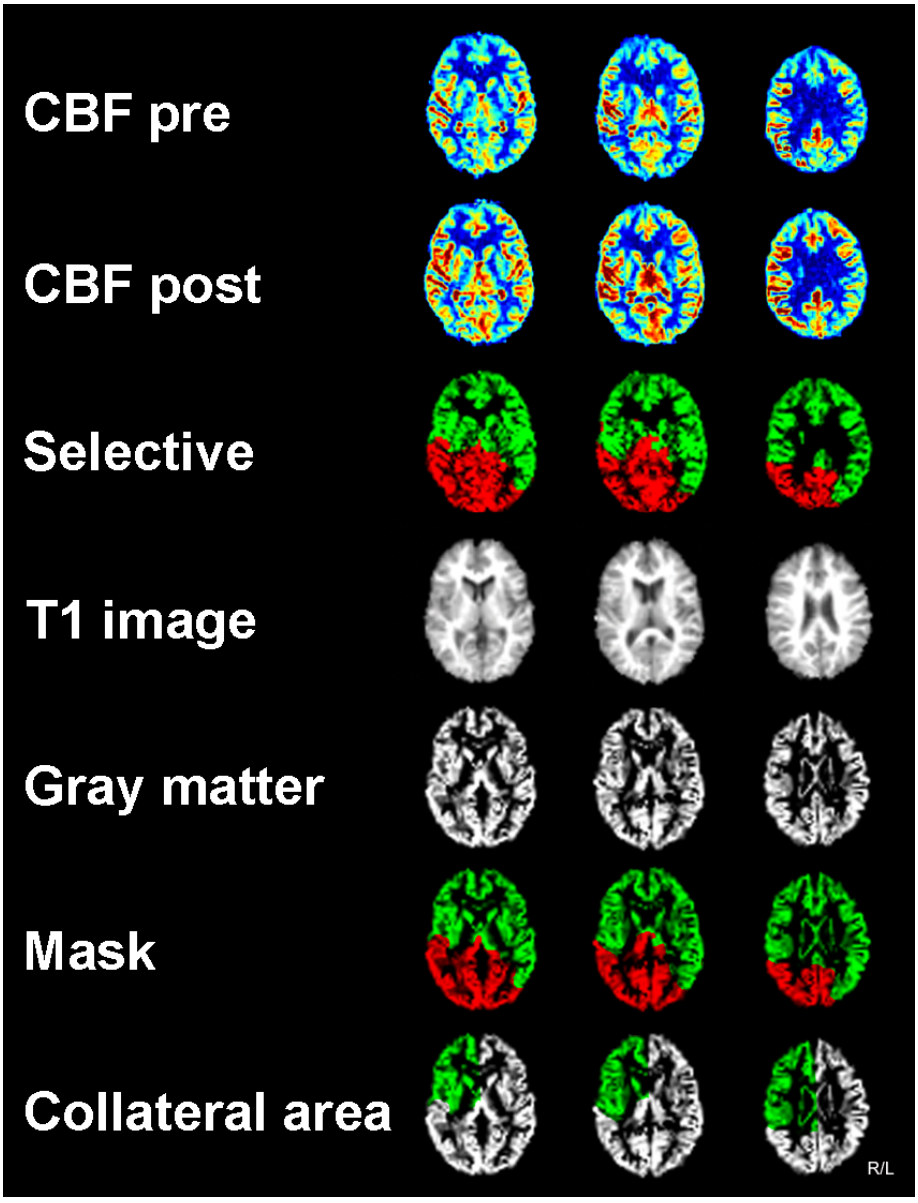

Figure 1: Pictorial description of the preprocessing steps in 3 of the 17 slices in a patient with an occluded right ICA. First shown are transverse CBF maps in mL·100mL^{-1}·min^{-1} before *(CBF pre)* and after administration *(CBF post)* administration of acetazolamide. Selective ASL images *(Selective)* show the perfusion territory of the ICA (green) and basilar artery (red). T_1-weighted image was segmented into a gray-matter probability map. By combining the segmented gray matter map with the perfusion-territory information, a gray-matter mask was obtained of the ICA, basilar artery and collateral pathways originating from the unaffected contralateral ICA.

Chapter 7

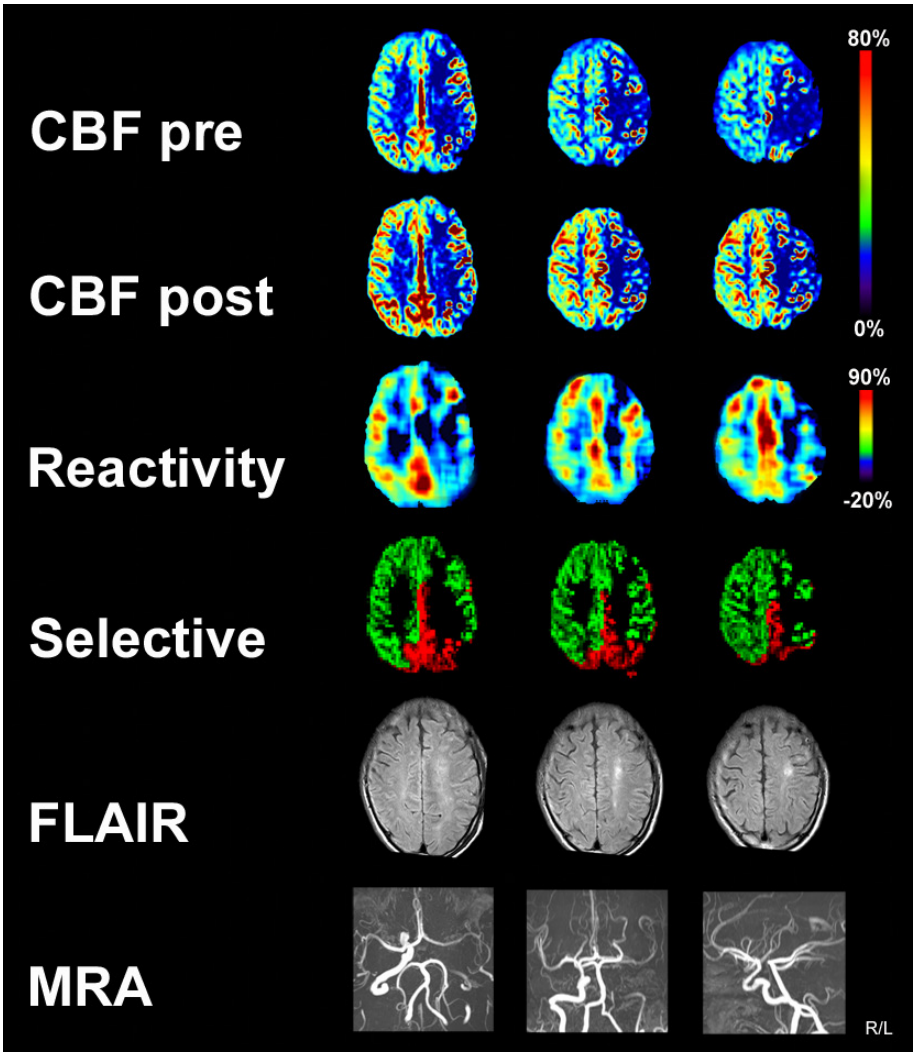

Figure 2: Transverse CBF maps in mL·100mL^{-1}·min^{-1} before *(CBF pre)* and after *(CBF post)* administration of acetazolamide of a 47-year old man with a symptomatic occlusion of the left ICA and collateral flow from unaffected contralateral ICA (green on Selective ASL image). CBF and cerebrovascular reactivity (percentage CBF increase) are decreased in the left hemisphere. On the anatomical fluid-attenuated inversion recovery (FLAIR) image, multiple hyperintensities are present in the left hemisphere. MRA, MR angiography.

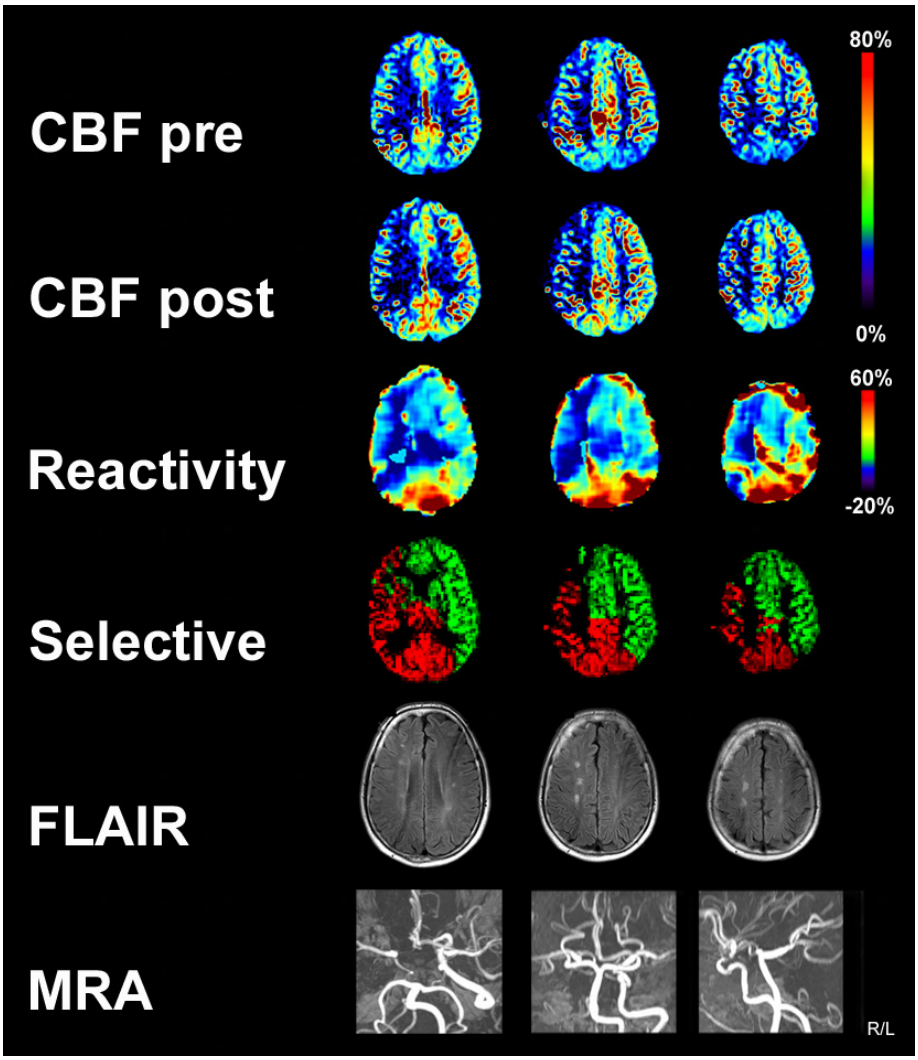

Figure 3: Transverse CBF maps in mL·100mL^{-1}·min^{-1} before *(CBF pre)* and after *(CBF post)* administration of acetazolamide of a 51-year old man with a symptomatic occlusion of the right ICA and collateral flow from the posterior circulation (red on Selective ASL image). CBF and cerebrovascular reactivity (percentage CBF increase) are decreased in the in the right hemisphere. On the anatomical fluid-attenuated inversion recovery (FLAIR) image, multiple hyperintensities are present in the right hemisphere. MRA, MR angiography.

Chapter 8

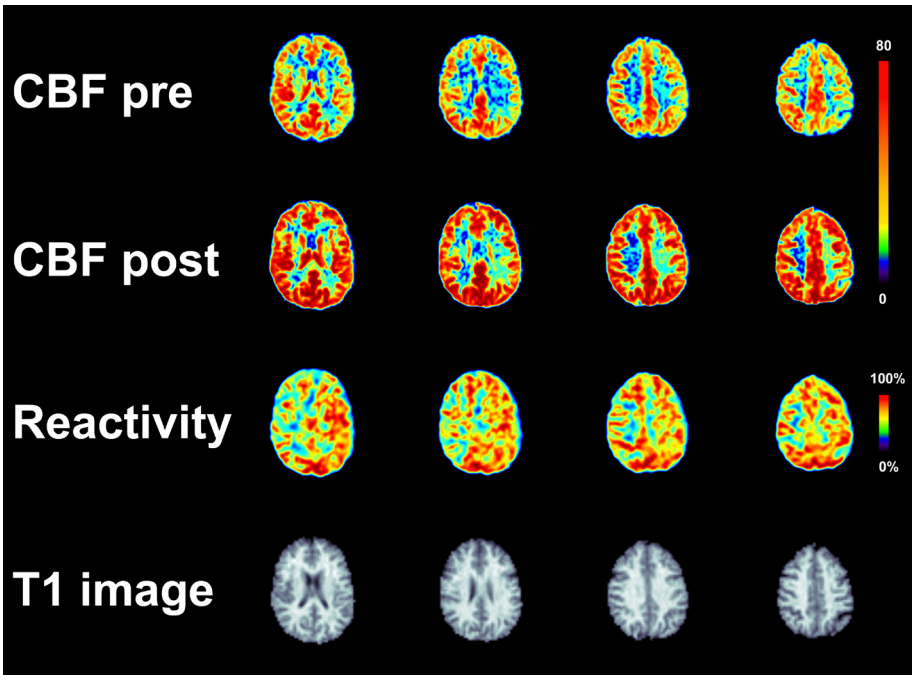

Figure 1. Clinical example of a 51 year old female with a right sided high-grade stenosis of the ICA. Decreased cerebral blood flow and cerebrovascular reactivity can be appreciated in the gray and white matter of the right hemisphere.

Chapter 8

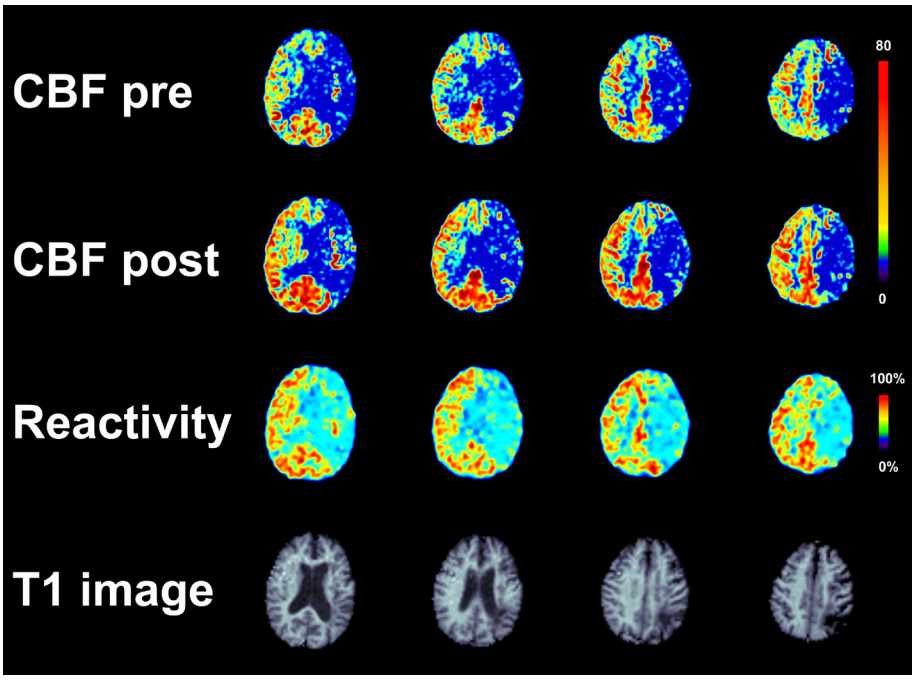

Figure 2. Clinical example of a 75 year old man with a left sided ICA occlusion. Decreased cerebral blood flow and cerebrovascular reactivity can be appreciated in the gray and white matter of the right hemisphere.